POLITECNICO DI TORINO

Dipartimento di Ingegneria Strutturale, Edile e Geotecnica

Corso di Laurea Magistrale in Ingegneria Civile

TESI DI LAUREA MAGISTRALE

BEHAVIOUR AND DESIGN OF COMPOSITE BEAMS WITH THE AUSTRALIAN CODE

Relatore:

Prof. Ing. Rosario Ceravolo,

Politecnico di Torino

Correlatore:

Prof. Ing. Gianluca Ranzi,

The University of Sydney

Tesista:

Borzelli Giuseppe

Anno accademico 2018/2019

To Cristina

and my family,

which have always encouraged

me to follow my dreams.

Abstract

This thesis focuses on the behaviour of composite beam using the Australian Code in which creep and shrinkage play the main role in long term response. The main aims of the thesis are:

i) design of composite beam using AS/NZS 2327:2017

ii) parametric analysis to understand the behaviour of the beam and check the parameters which influence most the service behaviour

iii) built a Finite Element Model to check the response of the beam and make a comparison with the Australian code

In the first part of the thesis, a state of the art shows the history and the behaviour of composite beam from 1961 since 2018 which analyses: the time-dependent behaviour of composite slab and beam, the shear lag effect, the shear deformability and the models used to describe this behaviour. Subsequently, the project of the composite beam is implemented using the new Australian code which focuses more on the effect of shrinkage during the serviceability limit state. To understand how much the effect of creep and shrinkage influences the behaviour of composite beam a parametric analysis is performed which analysed the displacements of several types of steel beams in function of the span and the effect on this beam due to creep, shrinkage and construction phases. In the last part, a Finite Element Model is developed to predict the service response of composite beam and make a comparison between the displacements related from the code and the model.

Sintesi

Questa tesi si concentra sul comportamento delle travi composite usando il codice australiano in cui fessurazione e rilassamento svolgono il ruolo principale nella risposta a lungo termine. Gli scopi principali della tesi sono:

i) progetto della trave composta usando AS/NZS 2327:2017

ii) analisi parametrica usata per comprendere il comportamento della trave e definire i parametri che influenzano maggiormente lo stato limite di servizio

iii) costruzione di un elemento finito usato per validare la risposta della trave e creare un confronto con i risultati ottenuti dal codice.

Nella prima parte della tesi, uno stato dell'arte mostra la storia e il comportamento delle travi composite dal 1961 dal 2018 ed analizza: il comportamento nel tempo della soletta e della trave composita, l'effetto di shear lag, la deformabilità a taglio e i modelli usati per descrivere gli effetti a lungo termine. Successivamente, il progetto della trave composita viene implementato utilizzando il nuovo codice australiano che si concentra maggiormente sull'effetto del rilassamento durante lo stato limite di servizio. Per comprendere quanto l'effetto dello scorrimento e del rilassamento influenzi il comportamento delle travi composite; quindi viene eseguita un'analisi parametrica che analizza gli spostamenti di diversi tipi di travi d'acciaio in funzione della campata, dell'effetto dovuto a scorrimento, ritiro e fasi costruttive. Nell'ultima parte, un modello ad elementi finiti è stato sviluppato per prevedere la risposta allo stato limite di servizio e fare un confronto tra gli spostamenti del codice e del modello.

Summary

List of figures

List of tables

Chapter 1 Introduction

1.1 Introduction

The thesis investigates the behaviour of composite beams in the serviceability limit state. Composite beam consists of a concrete slab (with or without a steel sheeting) connected by shear connectors with a profiled steel beam (**Figure 1.1**). During the action of the load, the two elements due to the effect of shear connectors guarantee a certain common behaviour which should be assimilated like a T-beam. Using this construction method, the advantage is maximizing the use of the two materials.

This technique is largely used in framed buildings, industrial buildings, hospital and multi-storey buildings and present this advantage:

1) speed of construction
2) saving in weight
3) saving in transport
4) faster construction phases because of the use of pre-fabricated components
5) concrete and steel are utilized effectively

6) higher stiffness which reduces the deflection respect to a steel beam

7) span bigger without the use of intermediate columns

8) if steel sheeting is used no additional formwork need to be used

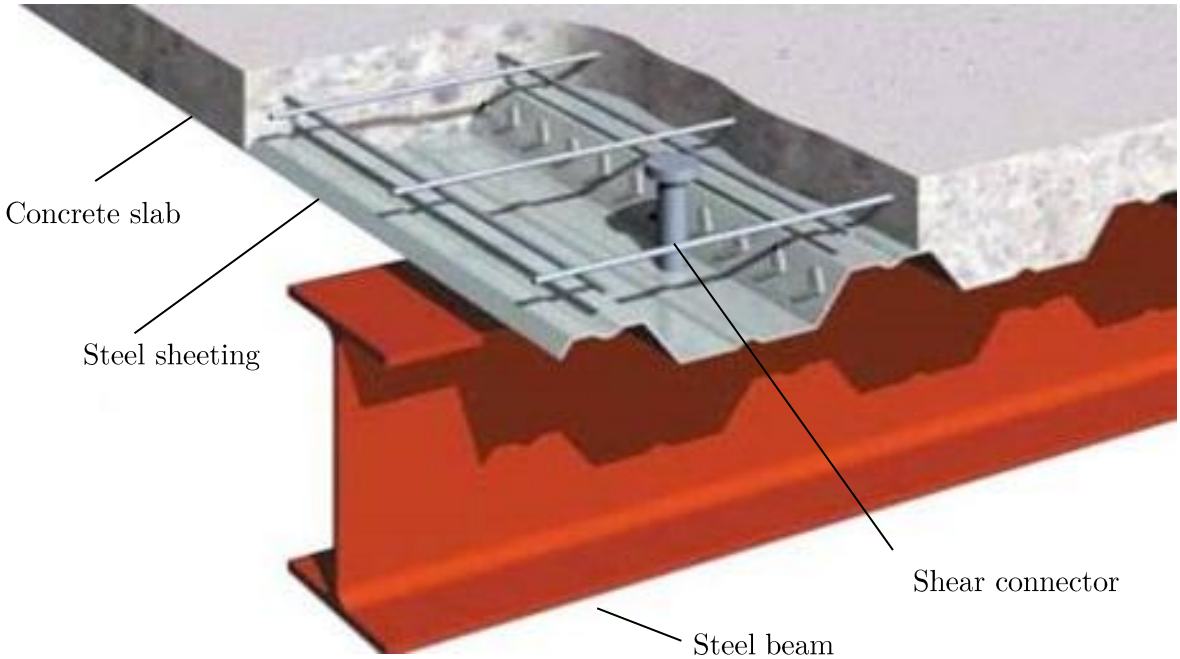

Figure 1.1 Composite beam

The use of this system increases during the years and also application in bridges are developed due to the fast construction procedures and the low value of deflections. However, some problems related to long-time effect are found related to the effect of creep and shrinkage especially when profile steel sheeting is used.

1.2 Objectives of the thesis

The objectives of the thesis should be defined as follow:

1) understand the design of a composite beam using the AS/NZS 2327:2017
2) to perform a parametric analysis able to define the main parameters engaged in the serviceability limit state
3) define the strength design actions along the constructions stages
4) build a Finite Element Model used to predict the response of composite beam during serviceability limit state and valeted using the Australian/New Zealand Standard

1.3 Layout of the thesis

This thesis is divided into 6 chapters and 2 appendices as detailed below:

Chapter 1 showed an introduction of the thesis.

Chapter 2 present a literature review about composite beams in which is described the researches carried in these years related to the time-dependent behaviour, the shear lag effect, the shear deformability of steel beam, the use of prestressing and the models adopted for considering the long-term effects.

Chapter 3 describes how the design of composite beam for strength and serviceability is developed using the Australian/New Zealand Standard AS/NSZ 2327:2017 in which the long-term effect due to shrinkage play a big role in the serviceability limit state.

Chapter 4 Parametric analysis, using different types of steel sections and spans, is developed to understand the parameters which influenced most the serviceability behaviour.

Chapter 5 A simplified Finite Element Model is developed on the composite beam and validated with the results obtained by the Australian Code

Chapter 6 Presents the conclusion of the thesis and some recommendation for future works which should be carried.

Appendix I Presents the main passage carried out for the design of the composite beam using AS/NSZ 2327:2017

Appendix II Shows the flowcharts used for helping the development of the MATLAB scripts related to the project of the composite beam and the Finite Element Model

Chapter 2 Literature review

2.1 Introduction

This chapter will outline the state of the art of composite beams and the works carried out from analysis and testing of it. In this chapter the time dependent behaviour is analyzed for composite slab and beam and subsequently the effects of shear lag and shear deformability are considered. In the final part a study related to prestressing beam is showed and the models used to describe the time dependent behaviour are defined.

2.2 Background

In many buildings and bridges, it is common to have a concrete slab supported by steel beams. To guarantee a good distribution of action from concrete slab to steel section, on the top flange of the steel beam are welded or bolted shear connectors that permit a common work of the concrete slab with the steel beam. Moreover, composite beam, in

sagging moment regions, has the advantage that the concrete in the slab takes all or most of the compression (for which it is best suited), while the steel beam takes all the tension in the overall system, so with this type of scheme, thereby we have the best use of the materials. Time-dependent behaviour of the concrete exhibit a great role because the concrete properties are affected by different drying conditions provided by the presence of profiled sheeting [1]

Moreover, the randomness about creep and shrinkage model is caused by different parameters:

a) compressive strength

b) elastic modulus

c) ambient humidity

d) the stiffness of shear connector

e) the magnitude of sustained load

2.3 Time-dependent behaviour

To analyze the history of the time-dependent behaviour it is possible to focus on the composite slab and on the composite beam.

2.3.1 Composite slab

During the 70s some experiments related to the time-dependent of composite slab were done. Bazant analyzed the effects of the creep and predicted creep effects using the age-adjusted effective modulus method [2].

The analysis of creep and shrinkage in the following years showed a continuous evolution due to the experimental tests, carried out on composite slabs, and due to the new concrete analysis models. An analytical model was proposed by the researchers based on theoretical model performed by Gilbert considering a uniform shrinkage profile and full shear interaction caused by the steel sheeting and the concrete [3] [4].

It was common to consider a constant shrinkage distribution through the depth of the concrete slab during the computation of the deflection [5] [6]; but in reality, a non-uniform shrinkage appears due to the effect of the steel sheeting which introduces an additional curvature and a consequent deflection in composite slabs that should be included in the calculations of the deflection predictions. Therefore some experiments were performed on composite slabs with different drying conditions [7] [8] [9].

Afterwards time-dependent analysis were performed to predict the non-uniform shrinkage through the slab thickness and the results obtained were compared with the experimental observation. These works shown the main role of the shrinkage gradient in predicting shrinkage deformation [10].

During the experiments were noticed a different behavior if it was used the profile steel sheeting. This element prevents moisture egress and causes a non-uniform shrinkage which were analyzed with a simplified method [11].

A parametric study was performed for long term: strains, deflection and stresses. It has been noted that the stresses increase during time from concrete to steel especially when it was considered a variation of the load history [12] [13].

Fem and parametric analysis were performed to understand how change the behaviour of the composite slab in function of the shape of steel deck, the presence of intermediate stiffeners and the length of span [14]. The presence of this elements produced a reduction in deflection, stresses and a variation of stiffness in the composite slab if is present a change in shape of cold formed deck.

Some models which describe the full interaction were described by Gilbert. He compared the age-adjusted effective modulus method (used to include the effects of creep) the Dischinger's differential constitutive relationship for concrete and a rate of creep solution procedure (RCM) to understand the in-service behaviour of the structure [15].

The influence of drying shrinkage in composite slab was analyzed with the presence of the steel sheeting which create an impermeable layer which causes redistribution of internal action and variation of long term deflection [16] [17].

In 2018 these studies were implemented with a Hydro-mechanical analysis carried to understand, in a clearer way, the development of non-uniform shrinkage during the depth of the composite slab [18] [19].

2.3.2 Composite beam

In 1971 for understanding the importance of the serviceability limit state some case studies were performed. In those studies. Cracking on the top surface of the concrete slab over supporting steel girders appears and also excessive deflections of beams were noticed.

Besides, during the design of the element in analysis deflection the component of shrinkage was uncertain and this underestimate the measured deflections in structures [20] [21].

The model started with a full shear interaction theory [22] [23] [24] [25] between concreate slab and steel beam (**Figure 2.1**).

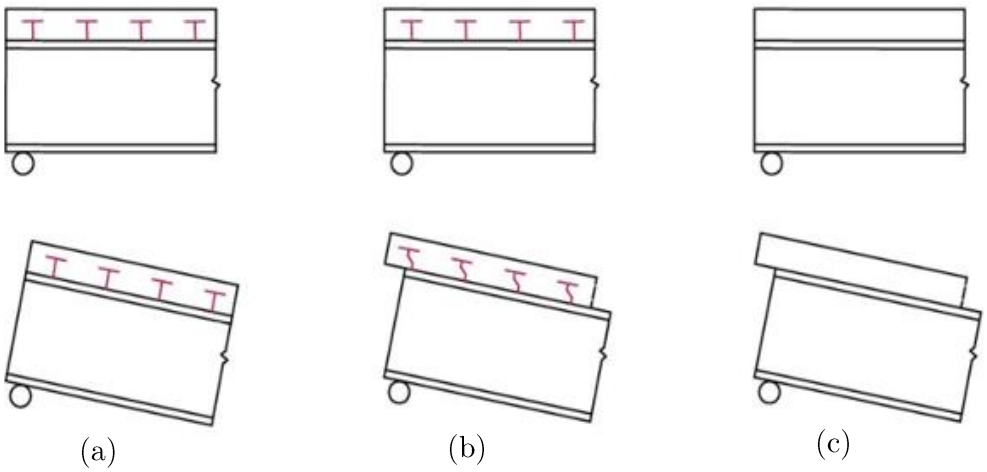

Figure 2.1 Full shear interaction (a), Partial shear interaction (b), No shear interaction (c)

After this stage, Bradford and Gilbert tried to analyze the non-linear behaviour involving a Newton Raphson method to investigate the response of composite cross-sections during the service load. At typical service load levels, the effect of creep and shrinkage cause a stiffness reduction [26] [27] [28] [29] [30] [31] [32].

In 1980 a ductile behaviour of the shear connector was noticed and the first model was implemented in the next years [33] [20].

In the early '90s, the effect of flexible shear connectors were performed by Tarantino and Dezi with a viscoelastic analysis of composite steel-concrete beams with flexible shear connectors. The effects of the connection device's deformability caused a migration of the stresses which occurs with time due to creep and shrinkage [34] [35] [36] [37] [38] [39] [40] [41] [42].

A distributed spring model is used to account the shear deformation at the interface of the two materials and long-term test was carried out [43] [44] [45] [46] [47] [48].

In the next years numeric method was performed to describe in a more accurately way the long-term experiments conducted before [49] [50] [51] [52] [53] [54] [55] [56] [57] [58] [59] [60]. The first method was the Effective Modulus Method (EMM) [2], however, Trost modified it with an age adjustment (AEMM). With this method, two analysis need to be carried out [10].

Analytical solution and stiffness method appear with the study of Ranzi e Gilbert [61] [62] [63] [64] [65].

In 2006 Ranzi proposed a closed form solution for predicting the behaviour of composite beams using algebraic representations of the viscoelasticity (AEMM and MSM) and a second-order linear differential equation [66].

To describe the main parameters involved in the behavior two different analysis were performed: Latin Hypercube and a Montecarlo method [67].

Concrete is less susceptible to creep and shrinkage at higher ages, in fact, Criel et al. show that the deflection due to creep and shrinkage is underestimated when the fully cracked section properties are assumed [68].

Some experiments also notice that the shrinkage stresses in steel-concrete interface reduce the stresses from external load and permit to neglect concrete adhesion to steel girder flange because its influence is lower respect to the shrinkage stresses [69].

Hydration heat and shrinkage developing in concrete at an early age and are responsible for cracking [70] which can be caused also by thermal effects, due to the heat, produced by cement reaction and shrinkage deformations affecting concrete result in stresses [71].

In 2015 Furtak settled some analysis to define the time-dependent behaviour. Creep and shrinkage models are randomness and depends on various parameter like: compressive strength, the elastic modulus of concrete, humidity, type of load, the presence of shear connectors and also some studies are related to the fatigue strength [72]. During the same year Ban and Uy used blind bolts in steel-concrete composite beams and demonstrated that time-dependent behaviour changed due to the stiffness and the bolt-to-hole clearance of connectors which causes lower deflection for the effect of creep and shrinkage [73].

In 2018, Tong et al. and Yuan et al. developed some experiments related to prestressed structure and their effects on creep, shrinkage and cracking. Parametric study and tridimensional model and non-uniform shrinkage were developed to controlling the concrete behaviour [74] [75].

The new researches focus also on the structure durability and the effect of corrosion caused by the external environment which accelerates the effect of creep and shrinkage [76].

2.4 Shear lag effect

When a flange is subjected to a bending moment, the stress distribution differs from the one given by the classic theory of the beam; this is caused by the effect of the "shear-lag action", which permits the development of shear deformations on it [77].

Theoretical models and experiment were performed to define the distribution of the load in the concrete flange [78] [79] [80] [81].

Partial interaction was introduced in the model with a flexible shear connector to analyze the shear lag effect by Dezi [82]. More refined finite element introduces a three-dimensional non-linear analysis which permits to define the actual effective slab width of

steel composite bridge girders [83]. Other studies were performed also when a negative moment is applied [84].

Analytical and fem model was compared and shown a shear lag effect in the composite slab and slip effect in the interface are coupled. The shear lag effect decreases when appear a reduction of shear stiffness of interface or when slip deformation and deflection of composite beam increase or when the thickness of the concrete slab has little impact [85] [86].

Moreover, the accuracy in calculating the effective flange width has a pronounced effect on the computed ultimate moment and serviceability limit states, such as deflection, fatigue, and overloading.

Long term analysis was also performed considering the shear lag effect [87] [88].

Closed form solution was implemented and validated by experiments showing the necessity of accounting for the shear deformation of composite beams. In addition, it is found that significant errors result from employing Timoshenko beam elements for the steel beam [89] [90].

Using stiffeners reduced the magnitude of the top flange longitudinal stresses by 40%, but didn't affect the shear lag [91].

2.5 Shear deformability of steel beam

An analytical model for the analysis of steel-concrete composite beams with partial shear interaction including the shear deformability of the steel component was proposed by Ranzi and Zona. This model is obtained by the sum of a Euler-Bernoulli beam for the

reinforced concrete slab and a Timoshenko beam for the steel beam. Extensive numerical simulations are carried out to evaluate the effects of the shear deformability of the steel member on the overall structural response [92].

More models by Dezi et al. was investigated for the analysis of composite beams with the constrained kinematics encompasses the overall shear deformability, warping of the slab cross-section and steel beam and partial shear interaction between slab and girder [93].

An analytical model for the short- and long-term analysis of steel beams with partial shear interaction considering the shear deformability was defined by Ranzi, Zona and Vrcelj. The time-dependent behaviour of the concrete was considered using a step-by-step procedure while the steel of the reinforcement and joist is assumed to remain in the linear-elastic range. The analytical model and the numerical solution was obtained using the principle of virtual work and the finite element method. Extensive numerical simulations are carried out on realistic simply supported composite beams to evaluate the effects of the shear deformability of the steel member on the overall structural response [94].

2.6 Internal and external prestressing

It is possible to use composite beam with external and internal prestressing. Internal prestressing is installed in the slab of the composite beam while external is installed in the bottom part of the steel section. This type of composite beam offers some advantages [95]:

a) limit tensile stress in concrete

b) prevent the occurrence of cracking

c) smaller values of concrete stresses due to the effect of creep

d) less steel and less deflections

In the positive moment region, the steel beam is prestressed along the bottom (tension) flange before the concrete deck is cast. In the negative moment region, the steel beam and the concrete deck can be prestressed either separately or jointly along with the top (tension) flange [96].

A time-dependent analysis for prestressed composite beams with a flexible shear connection was performed. Cable anchorages produce peaks on the shear force distribution at the beam-slab interface and stiffness of shear connection has only a local influence in the proximity of the inner supports, the cable anchorage cross sections and the beam ends. Shrinkage influence on the prestress losses is low, so the time evolution of the slab axial force is strongly modified [97] [98].

Numerical models, used from 2007 to 2010 by Uy, Xue and Giussani, were based on the Age-Adjusted Effective Modulus Method and parametric analysis were performed for various level of pre-stressing and their effects on deflection [99] [100] [101].

To investigate the effects of material nonlinearity on structural behaviour, an analytical model of the continuous composite beams, under sustained service loads, is useful [102].

2.7 Models for time effects

In 90s century few material researchs was defined related to the study of creep and shrinkage. The models were simple (caused by fewer materials research) and some simplification of analysis which avoids the complexities of real analysis were done. The most widespread method since 1972 was the Effective Modulus Method (EMM) that

increase its error when we considered the ageing of concrete; however, guarantees good result when:

$$\begin{cases} \sigma = cost \\ \boldsymbol{\varepsilon = \varepsilon_0[1 + \phi(t, t_0)]} \end{cases} \tag{2.1}$$

Therefore, if strain varies linearly with the creep coefficient and instant strain in the first loading being admissible this type of method gives good results.

Trost defined another simplified method that gives an exact solution in many cases with constant σ, constant ε and in case of straining of a structure with differential creep [2].

A time analysis using the Effective Modulus Method is an elastic analysis in which E_e (t, τ_0) is used instead of E_c(τ0). Moreover, the creep strain is only the function of current stress in the concrete; consequently, we lost the previous stress history and creep recovery is also assumed (that is a wrong hypothesis and represents the limit of this approach). Therefore, creep is overestimated for an increasing stress history and underestimated for a decreasing stress history.

Trost proposed an adjustment of this method (AEMM) and then Neville and Bazant gave their essay in the formulation. It was defined a new creep coefficient $\chi\ t, \tau_0\ \ \varphi(t, \tau_0)$ that considers a gradual application of stresses because their value is less than one and reduce the creep strain as shown in **Figure 2.2**:

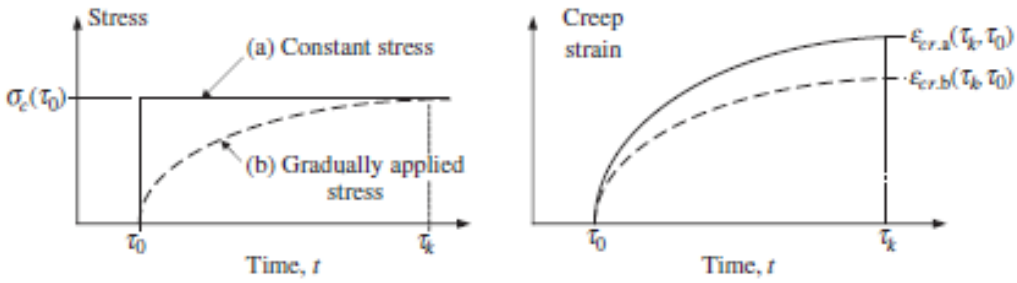

Figure 2.2 Variation of stress and strain caused by creep coefficient

Using the AEMM, the total strain at time t may be expressed as the sum of the strains produced by $\sigma_c(\tau_0)$ (instantaneous and creep), the strains produced by the gradually applied stress increment $\Delta\sigma_c(t)$ (instantaneous and creep), and the shrinkage strain:

$$\varepsilon\ t\ = \frac{\sigma_c(\tau_0)}{E_e\ (t,\tau_0)} + \frac{\Delta\sigma_c(t)}{E_e\ (t,\tau_0)} + \varepsilon_{sh}(t) \tag{2.2}$$

where $E_e\ \ t,\tau_0$ is the effective modulus and $E_e\ \ t,\tau_0$ is the age-adjusted effective modulus. With the AEMM, two analyses need to be carried out: one at first loading (time τ_0) and one at time t after the period of sustained stress [103].

In 2001 Dezi et al. used a finite difference method to analyse the shear lag effect with deformable shear connectors with long term behaviour. They define a variational approach to handle the differential equations [88].

In the 2002 Oehlers et al. introduced a criterion to determine the strength of a shear stud at partial composite state, and proposed the load–slip relation of the shear stud. Bradford and Gilbert analysed partially composite beams using an equivalent transformed section approach, with the linear load–slip relation of a shear connector. In addition, Dezi and Tarantino directly solved the governing differential equations by using the finite differential method to calculate the deflection change caused by the slip between the steel beam and concrete slab. Besides, many mathematical models based on the differential

equations have been introduced for simply supported composite beams with the partial shear connection. These methods give an exact solution and are very useful for analysing partially composite beams, but they have some restrictions in applications. Since these methods are greatly affected by the boundary conditions, only the symmetric structures with zero slip at midspan can be analysed. To overcome those limitations and to account for the slip effect in the partially composite beams, a few numerical models have been proposed. This requirement leads not only to a considerable increase in the number of degrees of freedom but also to a complexity in mesh definition. In addition, the use of a double node makes it difficult to analyse a multi-span continuous composite structure because of the increasing number of nodes and elements [104].

Finite difference procedures give an estimated solution of the analytic model and it can give problem in statically indeterminate structures for instance in continuous beams. Moreover, finite element procedures lead to approximate solution present a degree of accuracy depending on the choice of the shape functions. Newmark's differential equation can solve this problem evaluating the flexibility coefficients of the simply support composite beam analysing the problem with a force approach (**Figure 2.3**).

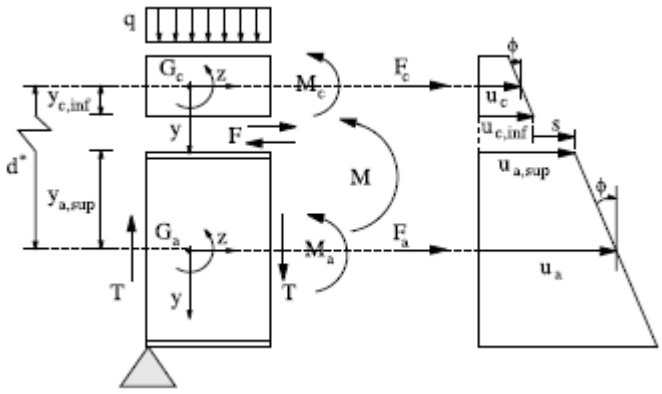

Figure 2.3 Newmark force approach

Faella et al. during 2002 used the exact solution of the matrix stiffness and the vector of equivalent nodal forces given by Newmark's equation and define a finite element model more accurate [105].

In 2004 Ranzi used a direct stiffness formulation based on an element possessing 8DOF to describe vertical displacement, rotation and slip. It is usual to try to minimize (rather than to eliminate) the locking phenomenon by using elements with larger numbers of degrees of freedom (10-DOF and 16-DOF elements), but these elements only produce a gradual improvement on the results as the degrees of freedoms increase. While the direct stiffness technique eliminates the locking phenomenon, it can produce numerical instabilities for low values of the shear connection stiffness, owing to the manipulation of exponential terms of highly disparate magnitude in the stiffness relationships. This difficulty was shown to be overcome adequately by recourse to a truncated Taylor series expansion of the exponential function for the slip within the stiffness matrix for an element [106].

Subsequent studies focus on the effect of shear connects on the composite beam. Numerical simulation performed by Jurkiewiez and Braymand observed that the effects of slip and strains in studs depends on the shrinkage crack and need to be considered [107].

In 2006 Ranzi modified the generic solution defined for the composite beam with PI for instantaneous or short-term loading into the time domain for including viscoelastic behaviour of a concrete slab. He proposed a closed form solution for predicting the behaviour of composite beams using algebraic representations of the viscoelasticity (AEMM and MSM) and a second-order linear differential equation [66].

In 2007 Chaudhary et al. propose a hybrid procedure has been presented to take into account the effect of concrete cracking and time-dependent effects of creep and shrinkage in composite beams of the composite frames subjected to service load. The procedure is analytical at the element level and numerical at the structural level [108].

In 2009 some research tries to blend the effect of creep and shrinkage with the behaviour of shear connectors; when creep and shrinkage arise the shear connectors are affected by the stiffness and strength of shear connectors and the stiffness and strength of the surrounding concrete that is reduced during the time.

In 2010 to prove that an accurate finite element model has been developed to investigate the behaviour of the shear connection in composite steel-concrete beams for both solid and profiled slabs when creep and shrinkage are examined, and the FE models were compared with push test experimental.

The structural steel beam, profiled steel sheeting and steel reinforcing were each modelled in a piecewise linear fashion as an elastic-plastic material with strain hardening. The shear connectors were also modelled in a similar fashion as the structural steel beam, profiled steel sheeting and steel reinforcing but without the inclusion of strain hardening.

They observed that for the solid slab, the failure mode is shear connector failure, whilst failure in the profiled slabs can be attributed to concrete failure. It also can be observed that the solid slab generally had a higher ultimate shear capacity and slip capacity when

compared with the profiled steel sheeting slab. Lastly, it is concluded that creep caused by the slip of the shear connectors was noticeable in the first 400 days, and the Young's Modulus of the concrete is reduced accordingly, leading to significant reduction in the shear resistance of the headed stud shear connection. After 400 days, creep did not have a major influence on the mechanical behaviour of composite steel and concrete structures [59].

In 2010 Nguyen et al. define a time-discretised formulation for the time-analysis of composite beams adopting a step-by-step procedure for the discretization in time of the concrete constitutive relationship, the time-discretised governing equations of the problem are analytically solved. The solution is approximate in time and exacts in space. The space-exact expression of the stiffness matrix and the vector of equivalent nodal forces are deduced for a generic composite beam element. The proposed space-exact finite element model is used in a displacement-based procedure for the time analysis of continuous beams with partial interaction. The concrete cracking effects in the slab are taken into account by neglecting the concrete's contribution along 15% of the beam length on each side of the internal support as suggested by Eurocode 4 so this model is able to perform a cracked and uncracked analysis. The numerical results have been indicated that the effects of concrete cracking must be considered for continuous composite beams even under serviceability loads. Furthermore, it has been observed that the choice of the creep and shrinkage models has a certain influence on the time-deflection responses and give the best result up to 340 days furthermore the numerical results show that shrinkage of the concrete slab plays an important role in the behaviour of composite beams. It leads to a large increase in deflection and significant redistribution of internal forces [64].

In 2012 Wenbin Yu proposed a new method: the GEBT. The Geometrically Exact Beam Theory (GEBT), is developed as a general-purpose tool for nonlinear analysis of composite

beams. It can capture all geometric nonlinearities due to large deflections and rotations, subject to the strains being small. GEBT not only effectively analyses geometric nonlinear static or dynamic behaviour of composite beams but also can carry out eigenvalue analysis of the linear system or a linearized state of the original nonlinear system to obtain eigenvalues and mode shapes of the composite beam [109].

In 2015 was developed analytical model and closed-form solution are derived for the long-term effect [110]. The time-dependent analysis with partial interaction was refined using a three-dimensional numerical model [111]. Gholamhoseini et al. developed a time-dependent deflection of composite concrete slabs with a simplified design approach and analysed the effect of drying shrinkage [112].

In 2016 most of the model was compared with the behaviour of real structure like truss bridge span or prestressed bridge; two-dimensional model and crack width was defined due to shrinkage and gravity load [113] [114] [115]. For considering the non-linear time-dependent, mixed finite element model was used in which a viscoelastic model was used for the concrete slab and a nonlinear constitutive relationship is utilized for the shear stud [116]. Also, Bernardi et al. developed non-linear analysis for showing that shrinkage in short term, which is always neglected, in service condition is relevant [117].

In 2017 an efficient one-dimensional finite element model is developed for an accurate prediction of the inelastic response of steel-concrete composite beams with partial shear interaction using a higher-order beam theory (HBT). This is achieved by taking a third order variation of the longitudinal displacement over the beam depth for the two layers separately. The deformable shear studs used for connecting the concrete slab with the steel girder are modelled as distributed shear springs along the interface between these two material layers.

In reality, the materials of these beams are having inelastic deformations even with a low to moderate range of loading; in order to address this issue, Yasunori incorporated the effect of inelastic material behaviour in their finite element model of composite beams using the von Mises yield criterion. The proposed model is based on a 3rd order beam theory (HBT) but it can easily be converted to a lower order beam theory by eliminating the higher order terms. The model based on TBT is able to predict the global response satisfactorily with the help of the shear correction factor. The model based on TBT doesn't predict the distribution of stresses across the beam section but the major advantage of the proposed model is it can predict results very close to those produced by a detailed finite element with a less computational cost. The proposed model is also used to examine the effect of different levels of shear interaction between the concrete and steel layers of the composite beam. It is observed that the full shear interaction condition predicted deflection less than that for the partial interaction as expected [118].

During 2016 the effects due to creep cracking of concrete and shrinkage were analyzed by Kelvin chain model. It was noticed that deflection became bigger when nonlinear behaviour of concrete is combined with creep and shrinkage and time effect produce redistribution of internal action under serviceability load [119] [120].

The new analytical solution was proposed which is able to simulate the effect of slippage, shear lag and time-dependent effects which show the importance of considering the creep and shrinkage effects [121].

In 2017 Altoubat et al. made experiments considering the different amount of fibres in concrete and for developing in a faster way the experiments they use a high value of w/c for aggravating the drying shrinkage. They notice that that the shrinkage stabilizes between 75 and 100 days and an increase of fibre causes a decrease of the average crack width and displacement in midspan if we considered long term results [122]. In the same

year Zhu et al. propose a new solution method to solve the one-dimensional analytical model of composite beams which is able to simulate the effects of interface slippage, and shear-lag and time-dependent effects [123].

In the same year, real case study of temperature and shrinkage was analyzed because they cause damage of structure during its life. A case study was analyzed starting from the observation of cracking which permitted to define stresses in the slab caused by shrinkage and temperature change [124].

In 2018 some analysis on the effect of the long terms were done. Cao et al. investigate the effect of corrosion of the studs and load with a test of 200 days. They notice that long term load influences the development of strain and creep in concrete structures and corrosion of studs strongly affects the stiffness of connectors but have a neglectable effect on concrete strain [125]. To modify the thermo-mechanical behaviour of concrete Klemczak et al. tried to modify the type of cement and aggregate to limit the early age deformation and possible crack in the beam [126].

Chapter 3 Design of composite beams

3.1 Introduction

The purpose of this chapter is to describe the steps provided in the code for the design of composite beams using the Australian Standard AS/NZS 2327:2017. The composite beams analyzed in this thesis are composed by a beam in steel and a concrete slab or a composite concrete slab place on it. The design starts choosing:

a) a steel beam

b) a concrete slab or a composite slab

Then, analyzing the effective section which carries the loads, the design of the load is performed on the composite beam. Subsequently, the design of strength and serviceability are performed. If both the design satisfy the verification limits the project is finished but if one of it does not respect the limit imposed by the code another section will be considered and the analysis will be performed a second time.

At the end of the thesis are defined some flowcharts which shows an overview of all the process.

3.2 Elements requirements

A description of the elements which compose the composite beam is developed.

3.2.1 Steel beam

The code is defined for different use of profile steel beams as shown in **Figure 3.1**:

a) a hot-rolled I-section, or channel section

b) a welded I-section

c) a rectangular cold-formed hollow section

d) a fabricated I-section, Tee section, channel section or rectangular hollow section

e) any of the above sections where an additional plate is welded to the bottom flange

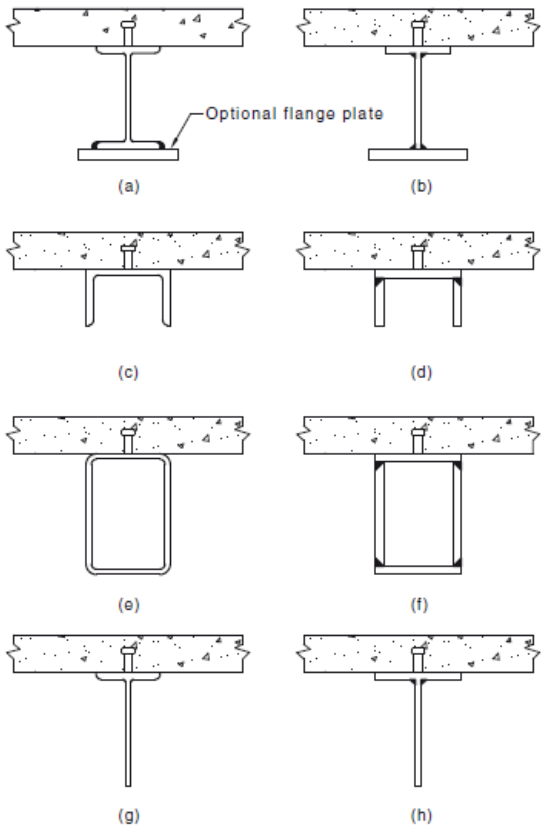

Figure 3.1 Steel beams types

3.2.2 Shear connectors

Shear connectors are the elements that connect the beam with the top slab, it is possible to use three types of connectors as shown in **Figure 3.2**:

a) head studs

b) channels

c) high-strength structural bolts

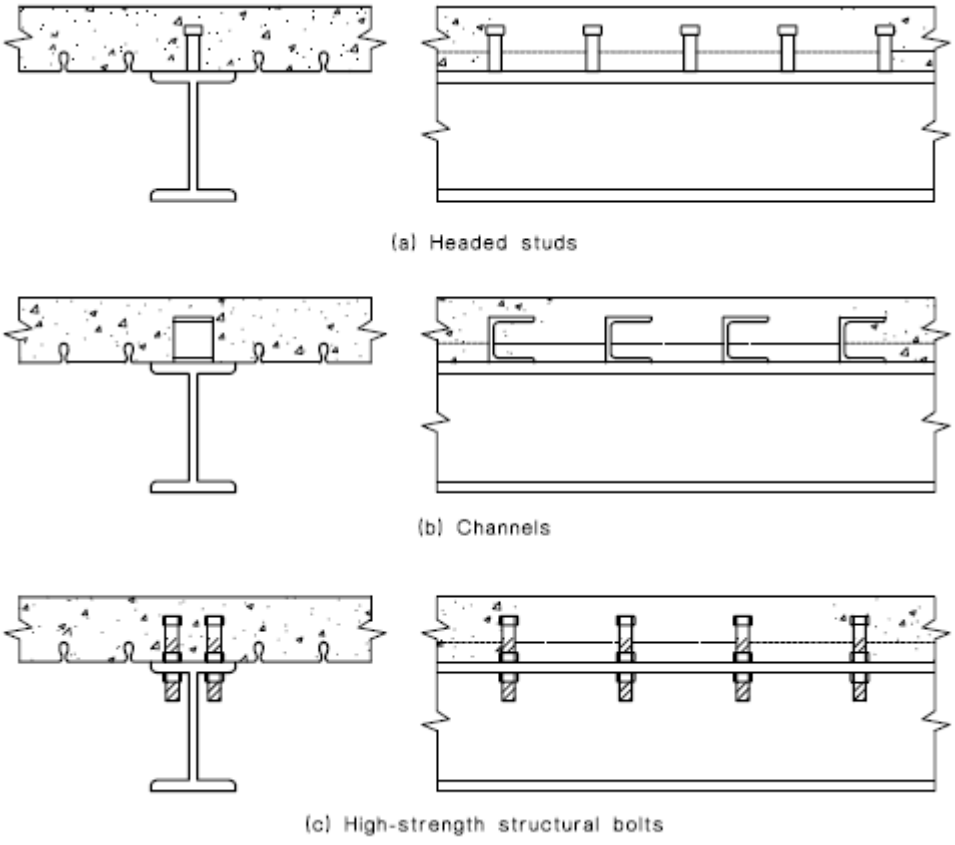

Figure 3.2 Shear connectors types

3.2.3 Concrete slab

It can be used two different types of reinforced concrete slabs as shown in **Figure 3.3**:

a) solid slab

b) composite slab using a profiled steel sheeting

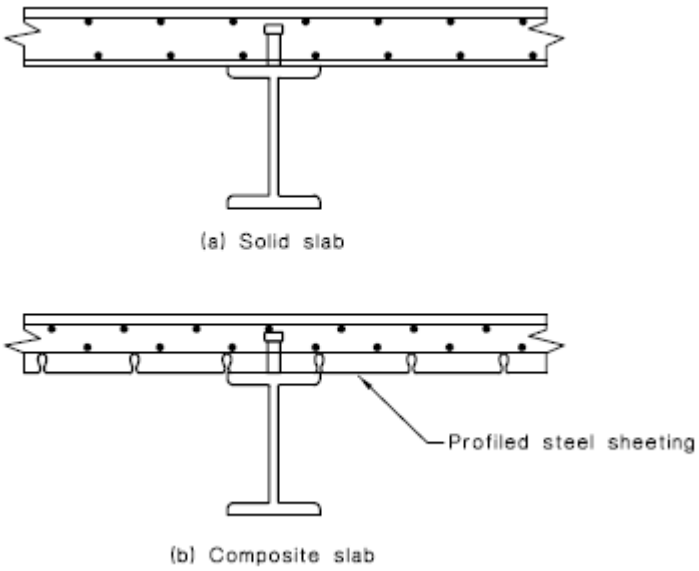

Figure 3.3 Types of slabs

3.2.4 Profiled sheeting

It is possible to choose every profiled sheeting in commerce but they need to satisfy some requirements as shown in **Figure 3.4**:

a) the overall height of a steel rib (h_r) shall be not greater than 80 mm, excluding any embossments

b) the width of the opening at the base of a steel rib shall be not greater than 20 mm

c) the area of the voids formed by the steel ribs in the concrete shall be not greater than 20% of the area of the concrete within the depth of the steel ribs

d) the width of the concrete between the mid-height of adjacent steel ribs (b_{cr}) shall be not less than 150 mm

e) the cover slab thickness shall be not less than 65 mm

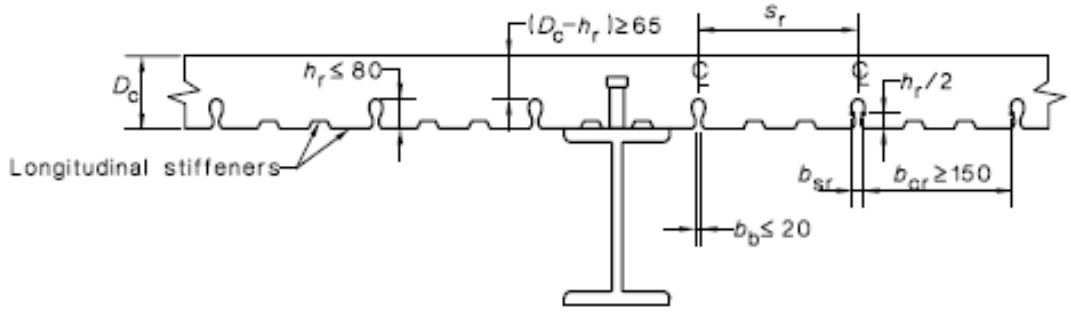

Figure 3.4 Limits of profiled sheetings

The meaning of this profile is to transmitting horizontal shear at the interface between sheet and concrete as shown in **Figure 3.5** that is ensured by:

a) mechanical interlock

b) frictional interlock

c) end anchorage

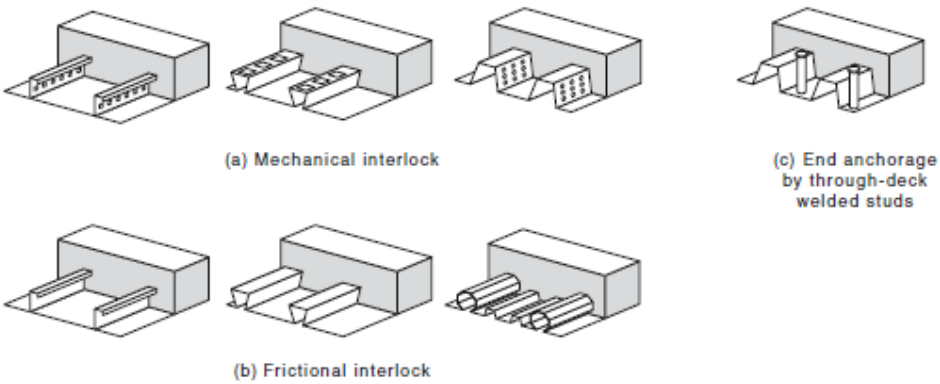

Figure 3.5 Interlock types in composite slabs

3.3 Design process

The design process starts with the definition of constructions faces that permit the birth of composite action in the structural system. For any construction stages are defined some load arising by the construction procedure.

3.3.1 Design stage

Before defining the design process, it is suitable to make some assumptions:

a) the beams are assumed to be simply supported during all the construction stage and during the service condition

b) the sheeting is unpropped throughout all the construction phases and there is a limitation on the deflection

c) the slab is one way continuous

d) deflection limits are: total deflection of the beam/slab ≤ L/250 and incremental deflection after installation of partition ≤ L/500

After this assumption is useful to choose a trial dimension of the element that we want to use and then verify if the pre-dimension is correct. The design stages are:

a) choose a trial steel beam and a concrete slab

b) determine the construction loads and the deflection limit for the profile sheeting steel

c) define detail for durability

d) design the composite beam by prototype testing or not

if we don't want to design it by prototype testing

e) calculate the design load

f) determine the effective section and calculate the design action effect

g) verify the strength of the beam cross-section and if it is not satisfying change the steel beam or the concrete slab

h) verify the serviceability limit and if it is not satisfying change the steel beam or the concrete slab

i) design and detail the shear connection

j) detail concrete slab for durability (if we design the composite beam with prototype testing we pass from point d to point j)

k) design for fire resistance

3.3.2 Construction stage

To permit to improve the correct behaviour there are some steps for the construction stages to follows for guarantee the birth of the composite action.

a) Stage 1: erection of steelwork and installation of falsework, then we make the placement of formwork and fix the profiled steel sheeting to steel beams (this is put in position with a certain curvature opposite to the deflection that will have the slab in order to have a plane slab)

b) Stage 2: attachment of shear connectors and fixture of reinforcement

c) Stage 3: commencement of casting slab until initial set of concrete and sample of concrete for laboratory test

d) Stage 4: Hardening of concrete until it reaches a compressive strength of 15 MPa

After Stage 4 begin the commencement of composite action.

e) Stage 5: Hardening of the concrete slab that reaches a design value of f'_c

After Stage 5 the composite action is fully developed.

f) Stage 6: Commencement of in-service condition

After this stage, the construction procedures are finishes and start the composite beam design stage.

3.4 Design load

After the definition of all the constructive phases, it is possible to consider the design due to the different types of load and the combinations for strength, serviceability and fire

limit state. In this part are defined all the combination of load at ultimate limit states, serviceability limit state and fire limit state.

When the ultimate limit state is analyzed we need to verify that the design capacity is not less than the design action for all critical cross section.

When we consider the serviceability limit state: deflection, vibration and control of the crack are checked.

The actions that operate on the structure are:

a) permanent and imposed, wind, snow, earthquake

b) construction load

c) any other specific loads

Other actions that it is necessary to consider in strength or serviceability are:

a) removal of construction props

b) foundation movement

c) temperature changes and gradient

d) dynamic action

e) shrinkage and creep of concrete

3.4.1 Load combinations at limit state

The load combination for strength at an ultimate limit state is:

$$W = 1.25\ G + 1.5\ Q \tag{3.1}$$

Where: wind, snow and earthquake are not relevant.

For the serviceability limit state, for short term effect:

$$W = G + \psi_s Q \tag{3.2}$$

For long term effect:

$$W = G + \psi_l Q \tag{3.3}$$

Where the value of ψ_l and ψ_s are scheduled in **Table 3.1**:

Table 3.1 Value of ψ_l and ψ_s in AS/NZS 1170.0:2002 R(2016)

SHORT-TERM, LONG-TERM AND COMBINATION FACTORS

Character of imposed action	Short-term factor (ψ_s)	Long-term factor (ψ_l)	Combination factor (ψ_c)	Earthquake combination factor (ψ_E)
Distributed imposed actions, *Q*				
Floors				
Residential and domestic	0.7	0.4	0.4	0.3
Offices	0.7	0.4	0.4	0.3
Parking	0.7	0.4	0.4	0.3
Retail	0.7	0.4	0.4	0.3
Storage	1.0	0.6	0.6	0.6
Other	1.0	0.6	0.6	0.6
Roofs				
Roofs used for floor type activities (see AS/NZS 1170.1)	0.7	0.4	0.4	0.3
All other roofs	0.7	0.0	0.0	0.0
Concentrated imposed actions (including balustrades), *Q*				
Floors	1.0	0.6	as for distributed floor actions	0.3
Floors of domestic housing	1.0	0.4		0.3
Roofs used for floor type activities	1.0	0.6		0.3
All other roofs	1.0	0.0	0.0	0.0
Balustrades	1.0	0.0	0.0	0.0
Long-term installed machinery, tare weight	1.0	1.0	1.2	1.0

3.5 Effective section and action effect

To understand the behaviour of the composite beam it is necessary to define the portion of slab and steel that carry the loads. Two analyses are performed:

a) the effective width of concrete in compression

   i) solid slab

ii) composite slab

b) the effective portion of steel beam

3.5.1 Effective width: solid slab

For the internal support or midspan the total effective width is defined by the current relation:

$$b_{eff} = b_0 + \sum b_{ei} \tag{3.4}$$

where:

a) b_0 is the distance between the centers of the outstand shear connectors

b) b_{ei} value of the effective width of concrete flange on each side of the web and taken as $\frac{L_{ef}}{8}$ but not greater than b_i

If it is analyzed an end support:

$$b_{eff} = b_0 + \sum \beta_i b_{ei} \tag{3.5}$$

where:

$\beta_i = \left(0.55 + 0.025\frac{L_{ef}}{b_{ei}}\right)$ is the distance between the centers of the outstand shear connectors

b_0 usually during the analysis is assumed to be zero

3.5.2 Effective width: composite slab

For composite slabs with ribs parallel or within 15° respect to the steel beam axis the effective width is calculated like the previous paragraph instead if the angle is bigger than 15° only the contribution of concrete above the ribs shall be considered based on the effective width calculated before and the first formula is used. **Figure 3.6** shows the evolution of b_{eff}.

If the slab is voided the code give another formulation of b_{eff}.

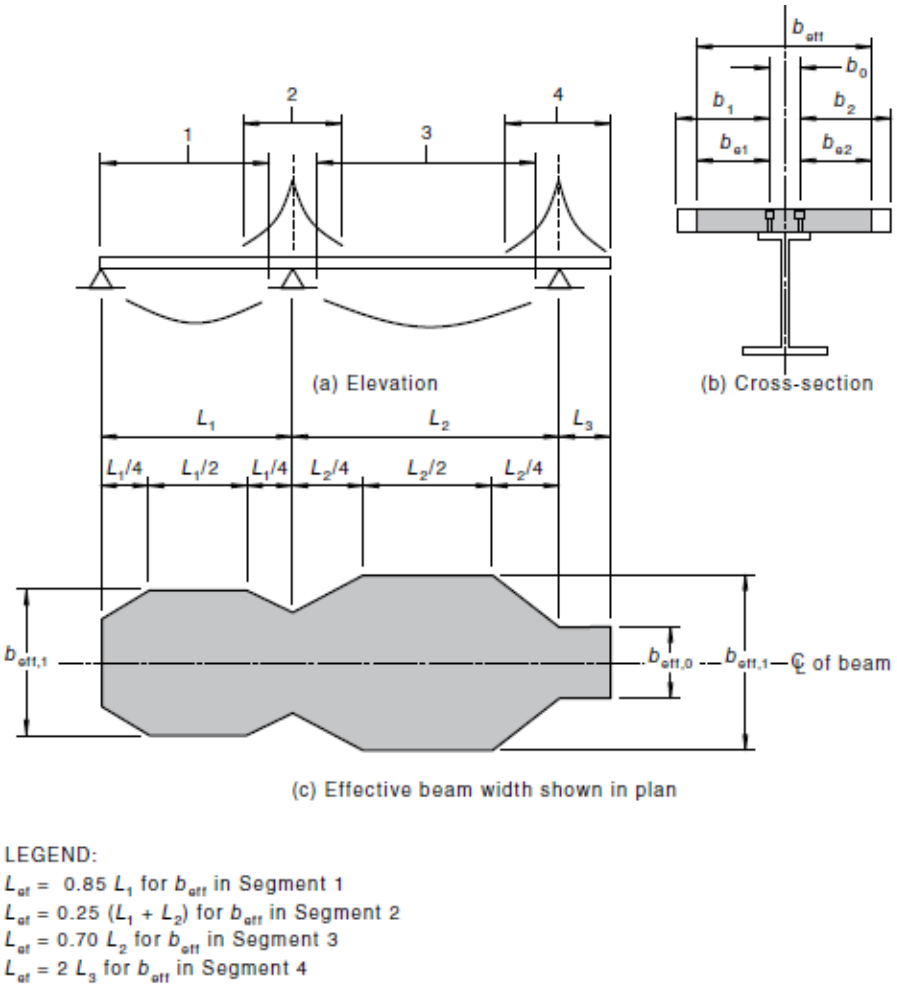

Figure 3.6 Effective spans for effective width of concrete

3.6 Effective portion of steel beam

In function of β that represent the degree of shear connection it is possible to define the effective section of composite beam cross section.

3.6.1 $\beta \leq 1$

This is the case when part of the top flange or the top flange and part of the web of the steel beam is in compression so the plate slenderness of the flange and the web are:

$$\lambda_{e,flange} = \frac{b}{t}\sqrt{\frac{f_y}{250}} \tag{3.6}$$

$$\lambda_{e,web} = \frac{d}{t}\sqrt{\frac{f_y}{250}} \tag{3.7}$$

with:

a) b is the clear width of the element

b) d is the height of the beam

c) t is the element thickness

d) f_y is the yield stress of plate element used in design

Then it is possible to calculate the depth of compressive stress zone in steel beam using rectangular stress block theory.

Then define the slenderness for the flange and the web and compare it with the plasticity limit of the element λ_{ep} permit to observe that:

a) $\lambda_{ep} > \lambda_e$ the plate element is compact

b) $\lambda_{ey} \geq \lambda_e > \lambda_{ep}$ the plate element is non-compact

c) $\lambda_e > \lambda_{ey}$ slender plate element

Where $\lambda_{ep}, \lambda_{ey}$ are given by table and is function of the residual stresses, part of the steel beam, longitudinal edge support and stress distribution.

Comparing $\lambda_{e,flange}$ and $\lambda_{e,web}$ with $\lambda_{ep}, \lambda_{ey}$ it is possible to define the effective width of steel beam top flange and the effective thickness of non-compact web of steel beam.

Ultimately if the top flange and web are compact, the entire steel section shall be assumed to be effective; or if the outstand of the flange is non-compact, the effective flange width shall be the maximum width for which the flange is compact. If the web is not compact, the effective portion of the web shall be determined in accordance with the **Figure 3.7** in which the length "x" is ineffective.

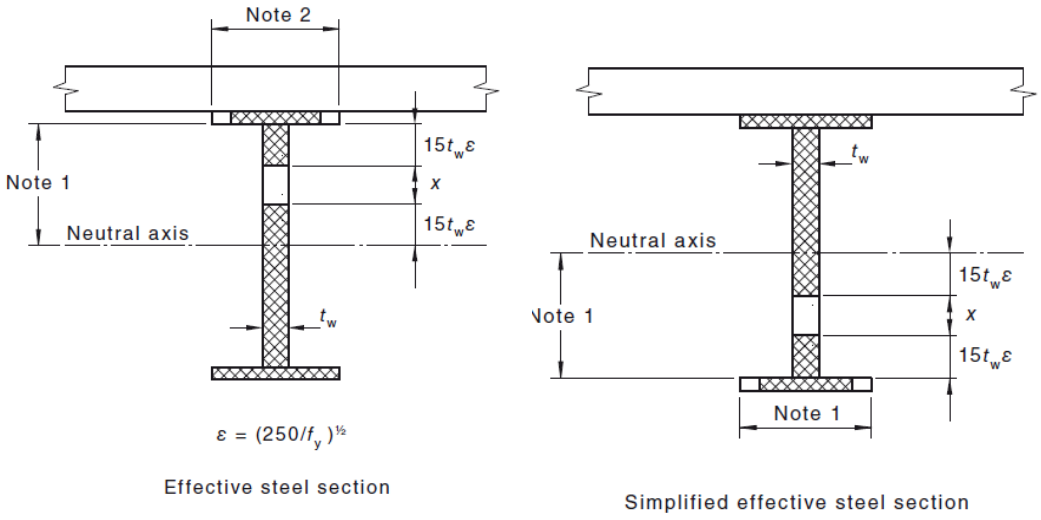

Figure 3.7 Effective portion of steel beams with non-compact section in sagging/hogging bending

If there are any compressive stress in the steel beam web we need to determine the new effective portion of the steel beam like the case defined before.

3.6.2 $\beta = 1$

It is possible to assume all the steel beam effective. Then it is possible to calculate the depth of compressive stress zone in steel beam using rectangular stress block theory. If there are any compressive stress in the steel beam web we need to determine the effective portion of the steel beam like done before, on the other hand the whole of the steel beam section at a cross section of a composite beam shall be assumed to be effective

3.6.3 β in unknown

It is conservatively able to ignore the composite action and calculate depth of compressive stress zone assuming only steel beam is present and determine the effective portion of steel like in the case of $\beta \leq 1$.

3.7 Design for strength

The first verify is the strength design. The first step is defining the potentially critical cross sections that are some particular parts of the beams defined in 3.7.1. Composite beams are designed for strength and they need to satisfy some limits at every potential cross section:

a) the design vertical shear capacity ϕV_u is to be not less than the design vertical shear force V^*

$$\phi V_u \geq V^* \tag{3.8}$$

b) the design moment capacity ϕM_{bv} is to be not less than the design bending moment M^* during construction and service condition

$$M_R \geq M^* \tag{3.9}$$

c) the effect of combined design moment and shear action shall remain within the design moment shear interaction diagram

$$\left(\frac{M}{M_{Rd}}\right)^3 + \left(\frac{V}{V_{comp}}\right)^6 = 1 \tag{3.10}$$

where:

M_{Rd} is the positive design moment resistance of the composite section

V_{comp} is the shear strength of the composite section

Another requirement is needed:

d) the flexural-torsional buckling requirements for hogging moment regions are satisfied

After defining the critical section, it is necessary to calculate the effective section of the potentially critical cross-section as shown in Chapter 3.5 -3.6 and then calculates the design action effects M^* and V^* and the design vertical shear capacity ϕV_u.

Defined the two shears the shear ratio at composite beam cross section is:

$$\gamma = \frac{V^*}{\phi V_u} \leq 1 \tag{3.11}$$

After the evaluation of the shear, the design of nominal moment capacity of a composite beam is performed in function of γ and β that need to be included in the range [0, 1]. The new moment is compared with the design action M^* to satisfy the following relation:

$$\phi M_{bv} \geq \ M^* \tag{3.12}$$

If this relation it is not satisfied we need to change the section choose when the design started.

Now to guarantee a connection from the steel beam and the concrete slab it is chief to outlines the minimum number of connectors between each potentially critical cross-section and ends of beam using:

$$n_i = \frac{F_{cp,i}}{P_{Rk}} \tag{3.13}$$

where:

$F_{cp,i}$ is the maximum compressive force in concrete in each section

P_{Rk} is the capacity of a single shear connector

At this point, it is possible to distribute the shear connectors along the beam and do the design of longitudinal shear reinforcement to complete the design of strength.

3.7.1 Potentially critical cross-sections

A critical cross section is a portion of the composite beams in which one of this critical event occurs:

a) section of maximum design bending moment

b) section of maximum design vertical shear force

c) a heavy concentrated load occurs with a positive moment region

d) a sudden change of cross section occurs

e) the member is tapered

f) the concrete flange is unusually large

3.7.2 Design of the moment capacity

In the computation of the moment capacity the following assumption shall be made in the design of full shear connection:

a) full interaction between structural steel, reinforcement and concrete

b) the effective area of the structural steel member is stressed to its design yield strength in tension or compression (f_y)

c) the effective areas of longitudinal reinforcement in tension and compression are stressed to its design yield strength in tension or compression (f_{sd})

d) the effective areas of concrete in compression resists a stress of 0.85 f'_c constant over the whole depth between the plastic neutral axis and the most compressed fiber of the concrete

The design axial force resisted by the steel section in full shear connection is:

$$F_{cc} = min(N_{y,d}, N_{c,d}) \tag{3.14}$$

where:

$N_{y,d} = f_{y,d}\, A$ is the design axial force by steel section at yield

$f_{y,d} = \phi\, f_y$ with ϕ capacity reduction factor listed by the code

$N_{c,d} = 0.85\, f_{cd}\, h_c\, b$

$f_{cd} = \phi_c\, f_c^{'}$ with ϕ_c capacity reduction factor listed by the code

$$M_R = M_p \tag{3.15}$$

Where the possible plastic stress distribution in sagging and hogging bending as shown in **Figure 3.9** and **Figure 3.8** are:

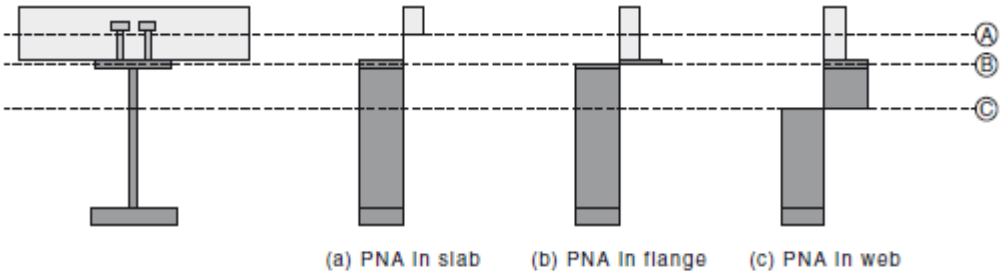

Figure 3.9 Plastic neutral axis in sagging bending for full shear connection

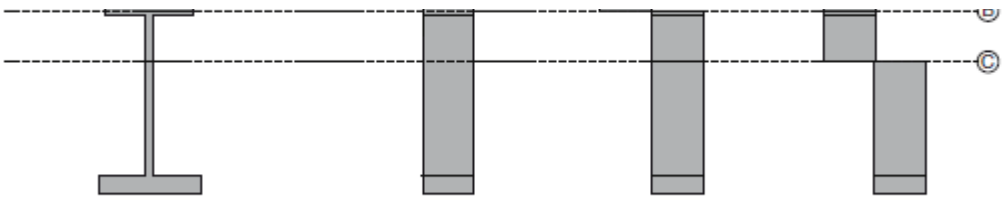

Figure 3.8 Plastic neutral axis in hogging bending for full shear connection

In the computation of the moment capacity made in the design of the partial shear connection M_R will be function of β that represent the degree of shear connection. The location of the plastic neutral axis shall be determined by F_{cp} that is a second plastic neutral axis which shall be used for the classification of the web as shown in **Figure 3.10**.

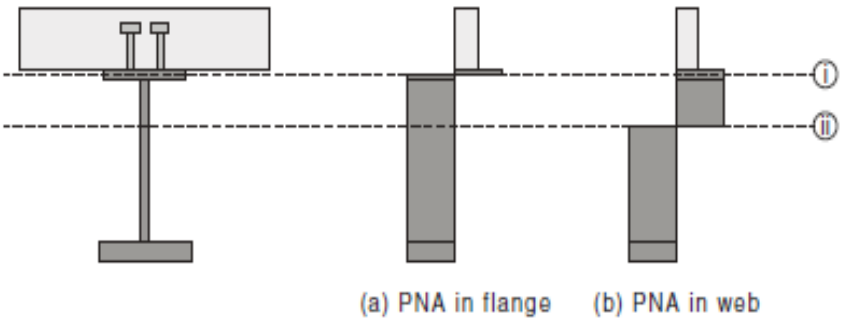

Figure 3.10 Plastic neutral axis in sagging bending for partial shear connection

The relation between M_R and β is given by a curve where M_R is determined by the line that join the two extreme points. For this reason, the value of M_R can be approximate as:

$$M_R = M_s + (M_p + M_s)\ \frac{F_{cp}}{F_{cc}} \tag{3.16}$$

If it is used high strength steel for the beam the bending capacity presents a reduction. The code gives also some requirement for define M_R if the material is in non-linear case due to the effect of shear connectors as shown in figure **Figure 3.11**.

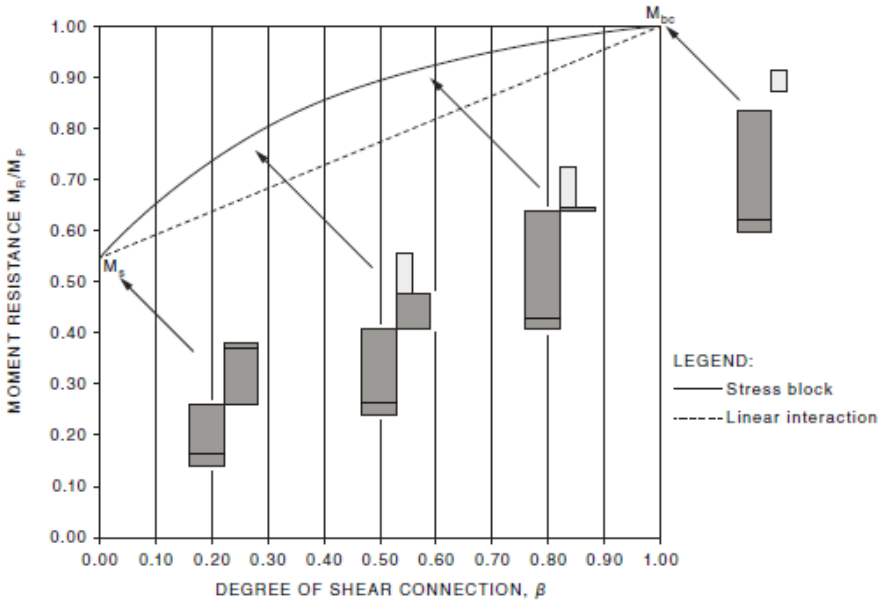

Figure 3.11 Relationship between design moment capacity and the degree of shear connection

To define the capacity moment it is possible to use two different approaches: analysis with continuous function (linear interaction) or a bilinear approximation. It can be possible to define two cases in which the value of γ can changes.

CASE 1: $\gamma \leq$ 0.5

The design moment capacity is independent of the shear ratio so it is constant as shown in figure **Figure 3.12**:

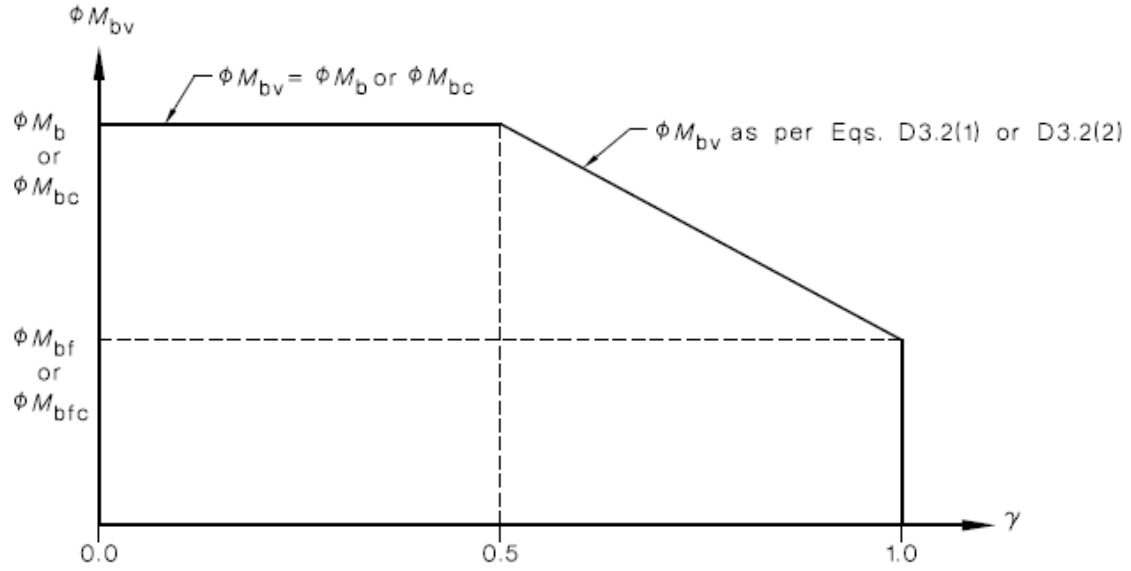

Figure 3.12 Relationship between design moment capacity and the shear ratio

If $\beta = 1$ it is the case of full shear connection and the moment M_{bc} is defined with the equilibrium of forces using stress block theory. If the neutral axis cuts the solid slab:

$$M_{bc} = F_{cc} \left(d_{sr} - \frac{d_c}{2}\right) \tag{3.17}$$

If the neutral axis cuts the part of concrete between two ribs:

$$M_{bc} = F_{c1} \left[d_{sr} - \frac{D_c - h_r}{2}\right] + F_{cc} - F_{c1} \left[d_{sr} - \frac{d_h}{2} - \frac{D_c - h_r}{2}\right] \tag{3.18}$$

If the neutral axis cuts the flange of the steel beam:

$$\begin{aligned} M_{bc} = F_{c1} \left[d_{sr} - \frac{D_c - h_r}{2}\right] + F_{sc} \left[d_{sr} - \frac{D_c + d_h}{2}\right] \\ + F_{c2} \left[d_{sr} - D_c + \frac{h_r}{2}\right] \end{aligned} \tag{3.19}$$

If the neutral axis cuts the web of the steel beam:

$$M_{bc} = F_{c1}\left[d_{sr} - \frac{D_c - h_r}{2}\right] + F_b\left[d_{sr} - \frac{D_c + d_h + t_{fl}}{2}\right] + F_{c2}\left[d_{sr} - D_c + \frac{h_r}{2}\right] + 2\ F_{scf}\left[d_{sr} - D_c + \frac{h_r}{2}\right] \tag{3.20}$$

where:

F_{st} is the tensile force in steel beam

F_{cc} is the compressive force in concrete

F_{c1} is the longitudinal compressive capacity of concrete cover slab within slab effective width

F_{c2} is the longitudinal compressive capacity of concrete between the steel ribs within slab effective width

F_{scf} is the compressive capacity of the top flange of steel beam

If $0 \leq \beta < 1$ it is the case of partial shear connection and the moment M_b is defined considering a double neutral axis.

CASE 2: $0.5 \leq \gamma \leq 1$

The design of moment capacity depends on the shear ratio, for defining ϕM_{bf} and ϕM_{bfc} is possible to use a continuous function of β with which it is possible to express the moment capacity ϕM_b like the previous

3.7.3 Design of vertical shear capacity

The shear strength of composite section is a function of the shear capacity of the steel beam alone $V_{pl,Rd}$ and the shear capacity of the concrete slab V_{slab}

$$V_{comp} = V_{pl,Rd} + V_{slab} \tag{3.21}$$

where:

$V_{pl,Rd} = \phi\, V_{uw}$ is the shear strength of steel beam alone

$V_{slab} = \phi_s\, f_{\lambda sd}\, (b_f\, D_{slab})^{0.7}\, \sqrt{f'_c}$

D_{slab} is the depth of slab

$f_{\lambda sd} = 110\, \lambda_{sd} + 13$

For the calculation of the strength of a partially connected composite beam:

$\lambda_{sd} = \frac{D_s}{D_{comp}}$

and for $\beta \leq 1$

$\alpha = \frac{1-\beta}{0.76\, \lambda_{sd}+0.92} + \beta$

$$V_{comp,\beta} = \alpha\, V_{comp} \tag{3.22}$$

3.7.4 Design of shear connectors

The function of the shear connection is to transmit the longitudinal shear force between the concrete and the steel beam ignoring the effect of the bond. They will be ductile and this property is defined with the slip capacity δ_{uk} that can be at least 6 mm.

Moreover, if different types of shear connectors are used on the same beam it needs to be considered for the different load slip that they produce.

Due to the effect of the force applied on the shear connectors longitudinal shear failure and splitting of the concrete slab is prevented. The number of shear connectors will be at least equal to:

$$n'_{ci} = \frac{F_{cc}}{P_{Rk}} \tag{3.23}$$

For full shear connectors. For partial shear connectors, the previous relationship is multiplied for a coefficient β_m that represent the degree of shear connection at the maximum moment cross-section of a composite beam:

$$n'_{ci} = \beta_m \frac{F_{cc}}{P_{Rk}} = \frac{F_{cp}}{P_{Rk}} \tag{3.24}$$

For stud connectors shall be the number of shear connectors is defined in a different way. If it is considered a solid slab the value of shear capacity is:

$$P_{Rk} = min\ \left(\alpha_{shear}\ f_{cu}\ d_{bs}^2\ , 0.29\ d_{bs}^2\ \sqrt{E_c\ f'_{cj}}\ \right) \tag{3.25}$$

where:

d_{bs} is the nominal shank diameter of a shear stud and 15.9 mm $\leq d_{bs} \leq$ 25 mm

f_{cu} is the strength of the shear connector

f'_{cj} is the characteristic strength of concrete

α_{shear} assume a value of 0.7 for headed stud connectors welded and 0.5 for hish strength structural bolts

If it is considered a composite slab the value of shear capacity with ribs parallel to the supporting beam (**Figure 3.13**) is the same as the previous but multiplied for a reduction factor k_l:

$$k_l = 0.6 \ \frac{b_0}{h_p} \ \left(\frac{h_{sc}}{h_p} - 1\right) \leq \ 1 \tag{3.26}$$

where:

h_{sc} is the overall height of the stud after welding, and it cannot be greater than $h_p + 75 \ mm$

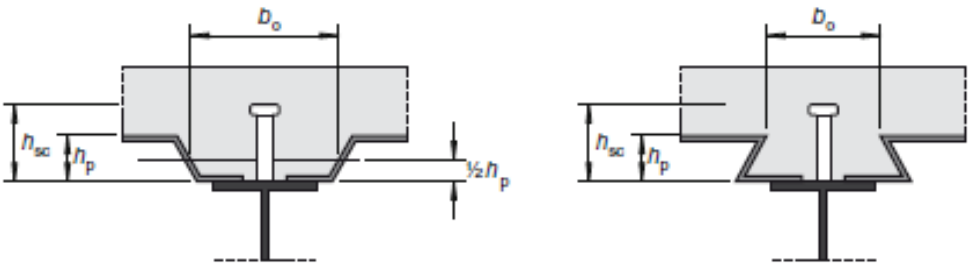

Figure 3.13 Beam with profiled steel sheeting parallel to the beam

If the ribs are in transverse position respect to the supporting beams:

$$k_l = \frac{0.7}{\sqrt{n_r}} \ \frac{b_0}{h_p} \ \left(\frac{h_{sc}}{h_p} - 1\right) \leq \ k_{t,max} \tag{3.27}$$

where:

n_r is the number of stud connectors in one rib at a beam intersection that it is not bigger than two

$k_{t,max}$ is the upper limit of reduction factor given by table and function of the number?

It is useful to notice that if the shear connectors in near the edge of the slab transverse reinforcement is provided to prevent longitudinal splitting of the concrete flange and if the distance from the edge of the concrete flange to the centerline of the nearest row of the shear connectors is less than 300 mm it is necessary to put U-bars passing around the shear connectors.

The total number of shear connectors shall be distributed along the length of the beam, in continuous beam they will be placed more closely in hogging moment zone to suit the curtailment of tension reinforcement and in cantilevers the spaced shall be based on the curtailment of tension reinforcement.

The number of shear connectors considered to contribute to the design moment capacity of potentially critical cross section and shall be equal or less of the number of connectors provided on each side of the cross-section.

3.7.5 Design of longitudinal shear reinforcement

The design shear stress acting on the interface of concrete slab and steel beam for full shear connection is:

$$\nu_L^* = \frac{F_{cc}}{s} \tag{3.28}$$

For ductile shear connection is:

$$\nu_L^* = \frac{F_{cp}}{s} \tag{3.29}$$

For non-linear resistance is:

$$\nu_L^* = \frac{A_t \; y_c \; V^*}{I_t} \tag{3.30}$$

where:

V^* is the design shear force at the cross section

A_t is the area of the section to one side of the shear plane under consideration

y_c is the distance from the neutral axis of the composite section to the centroid of area A_t

I_t is the second moment of area of the transformed composite cross-section

Distributing this area along the affected shear plane defined in figure permit to define the design longitudinal shear force per unit length ν_{Lp}^* as shown in **Figure 3.14** and **Figure 3.15**.

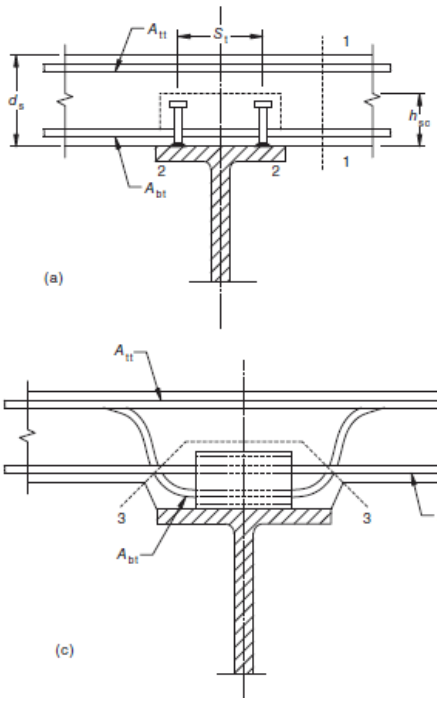

Shear plane type	A_{ts}
1-1	$(A_{tt} + A_{bt})$ or $(A_{tt} + A_{bs})$
2-2	$2A_{bt}$
3-3	$2(A_{bt} + A_{bs})$
4-4	$2A_{bt}$

Figure 3.15 Transverse reinforcement

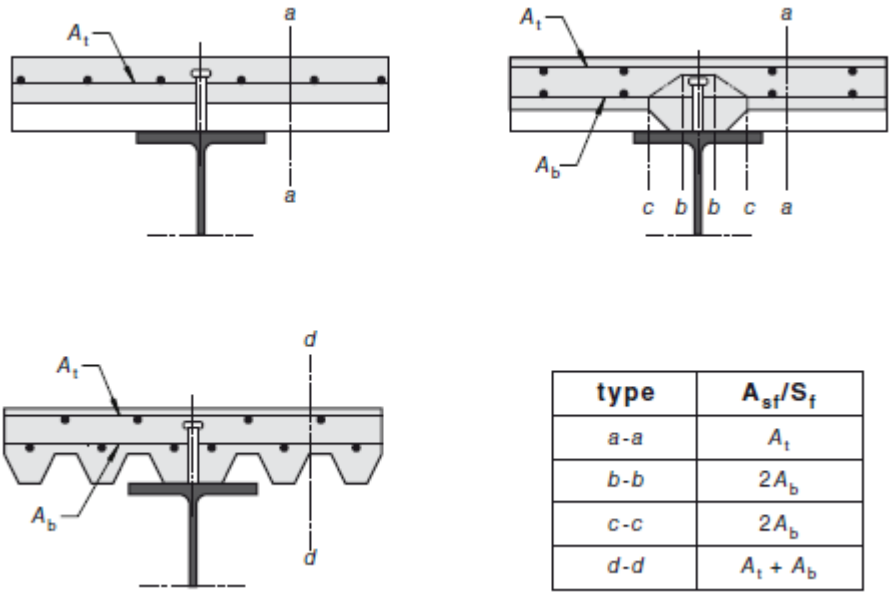

type	A_{sf}/S_f
a-a	A_t
b-b	$2A_b$
c-c	$2A_b$
d-d	$A_t + A_b$

Figure 3.14 Potential; surface of shear failure with profiled steel sheeting

This stress will be compared with the longitudinal shear strength on the surface considered:

$$\nu_{Lp}^{*} \leq \phi \ \tau_u \tag{3.31}$$

$$\tau_u = (\mu \ A_{rs} \ f_{sy} \ + \ k_{co} \ f'_{ct} \ A_{tc}) + \frac{P_{pb,Rd}}{s} \tag{3.32}$$

This will be lesser than:

$$\begin{cases} 0.2 \ f'_{ct} \ A_{tc} \\ 10 \ A_{cv} \end{cases} \tag{3.33}$$

where:

μ is the coefficient of friction

k_{co} is the cohesive coefficient given by the table

A_{ts} is the cross-sectional area of transverse reinforcement per unit length of beam

A_{tc} is the cross-sectional area per unith length of beam of the concrete shear surface

$P_{pb,Rd}$ is the design bearing resistence of a headed stud welded through the profiled steel sheet.

Table 3.2 Shear plane surface coefficients

SHEAR PLANE SURFACE COEFFICIENTS

Surface condition of the shear plane	Coefficients	
	μ	k_{co}
A smooth surface, as obtained by casting against a form, or finished to a similar standard	0.6	0.1
A surface trowelled or tamped, so that the fines have been brought to the top, but where some small ridges, indentations or undulations have been left; slip-formed and vibro-beam screeded; or produced by some form of extrusion technique	0.6	0.2
A surface deliberately roughened— (a) by texturing the concrete to give a pronounced profile; (b) by compacting but leaving a rough surface with coarse aggregate protruding but firmly fixed in the matrix; (c) by spraying when wet, to expose the coarse aggregate without disturbing it	0.7	0.4
Monolithic construction or mechanical shear keys.	0.9	0.5

NOTE: Where a beam is subjected to high levels of differential shrinkage, temperature effects, tensile stress or fatigue effects across the shear plane, the values of μ and k_{co} in the above table do not apply.

If more reinforcement is required to increase the longitudinal shear strength the maximum centre-to-centre spacing shall not exceed the maximum:

$$s_{max} = 3.5\ t_f \tag{3.34}$$

where:

t_f is the thickness of flange anchored by the shear reinforcement 30 $mm \leq t_f$

3.8 Design for serviceability

In this design stage the focus is on the deflection of the composite beam that shall be calculated in accordance with AS 4100 and there are two methods:

a) refined calculation

b) simplified calculation applied only in case of steel section of the beam classified as compact or non-compact

3.8.1 Refined calculation

The step to follow are described below:

a) cracking and tension stiffening of the concrete

b) shrinkage and creep properties

c) shear lag effect

d) slip between slab and steel

e) load history

f) construction procedure and changes in cross section

g) deflection of formwork

h) inelastic behaviour of the steel and reinforcement

i) torsional and distortional warping

j) yielding in steel beam

k) residual stresses in steel beam

l) temperature changes

m) end restraints

n) precambered of the steel beam

o) flexibility of the joints

3.8.2 Simplified calculation

For using this method, the maximum stress in the steel beam must be less than 0.9 f_{yb}. The step to follow are described below:

a) determine which of the deflection components defined are relevant to the design, and calculate the corresponding serviceability design loads

b) identify the different cross-sections along the steel beam during Construction Stages 1 to 3, and along the composite beam during Construction Stages 5 and 6 and the in-service condition. Calculate their elastic section properties, which in the case of the composite beam shall initially be performed assuming full interaction

c) calculate the maximum stress that occurs in the steel beam during Construction Stages 1 to 6 and the in-service condition

d) identify the maximum moment cross-section of the composite beam during the in-service condition and calculate the degree of shear connection at this cross-section

e) calculate the effective second moment of areas I_{eti} (for short-term) I_{etl} (for long-term) of the different composite beam cross-sections identified in Step (b) accounting for the degree of shear connection β m calculated at Step (d)

f) calculate the magnitude of the relevant deflection components assuming linear-elastic behaviour, accounting for changes in cross-section along the length of the beam and the magnitude and distribution of applied loads

g) calculate the corresponding values of the total and incremental deflections according to the following equations as appropriate:

    i) Total deflection measured from slab top face:

$$\delta_{tot} = \delta_{C5,6} + \delta_{Ii} + \delta_{Il} + \delta_{Ish} \tag{3.35}$$

ii) Total deflection measured from steel beam soffit:

$$\delta_{tot} = \delta_{Cl3} + \delta_{C5,6} + \delta_{Il} + \delta_{Ish} - precamber \tag{3.36}$$

iii) Incremental deflection calculated assuming formwork/falsework or props removed before installation of brittle finishes

$$\delta_{incr} = \delta_{Il} + \delta_{Ii} + 0.6\ \delta_{Ish} \tag{3.37}$$

h) check that the limits chosen for the total and incremental deflections are not exceeded

where:

δ_{Cl3} is the immediate deflection of steel beam during Construction Stages 1 to 3 and represent the deflections arising from the weight of the steel beam, formwork, concrete and reinforcement

$\delta_{C5,6}$ is the immediate deflection of composite beam during Construction Stages 5 and 6 and represent the deflections arising from removal of formwork/falsework supporting dead loads and from the addition of any superimposed dead loads

δ_{Ii} is the immediate deflection of composite beam during in-service condition and represent the deflection arising from the short-term component of the live load

δ_{Il} is the long-term creep deflection of composite beam during in-service condition due to Creep deflections arising from the dead loads and the long-term component of the live load and for propped construction

δ_{Ish} is the long-term shrinkage deflection of the composite beam during the in-service condition

3.8.3 Short-term deflection, creep deflection and shrinkage deflection

The short-term deflection is analyzed diving the beam in cracked and uncracked zone as shown in **Figure 3.16**:

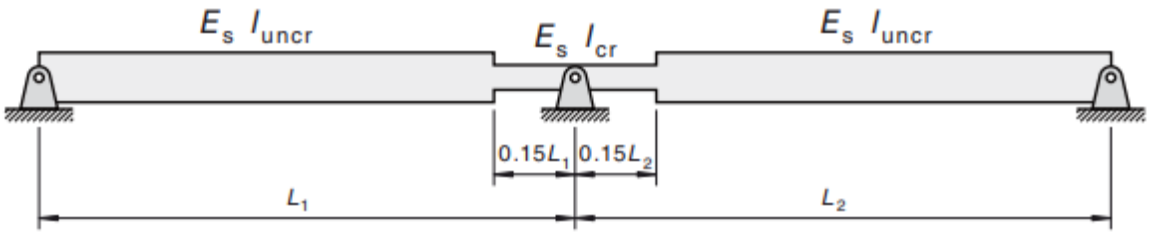

Figure 3.16 Inclusion of cracking regions in simplified approach

The envelope of the internal action should be defined using E_s and I_{uncr} and in region where the extreme tensile fiber exceeds the value of 1.4 $f'_{ct,f}$, the stiffness should be reduced by E_s and I_{cr}. If we consider a continuous composite beam in which the ratios of the length of adjacent spans the cracked zone is the 15% of each span and elsewhere is defined the uncracked zone. On the internal support the bending moment defined by the uncracked analysis is multiplied by f_1 which has a reduction function. This reduction function is shown in **Figure 3.17**:

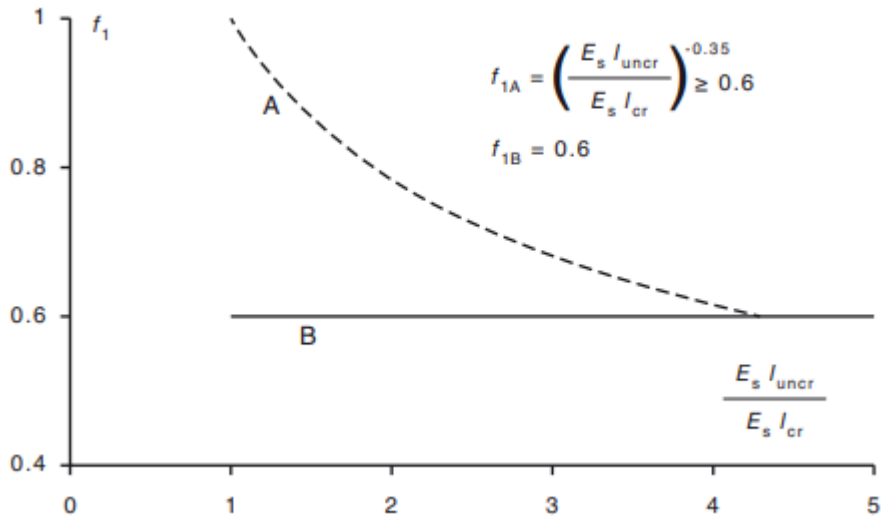

Figure 3.17 Reduction factor for bending moment at support

We can notice that curve A is used for internal span when the uniformed distributed load is equal in all the spans and the length of all the spans do not differ by more than 25% otherwise curve B is used.

The deflection component due to creep shall be determined with the effective modulus method using the corresponding modulus of elasticity:

$$E_{ef,cc} = \frac{E_c}{1 + \phi_{cc}} \tag{3.38}$$

where:

E_c is the elastic modulus at 28 days

ϕ_{cc} is the creep coefficient

The deflection component due to shrinkage shall be determined by the corresponding modulus of elasticity:

$$E_{ef,cs} = \frac{E_c}{1 + 0.55\ \phi_{cc}} \tag{3.39}$$

The strain caused by shrinkage is defined by:

$$\varepsilon_{cs,ef} = \varepsilon_{cs,top} - \ \kappa_{cs} \frac{h_c}{2} \tag{3.40}$$

$$\kappa_{cs} = \frac{\varepsilon_{cs,top} - \varepsilon_{cs,btm}}{h_c} \tag{3.41}$$

where:

$\varepsilon_{cs,top}$ is the shrinkage in the top part of the slab

$\varepsilon_{cs,btm}$ is the shrinkage in the bottom part of the slab

κ_{cs} is the curvature of the shrinkage profile

The moment generated by the shrinkage effect is:

$$M_{cs} = N_{cs}\ l_{cs} \tag{3.42}$$

where:

$N_{cs} = h_c\ b\ E_{ef,cs}\ \varepsilon_{cs,ef}$

l_{cs} is the distance between the line of action of N_{cs}

After, we calculate the deflection component of total and incremental deflection which should be compared with the code values in **Table 3.3** and **Table 3.4**:

Table 3.4 Suggested limits for deflection

Type of member	Deflection to be considered	Deflection limitation (δL_{el}) for spans[Notes 1-6]	Deflection limitation (δL_{el}) for cantilevers[Notes 1-6]
All members	The total deflection	1/250	1/125
Members supporting masonry partitions	The deflection that occurs after the addition or attachment of the partitions	1/500 where provision is made to minimize the effect of movement, otherwise 1/1000	1/250 where provision is made to minimize the effect of movement, otherwise 1/500
Members supporting other brittle finishes	The deflection that occurs after the addition or attachment of the finish	1/500	1/250
Members subjected to vehicular or pedestrian traffic	The imposed action (live load and dynamic impact) deflection	1/800	1/400
Transfer members (see Note 7)	Total deflection	1/500 where provision is made to minimize the effect of deflection of the transfer member on the supported structure, otherwise 1/1000	1/250

Table 3.3 Limits for deflection of profiled sheeting

LIMITS FOR CALCULATED VERTICAL DEFLECTIONS OF PROFILED SHEETING USED IN STEEL FRAMED CONSTRUCTION

Soffit requirements	Deflection limitation for spans
when the soffit requires a good visual quality finish	the lesser of $L_e/240$ and 20 mm when the effects of ponding are taken into account
when there is no requirement for the visual quality finish	the lesser of $L_e/180$ and 20 mm when the effects of ponding are not taken into account
when there is no requirement for the visual quality finish	the lesser of $L_e/130$ and 30 mm when the effects of ponding are taken into account

Chapter 4 Parametric analysis

4.1 Introduction

In this chapter is implemented a parametric analysis based on different types of longitudinal spans of composite beams and on different types of steel sheeting and size of the steel beams. The aim is to understand which types of sections satisfy the design limits under selected conditions.

In this chapter two types of analysis are performed:

a) parametric analysis in which different types of sections are considered for several lengths of spans under service limit state for AS/NZS 2327:2003 and AS/NZS 2327:2017. For this type of analysis three sets of beams are considered:

   i) Set1 represent big steel sections analyzed with the code of 2017

   ii) Set2 represent small steel sections analyzed with the code of 2017

   iii) Set0 represent small steel sections analyzed with the code of 2003

b) performance analysis in which deflections, stresses and design capacities actions are calculated

4.2 Parametric analysis

The parametric analysis is performed to speed up the design process and choose the section of steel beam in function of the problem.

This analysis is performed considering a beam with a span from 6 meters to 20 meters increasing every meter, so fifteen different spans are evaluated with likewise sections. The other parameter analyzed are the steel sections: different types of steel sections with different shapes are compared to evaluate what is the limit usage of the elements.

This study permits to investigate the behaviour of the different size of steel sections using AS/NZS 2327:2003 and AS/NZS 2327:2017. It is possible to notice that with the old version of the code small section can be used. Otherwise, in the new code, the behaviour of bigger sections and the same small sections, used previously, is observed to understand if something is changed and which parameters influenced more the serviceability limit state for a composite beam.

This parametric analysis is useful to comprehend which are the parameters that govern the service behaviour. In function of these elements more refined analysis are performed to understand the difference between the two codes in which the deflection due to the effect of shrinkage play a significant role.

Therefore, a more refined analysis of the shrinkage effect developed in the new code change the behaviour of the small steel sections beams used before and define a more restricted limit of usage. In fact, as is possible to read in this paragraph, small steel

sections should not be used in the service stage of AS/NZS 2327:2017 due to the huge effect of displacement which do not permit to stay in the imposed limit.

To make this comparison are taken into consideration:

a) the ratio between the design bending moment for a cross-section and the design moment capacity

$$\frac{M^*}{\phi M_{bv}} \tag{4.1}$$

b) the ratio between the design vertical shear force for a cross-section and the design shear capacity

$$\frac{V^*}{\phi V_u} \tag{4.2}$$

c) the ratio between the total deflection and the limit deflection imposed by the code ($\frac{L}{250}$):

$$\frac{\delta_{tot}}{\frac{L}{250}} \tag{4.3}$$

d) the ratio between the incremental deflection and the limit deflection imposed by the code ($\frac{L}{500}$):

$$\frac{\delta_{incr}}{\frac{L}{500}} \tag{4.4}$$

To understand better the behaviour, another comparison is made between the old version of the code AS 2327.1:2003 and the new version AS/NZS 2327:2017 which present difference in: creep coefficients (used during the design of service), in the computation of I_{ef} and in the consideration of curvature.

In fact, in the new code a different relation between I_{ef} and the different modular ratio α is only function of the ratio between E_s and E_c, while in the new code it is function of the effective modulus of elasticity for creep and shrinkage deflection as show in **Table 4.1**:

Table 4.1 Difference between the two code in service limit state

AS/NZS 2327.1 2003	AS/NZS 2327 2017
$I_{et,i} = I_{t,i} + 0.6\,(I_s - I_{t,i})(1 - \beta_m)$	$I_{ef} = I_{cr} + (I_{uncr} - I_{cr})\left(\frac{M_{cr}}{M_s}\right)^3$
$\frac{E_s}{E_c}$	$\frac{E_s}{E_{ef,cc}}$ $\frac{E_s}{E_{ef,cs}}$

Where:

$$E_{ef,cc} = \frac{E_c}{1 + \phi_{cc}} \tag{4.5}$$

$$E_{ef,cc} = \frac{E_c}{1 + 0.55\,\phi_{cc}} \tag{4.6}$$

In this analysis are also fixed some parameters like:

a) $D_c = 150\ mm$ the overall depth of concrete slab in compression flange including the steel sheeting

b) $Q = 3\ kPa$ the minimum value of variable loads in service condition

c) $f'_c = 32\ MPa$ the characteristic compressive cylinder strength of concrete

d) precamber equal to zero

e) $\beta = 0.5$ the degree of shear connection at cross section

All the elements in **Figure 4.1** are dimensionless and this trick permit to define which are the parameters that govern the problem in the service condition.

In **Table 4.2** are represented all the steel sections used for the different level of spans; in the first column are shown the small sections analyzed with the code of 2003 and in the second column bigger section are evaluated using the code of 2017.

Figure 4.1 shows which types of section verify the serviceability limit for the two codes analyzed. This graph compares composite beams with different types of sections, smaller sections are used for the oldest code and biggest section for the new code as shown in the table; moreover, the last section is the same for the final value of the span:

Table 4.2 Steel sections used for Figure 4.1

Span [m]	Steel sections	
6	360 UB 44	610 UB 101
7	410 UB 53	610 UB 113
8	460 UB 67	700 WB 115
9	460 UB 74	700 WB 115
10	530 UB 82	800 WB 122
11	610 UB 101	800 WB 146
12	610 UB 113	800 WB 146
13	700 WB 115	800 WB 168
14	800 WB 122	900 WB 175
15	800 WB 146	1000 WB 215
16	800 WB 146	1000 WB 215
17	800 WB 168	1000 WB 215

18	900 WB 175	1200 WB 249
19	1000 WB 215	1200 WB 249
20	1200 WB 249	1200 WB 249
	AS2327.1-2003	AS2327-2017

When we use the new code, we consider big sections to verify the limit imposed by the code in respect to the oldest.

The black line represents the sections analyzed with the code of 2003 while the red represents the new code. It is noticed that the total and incremental deflection governs the problem. In fact, they are close to the parameter one; moreover, the new code is more strict respect to the oldest, in which only the total deflection has a relevant role. This behaviour is caused by the effect of shrinkage which is underestimated in the computation of deflections. The values of moment and shear do not govern the design in service condition, but are more conservative in the oldest code.

A relevant aspect to take into account is that for every spans, the sections compared present different geometry properties and different weight so the comparison shows that for a smaller section, the ratio of moment is bigger because of the gap between: the design bending moment for a cross-section and the design moment capacity. This gap is little due to the high value of the design action used for big steel section, however the moment is not the most relevant parameter during the design project and the same reasoning are applicable to the shear.

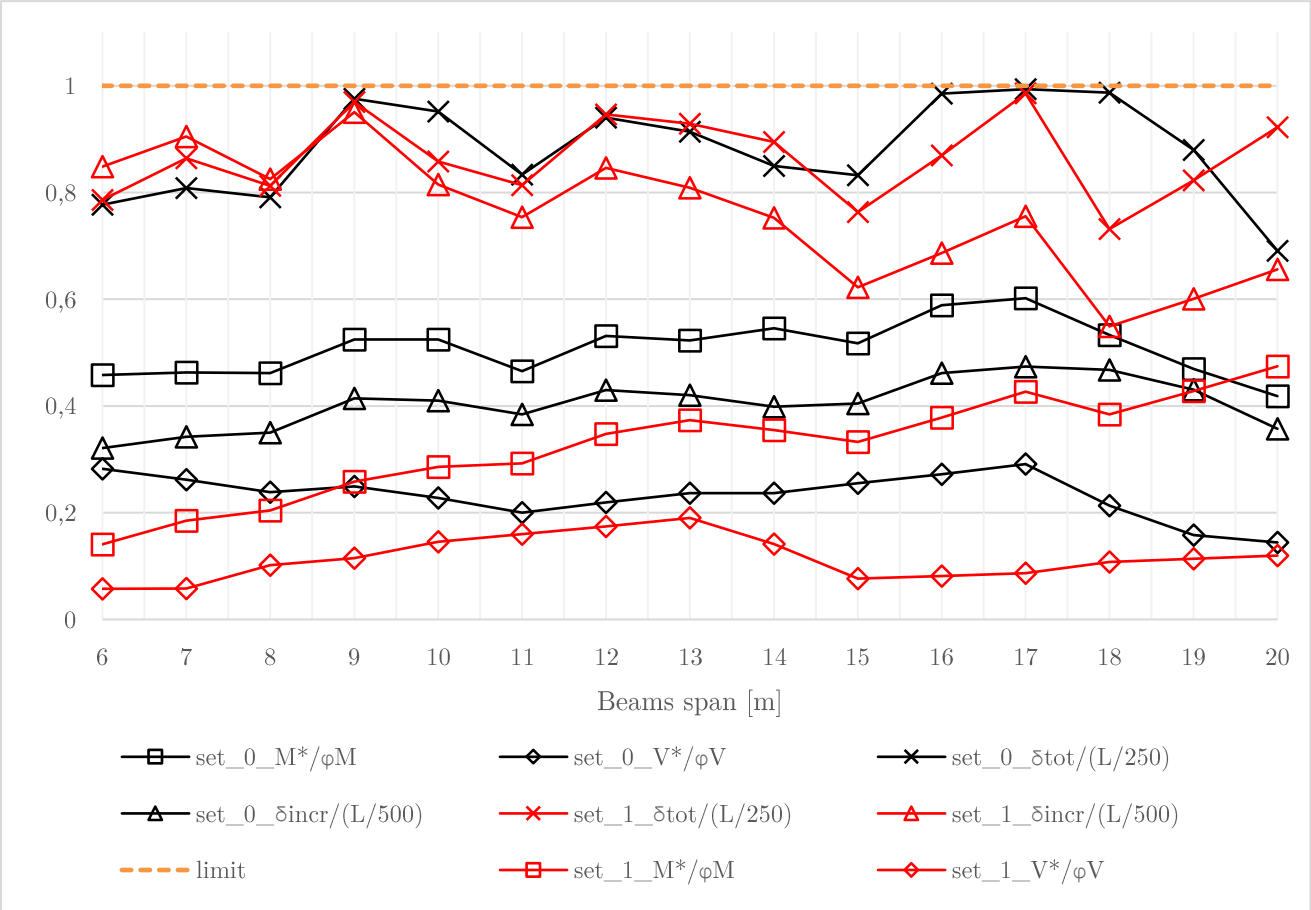

Figure 4.1 Percentage of influence in service condition using AS/NSZ 2327:2003 and 2017

Another analysis is performed when the same profiled steel sections are subjected to AS 2327.1:2003 and AS 2327:2017. The sections are defined in **Table 4.3**:

Table 4.3 Small sections analyzed with AS/NZS 2017

Span [m]	Steel Sections
6	360 UB 44
7	410 UB 53
8	460 UB 67
9	460 UB 74
10	530 UB 82
11	610 UB 101
12	610 UB 113
13	700 WB 115
14	800 WB 122
15	800 WB 146
16	800 WB 146
17	800 WB 168
18	900 WB 175
19	1000 WB 215
20	1200 WB 249

Steel beams smaller than the acceptable cannot be used in the code of 2017 because the design is controlled by the serviceability limit state, like it is possible to demonstrate in **Figure 4.2**. This graph, in fact, shows how the total and incremental deflections which arise in the composite beams are in the limit with the oldest code and cannot be used in the new. For this reason, in the previous figure, we increase the geometry of the sections for the analysis performed by the new code. This displacement problems are related to the effects of long term and shrinkage which are bigger in the new formulation. Only the last sections which are the same to the previous section is verified.

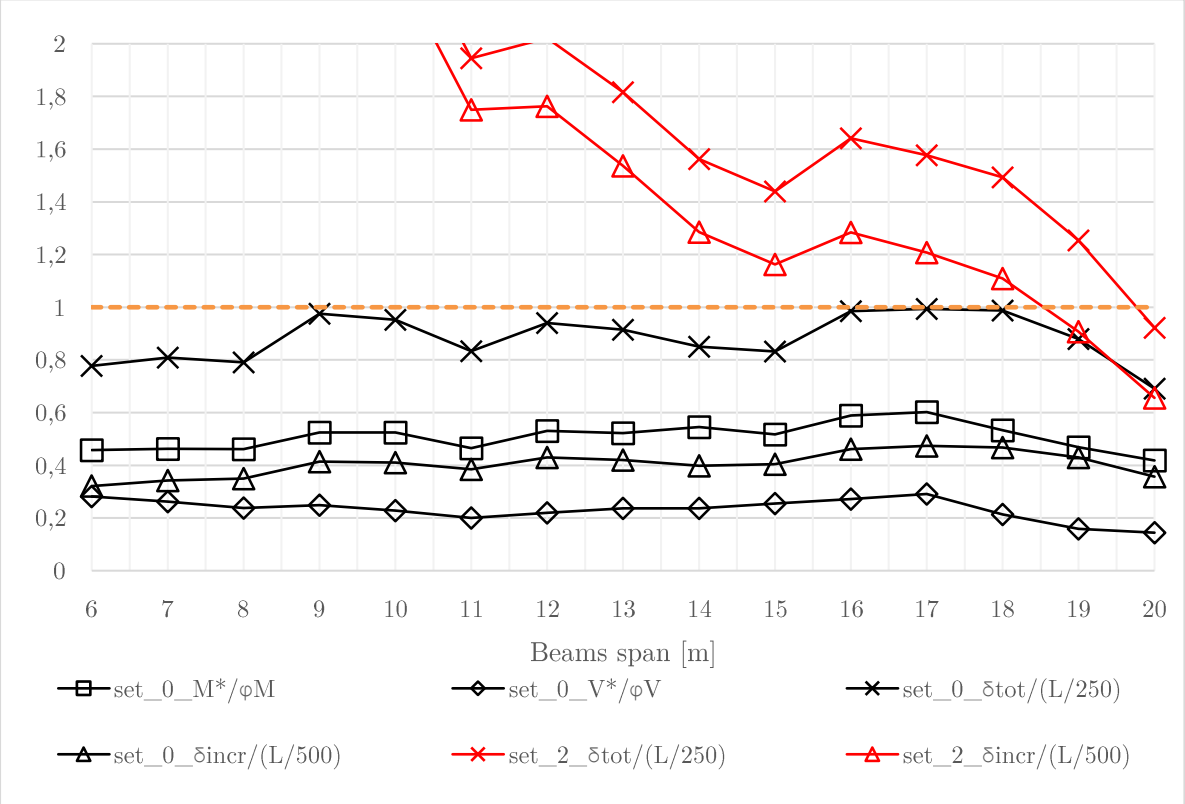

Figure 4.2 Percentage of influence in service condition using AS/NSZ 2327:2017

The new study on the creep and shrinkage effects change much the code and it is possible to appreciate the effect in the **Figure 4.3** and **Figure 4.4**:

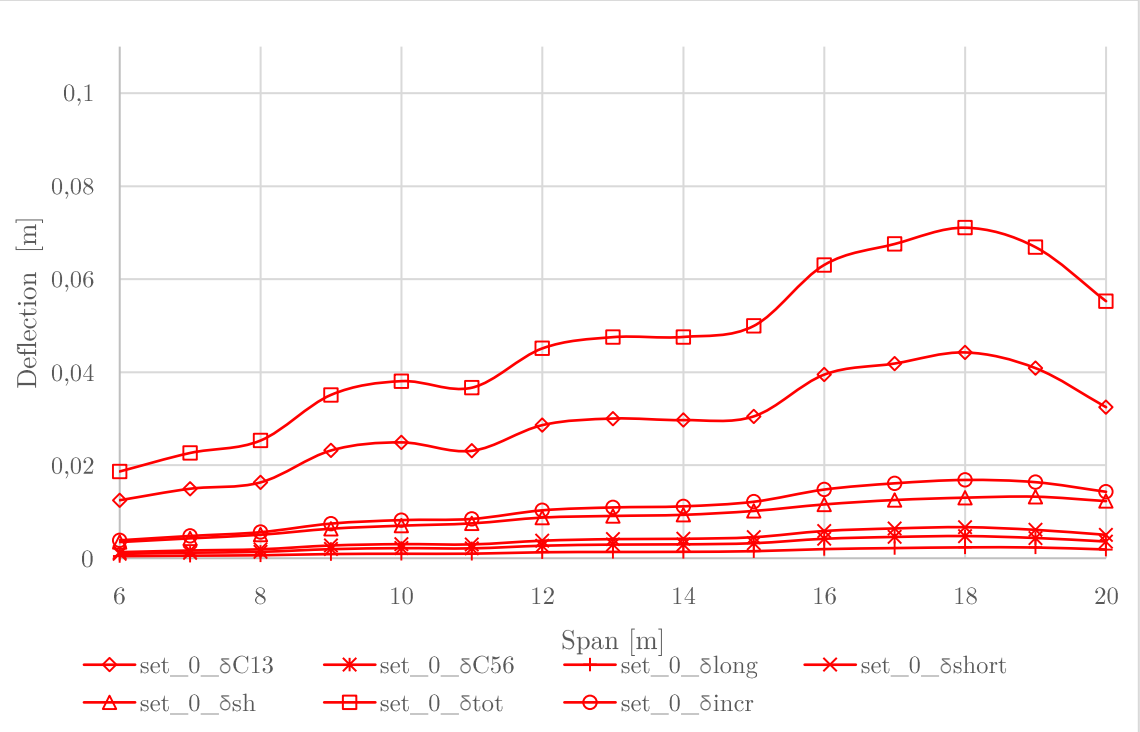

Figure 4.4 Deflections component of little sections using AS/NZS 2327:2003

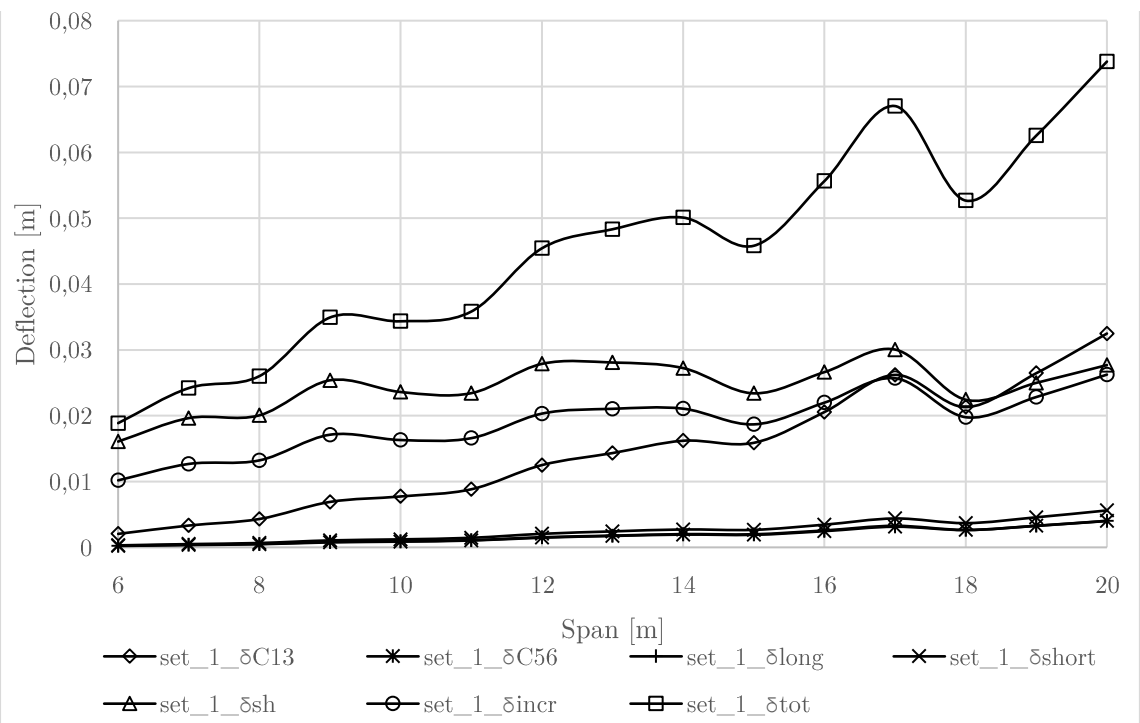

Figure 4.3 Deflections component of big sections using AS/NZS 2327:2017

The behaviour of the total deflection is quite the same, with the different sections, but different aspects are related to the displacement of long term due to shrinkage and the incremental displacement that is bigger in the new code.

The same sections with different code show that the computing of moment and shear is the same in contrast with deflection (**Figure 4.5**).

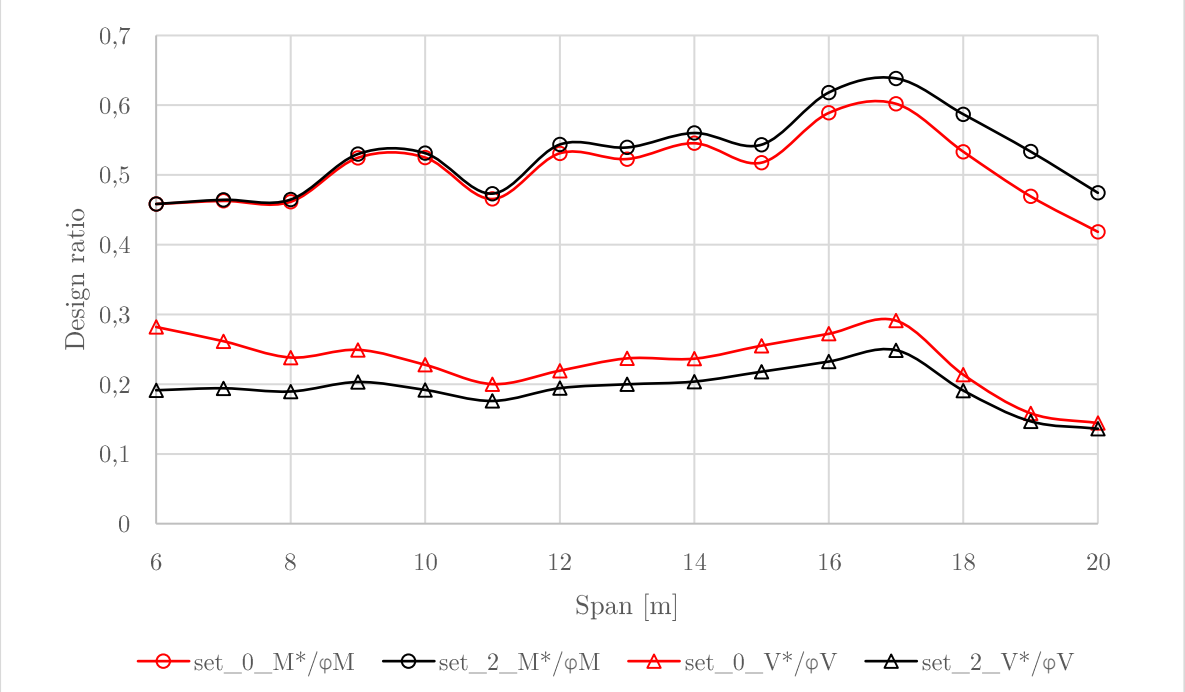

Figure 4.5 Comparison between little sections using AS/NZS 2003:2017 (moment and shear ratio)

In the project of composite beam, when the same section is used and when the behaviour of composite beam with the two code is analyzed, it is possible to observe that the value of shrinkage deflection changes a lot and increase the value of total deflection. δ_{c1-3} does not change and the others deformations are in the same range.

Another aspect, important to notice, is related to the shrinkage because in the new code it decrease when the span becomes bigger while in the oldest code it increases with the spans. This is caused because, in the AS/NSZ 2327:2017, the deflection component shall be determined by evaluating:

a) the deformation produced by the equivalent actions

b) the deformation induced by the effective shrinkage strain

    i) shrinkage strain in top slab

    ii) shrinkage strain in bottom slab

    iii) curvature of the shrinkage profile (equal to zero for solid slab)

Moreover, the modulus of elasticity of concrete is replaced with the effective modulus of elasticity $E_{ef,cs}$:

$$E_{ef,cc} = \frac{E_c}{1 + 0.55\ \phi_{cc}} \tag{4.7}$$

where:

ϕ_{cc} is the creep coefficient

Figure 4.6 shows the huge gap related to the total deflection which represent an amount of underestimate of the oldest code as shown in the **Table 4.4**:

Table 4.4 Variation of total and shrinkage deflections

Span [m]	$\Delta\delta_{tot}$ [%]	$\Delta\delta_{sh}$ [‰]
6.0	394.5	208.2
7.0	302.4	156.9
8.0	238.2	116.3
9.0	196.7	105.2
10.0	162.2	84.5
11.0	133.4	62.0
12.0	115.0	56.0
13.0	98.7	48.2
14.0	83.9	39.5
15.0	73.0	32.8
16.0	66.5	32.8
17.0	58.7	28.3
18.0	51.2	24.6
19.0	42.4	18.4
20.0	33.5	12.5

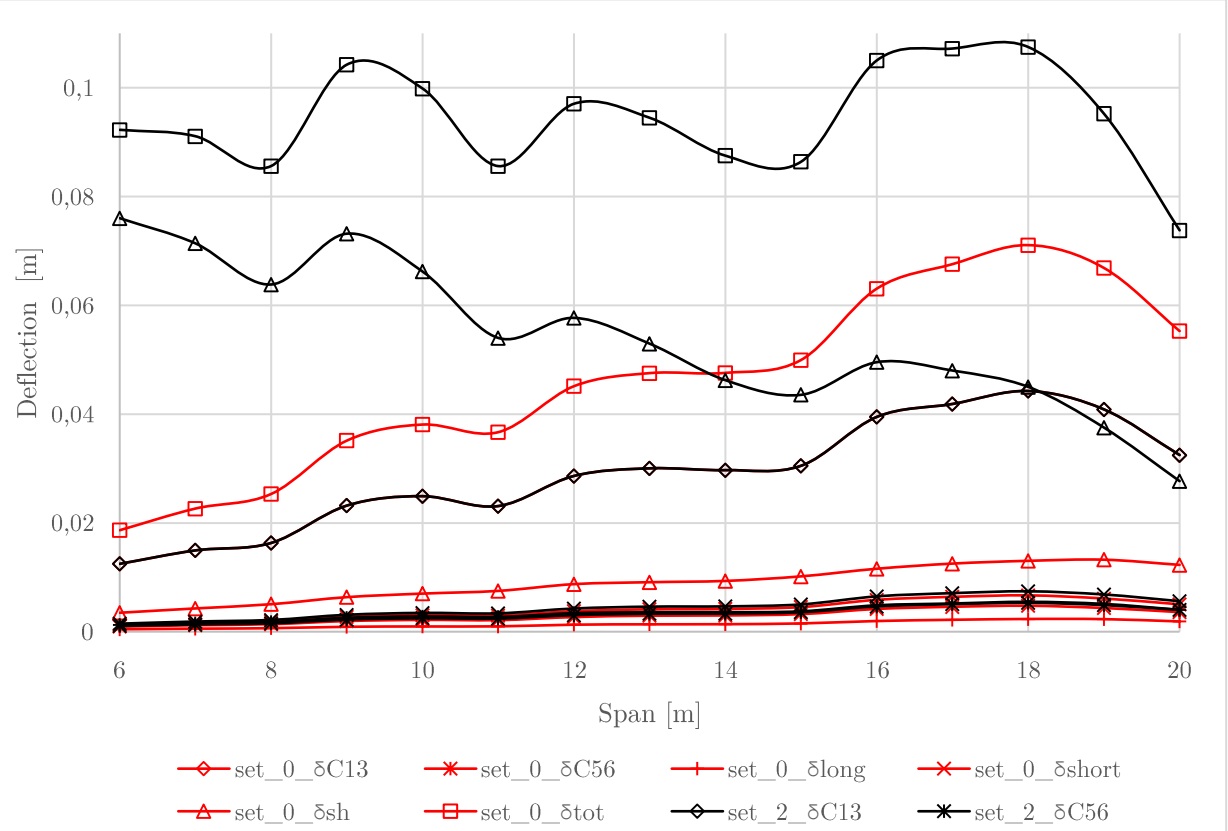

Figure 4.6 Comparison between little sections using AS/NZS 2003:2017 (displacements)

In **Figure 4.7** we need to notice that the shrinkage deflection, when the span increase in the new code, decrease due to the change of section. Both incremental and total deflections decrease when we increase the geometry property of the steel sections. Other differences are related to the evolution of the shrinkage, in fact, it increases with the old code and decreases with the new. This behaviour of deflections is caused by the reasons defined before.

We need to notice that the deflection due to shrinkage is bigger respect to the incremental, because in the incremental deflection is computed only a part of the effect of shrinkage. The gap between the incremental and shrinkage deflection are shown in the **Table 4.5**:

Table 4.5 Variation of total and shrinkage deflections

Span [m]	$\Delta\delta_{tot}$ [%]	$\Delta\delta_{sh}$ [‰]
6.0	1154.3	208.2
7.0	865.5	156.9
8.0	653.4	116.3
9.0	565.1	105.2
10.0	460.9	84.5
11.0	355.1	62.0
12.0	310.3	56.0
13.0	265.9	48.2
14.0	222.4	39.5
15.0	187.2	32.8
16.0	178.1	32.8
17.0	154.9	28.3
18.0	137.1	24.6
19.0	110.8	18.4
20.0	83.7	12.5

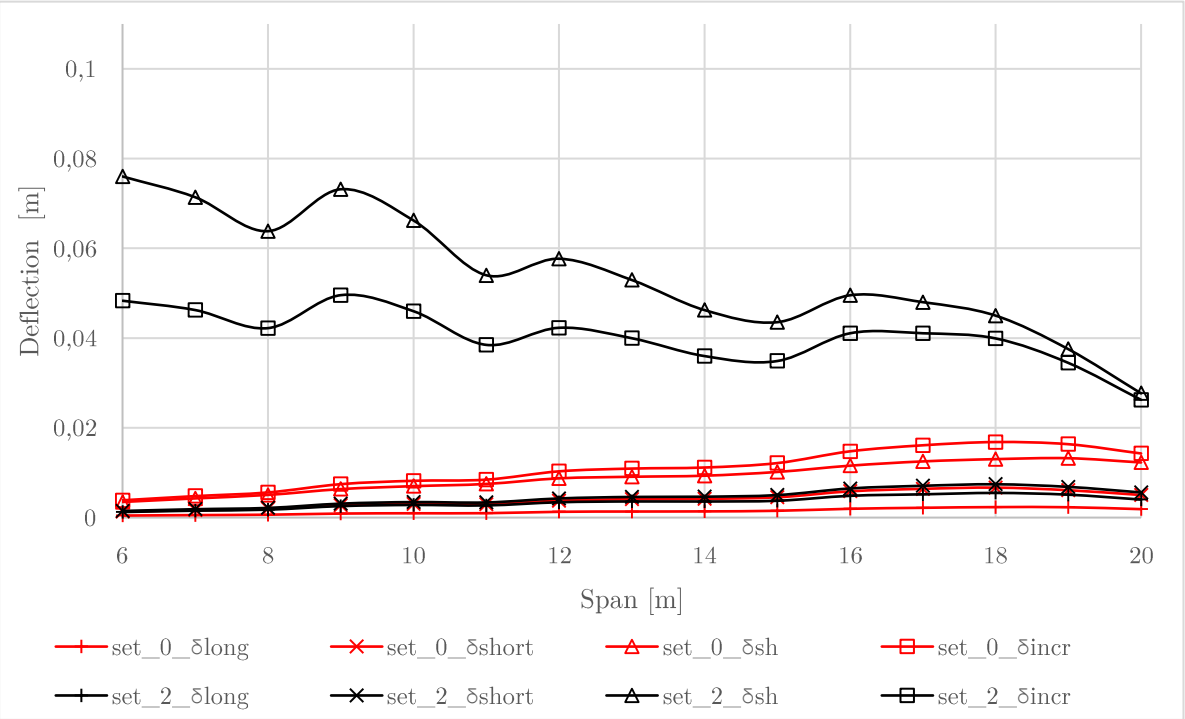

Figure 4.7 Comparison between little sections using AS/NZS 2003:2017 (displacements)

In the project of composite beam in service condition for the new code we need to adopt steel section bigger than the previous used in the 2003 code, however the total and incremental deflection represents the main critical parameters in the service design, the effect of the shear is neglectable and also the effect of the moment except for big value of span as shown in **Figure 4.8**.

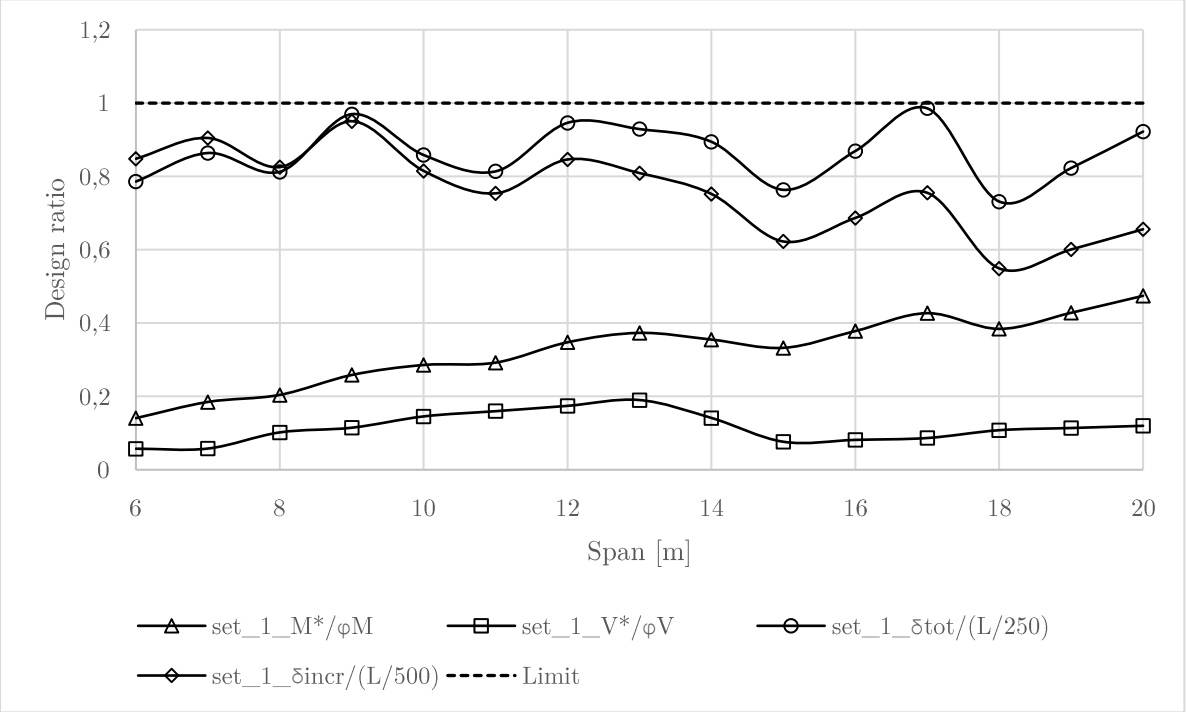

Figure 4.8 Percentage of influence using big sections in AS/NZS 2327:2017

Figure 4.9 shows the comparison between small sections computed with the 2003 code and big sections computed with the 2017 code. It shows the incremental deflections of different sections which satisfied the two codes. Bigger section shows a relevant incremental deflection caused by the shrinkage. We can notice that the incremental deflection for the same section, analyzing the last span, is bigger than 83% respect to AS2327.1-2003.

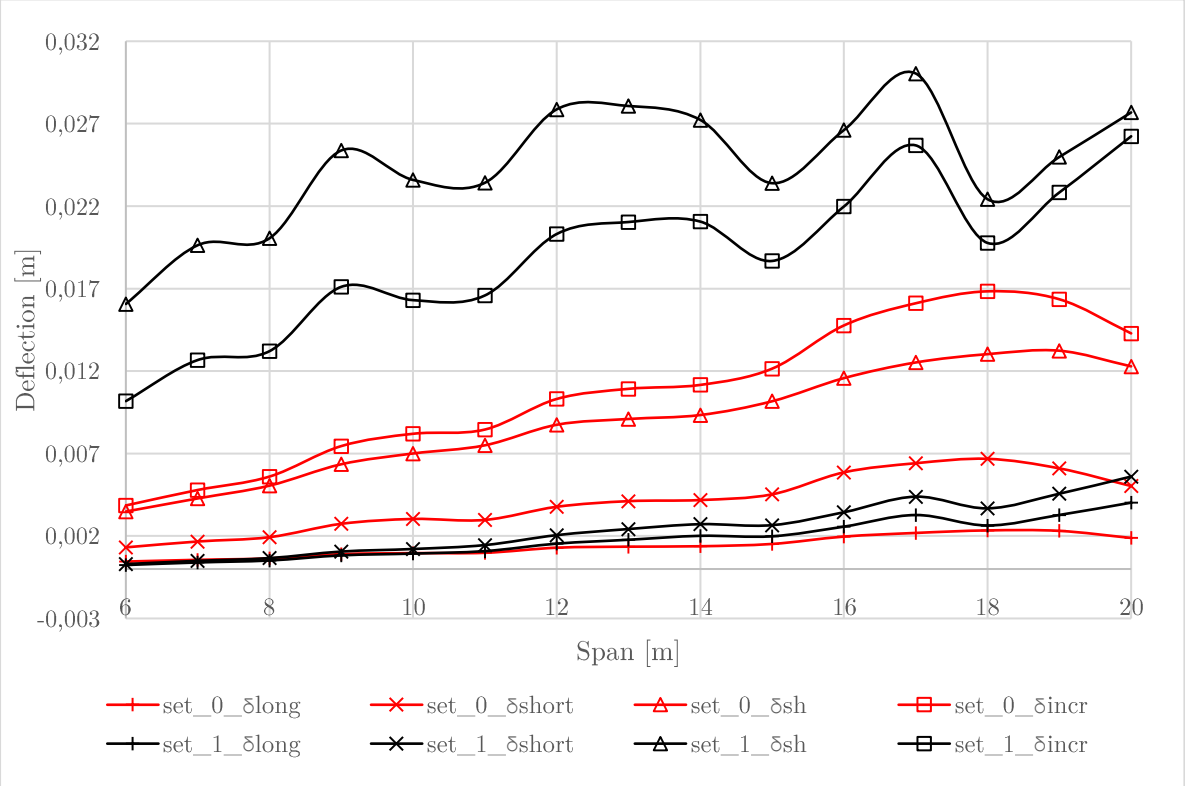

Figure 4.9 Comparison between little and big section using AS/NZS 2003:2017

In ultimate analysis, **Figure 4.10** clarify the comparison between different sections computed with the 2017 code. The use of big sections permits to decrease the effects of incremental and total displacements. Moreover, with the smallest sections, total displacements, is always in the same range; however, increases when we considered the biggest sections due to the effect of shrinkage.

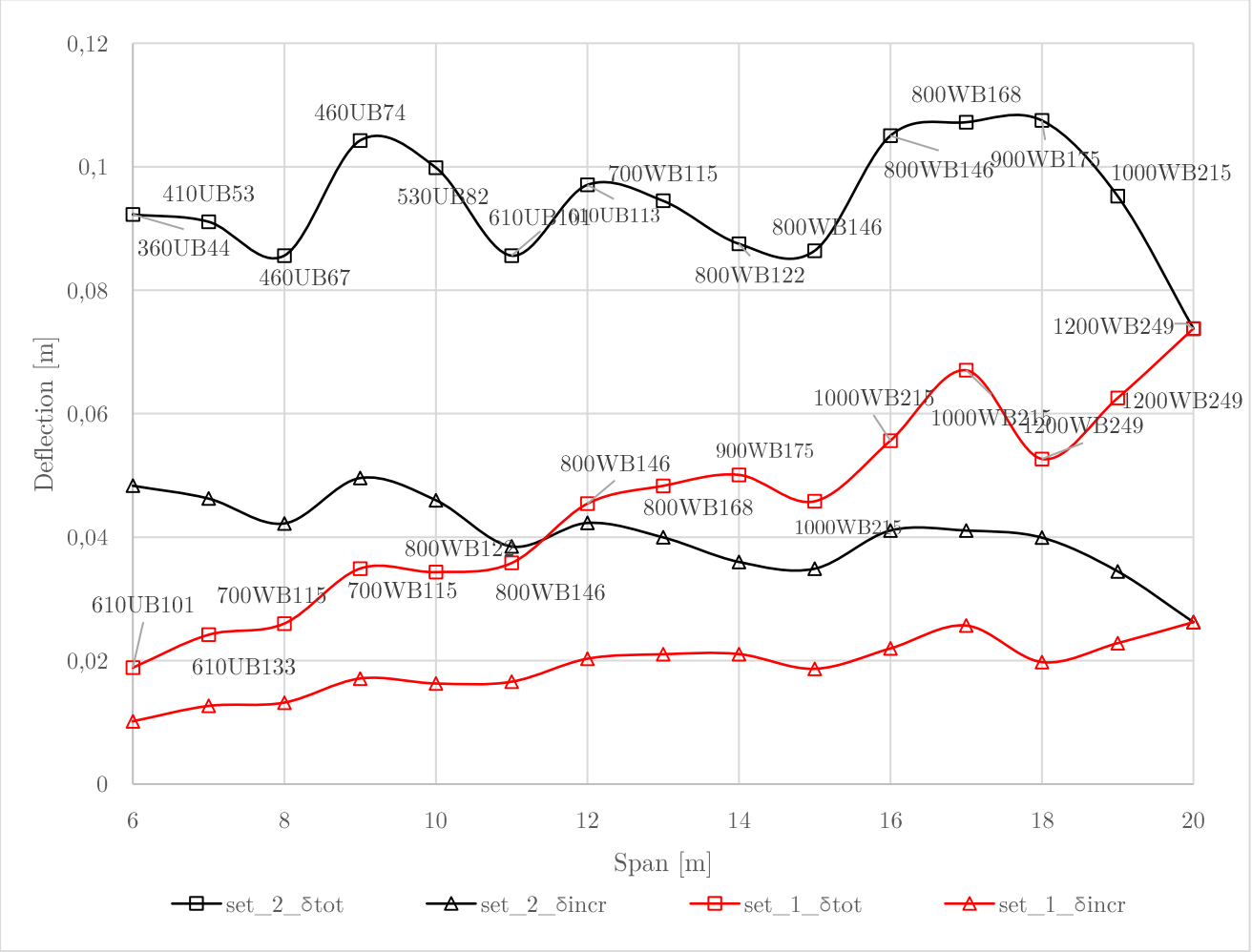

Figure 4.10 Comparison between little and big sections in the new code

4.3 Performance analysis

To analyze the performance of the composite beam a MATLAB script was developed. From the beams defined before it was chosen a steel beam with a span of 7 m divided in 21 elements with the profile steel 610 UB 113.

For this beam it was developed a strength design during the construction stage 3 where the slab is not casting yet and after the strength design is defined the in-service condition.

During the stage 3, the concrete does not reach the compressive strength of 15 MPa, so the design moment capacity and the shear capacity are constant along all the length (**Figure 4.11**).

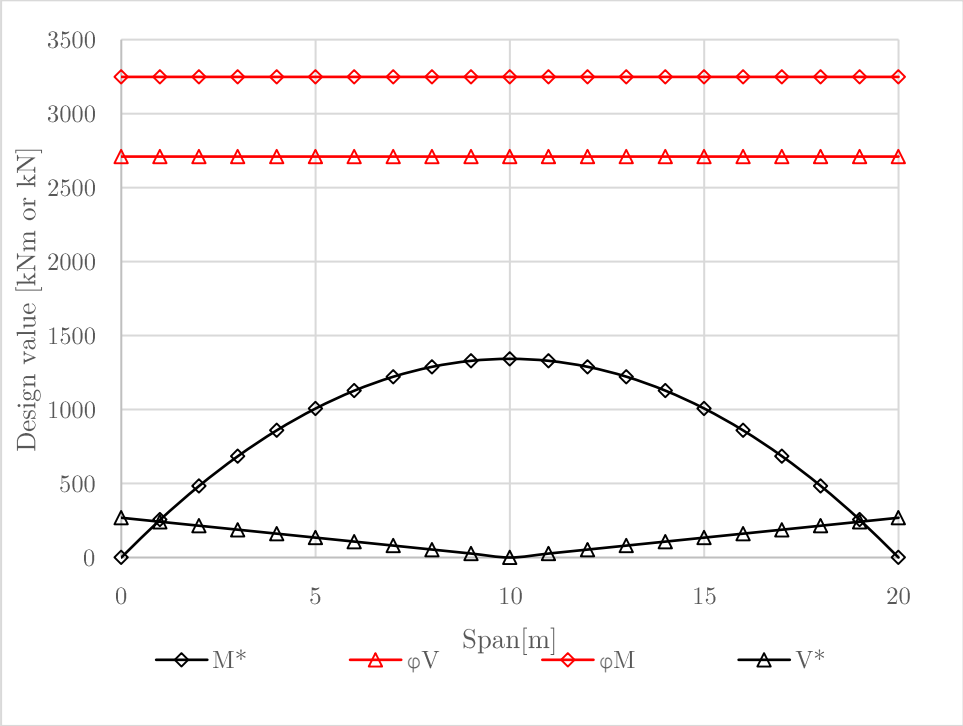

Figure 4.11 Stage 3 strength design actions and capacities

The value of the moment from the stage 3 to the in-service condition starts to develop as well as the design moment and shear due to the interaction of concrete with the shear connectors which guarantee a common behaviour of the two materials. The born of composite action permits to define the design moment capacity which, in this case, presents the same shape of the design moment (**Figure 4.12**).

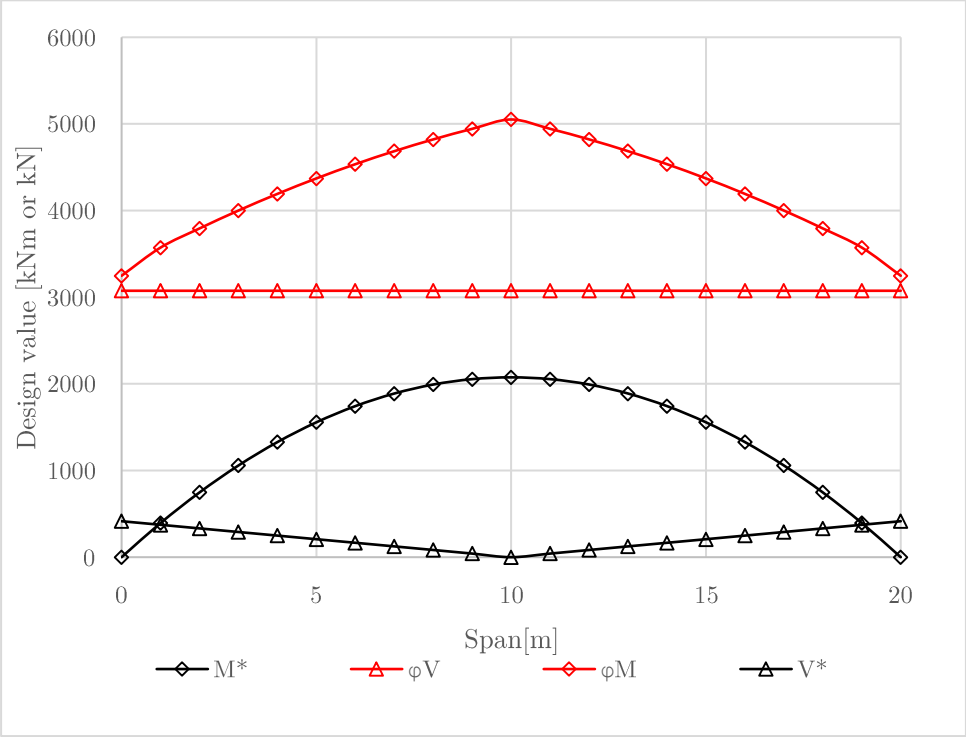

Figure 4.12 Composite strength design actions and capacities stage in service

In **Figure 4.13** the strength design is also satisfied in fact the stress after all the construction stage being less than the limit yield stress of 0.9 f_{yb}. Moreover, the reductions of stresses in the middle span of the beam is due the fact that is the sum of the initial stress in the beam with no composite action and the additional stress that results when the composite beam is loaded ignoring creep and shrinkage effects.

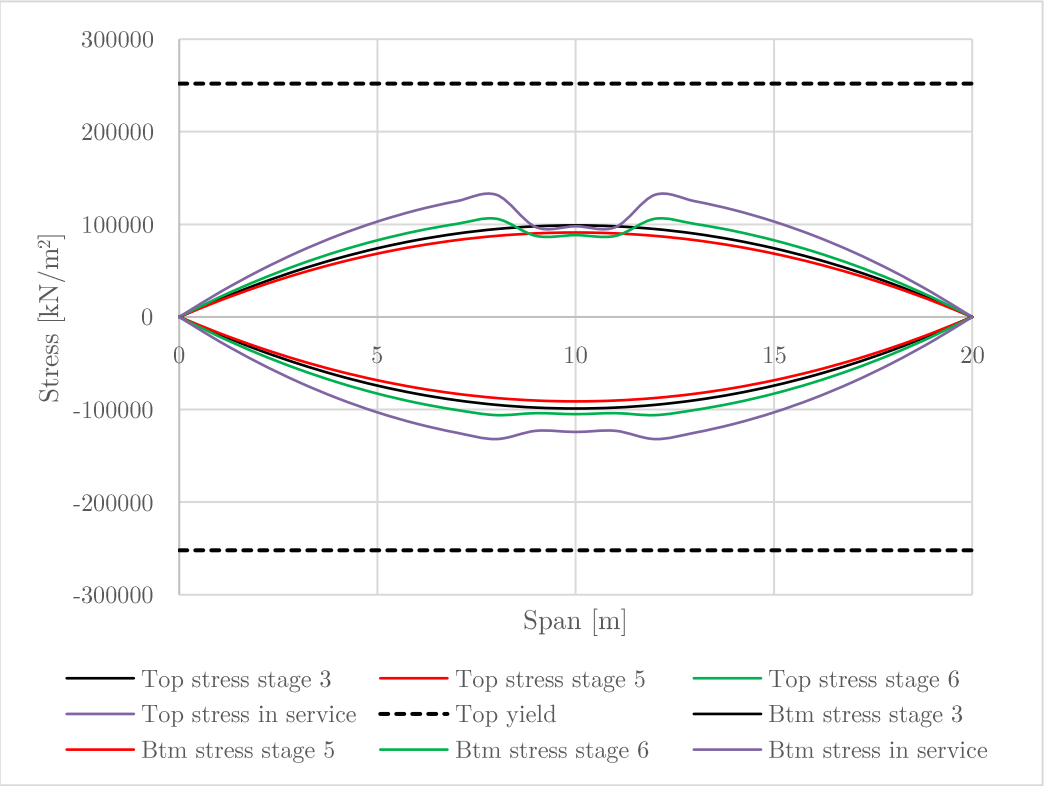

Figure 4.13 Top and bottom fibre flexural stresses

To validate the previous deflection analysis now are computed the various displacement for the effects of construction stages, creep and shrinkage. Shrinkage represents, like before, the worst amount of deflection which can occur (**Figure 4.14**).

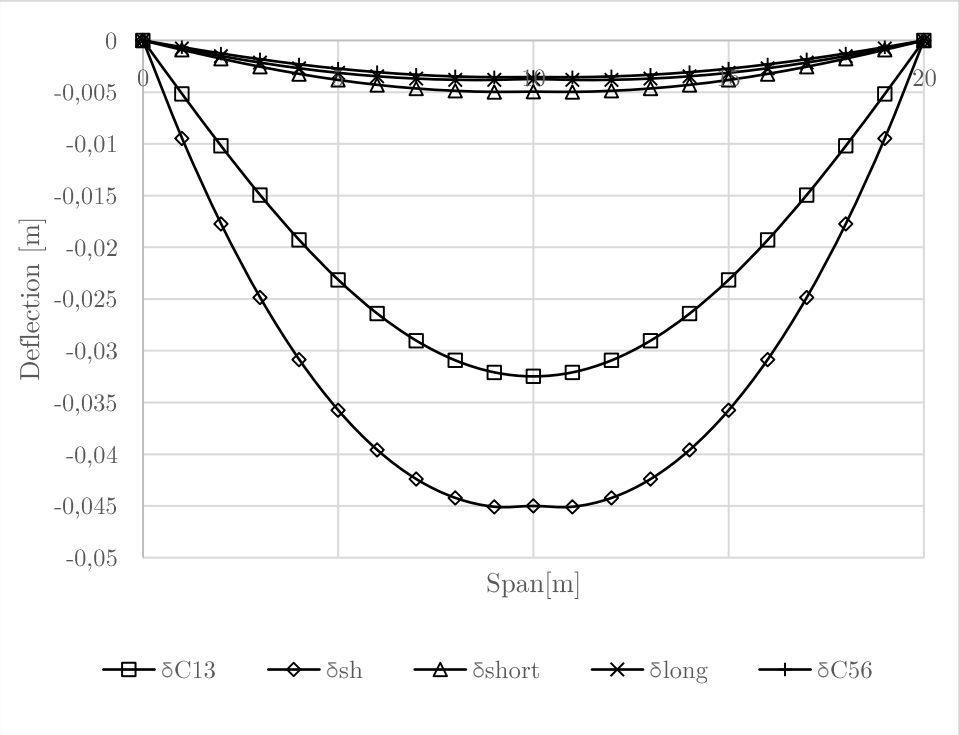

Figure 4.14 Deflection results

Chapter 5 Finite Element Model

5.1 Introduction

The objective of this chapter is to build a Finite Element Model with 7 degrees of freedom (dof). A span of 20 m discretized in 20 elements permitted to derive the displacement in service condition and to validate the Finite Element Model a comparison between the results obtained by the analysis and the code is done.

5.2 FEM

Finite element analysis (FEA) is a simulation of a phenomenon which occurs in a beam using a numerical technique.

The model used in this chapter is the Euler-Bernoulli beam model which is performed for statically and indeterminate beam. The differential equations are derived from:

a) equilibrium equations

b) constitutive equations

c) kinematic equations

The model used is the kinematic ones, in which we consider a prismatic section with these properties:

a) plane sections remain plain and perpendicular to the beam axis before and after any deformation

b) beam segment of length L

c) cross section assumed to be symmetric respect to the y-axis

d) no torsional and out of plane effects

During the kinematic analysis, if is considered a section of the beam (**Figure 5.1**), it is possible to find two types of displacements: axial displacement at the level of the level of the reference axis $u(x_P)$ and its deflection $v(x_P)$ (function also of the rotation $\theta\ x_P$) where x_P defines the position of a generic point P of the beam in the undeformed situation.

If we analyze also the displacements of a point Q, which is not positioned on the member axis it is possible to derive the horizontal and vertical displacements $d_x(x_Q, y_Q)$ and $d_y(x_Q, y_Q)$:

$$d_x(x_Q, y_Q) = u(x_Q) - y_Q \sin\theta\,(x_Q) \tag{5.1}$$

$$d_y(x_Q, y_Q) = v(x_Q) - y_Q + y_Q \cos\theta\,(x_Q) \tag{5.2}$$

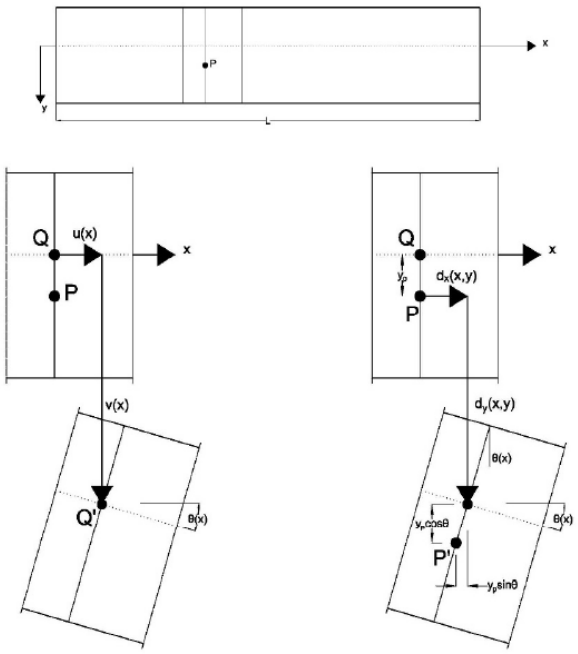

Figure 5.1 Displacement field

To simplify these expressions, it is useful to consider little displacements becouse this assumption is common for several typologies of structures which are commonly analyzed. In this way the sine is approximated by the angle and the cosine by one, so the generalised displacements are re-written like:

$$d_x(x,y) = u - y\,\theta = u - y\,v' \tag{5.3}$$

$$d_y(x,y) = v \tag{5.4}$$

$$d_z(x,y) = 0 \tag{5.5}$$

Deriving the previous elements, the strain fields are obtained:

$$\varepsilon_x = \frac{\partial d_x}{\partial x} = u' - y\,v'' \tag{5.6}$$

$$\varepsilon_y = \frac{\partial d_y}{\partial y} = 0 \tag{5.7}$$

$$\varepsilon_z = \frac{\partial d_z}{\partial z} = 0 \tag{5.8}$$

$$\gamma_{xy} = \frac{\partial d_x}{\partial y} + \frac{\partial d_y}{\partial x} = 0 \tag{5.9}$$

$$\gamma_{yz} = \frac{\partial d_y}{\partial z} + \frac{\partial d_z}{\partial y} = 0 \tag{5.10}$$

$$\gamma_{xz} = \frac{\partial d_x}{\partial z} + \frac{\partial d_z}{\partial x} = 0 \tag{5.11}$$

For analyzing the weak form, it is useful to consider a beam with a vertical distributed load w(x) and horizontal n(x), in which the edges are defined by the nodal action which can represent external load, internal action and support reactions.

We start comparing the work of internal stresses to the work of external actions:

$$\int_L \int_A \sigma_x\,\varepsilon_x\,dA\,dx = \int_L (w\hat{v} + n\hat{u})\,dx + \cdots$$
$$\cdots + S_L\widehat{v_L} + N_L u_L + M_L\theta_L + S_R\widehat{v_R} + N_R u_R + M_R\theta_R \tag{5.12}$$

Recalling the axial force and the moment expression as:

$$N = \int_A \sigma_x \, dA \tag{5.13}$$

$$M = -\int_A y \, \sigma_x \, dA \tag{5.14}$$

It is possible to write the integral force like:

$$\begin{gathered} \int_L (N \, \hat{u}' + M \, \hat{v}'') \, dx = \cdots \\ \cdots = \int_L (w\hat{v} + n\hat{u}) \, dx + S_L \widehat{v_L} + N_L \hat{u}_L + M_L \hat{\theta}_L + S_R \widehat{v_R} + N_R \hat{u}_R + M_R \hat{\theta}_R \end{gathered} \tag{5.15}$$

And using matrix relation:

$$\int_L \begin{bmatrix} N \\ M \end{bmatrix} \begin{bmatrix} \hat{u}' \\ \hat{v}'' \end{bmatrix} dx = \int_L \begin{bmatrix} n \\ w \end{bmatrix} \begin{bmatrix} \hat{u} \\ \hat{v} \end{bmatrix} dx + \begin{bmatrix} N_L \\ S_L \\ M_L \end{bmatrix} \begin{bmatrix} \hat{u}_L \\ \widehat{v_L} \\ \hat{\theta}_L \end{bmatrix} + \begin{bmatrix} N_R \\ S_R \\ M_R \end{bmatrix} \begin{bmatrix} \hat{u}_R \\ \widehat{v_R} \\ \hat{\theta}_R \end{bmatrix} \tag{5.16}$$

If the virtual displacements at the end are put equal to zero, we simplify the equation:

$$\int_L \begin{bmatrix} N \\ M \end{bmatrix} \begin{bmatrix} \hat{u}' \\ \hat{v}'' \end{bmatrix} dx = \int_L \begin{bmatrix} n \\ w \end{bmatrix} \begin{bmatrix} \hat{u} \\ \hat{v} \end{bmatrix} dx \tag{5.17}$$

If we want to describe this expression in function of linear elastic material properties the internal action will be:

$$N = \int_A \sigma_x \, dA \; = \int_A E \, (\varepsilon_r - \; y \, \kappa) \, dA \; = \; R_A \varepsilon_r \; - \; R_B \, \kappa \tag{5.18}$$

$$M = -\int_A y \, \sigma_x \, dA = -\int_A E \, y(\varepsilon_r - \; y \, \kappa) \, dA \; = \; - R_B \varepsilon_r \; - \; R_I \, \kappa \tag{5.19}$$

Changing the notation:

$$r = \begin{bmatrix} N \\ M \end{bmatrix} = \begin{bmatrix} \int_A \sigma_x \, dA \\ -\int_A y \, \sigma_x \, dA \end{bmatrix} \tag{5.20}$$

$$D = \begin{bmatrix} R_A & -R_B \\ -R_B & R_I \end{bmatrix} \tag{5.21}$$

$$\varepsilon = \begin{bmatrix} \varepsilon_r \\ \kappa \end{bmatrix} = \begin{bmatrix} u' \\ v'' \end{bmatrix} = \begin{bmatrix} \partial & 0 \\ 0 & \partial^2 \end{bmatrix} \begin{bmatrix} u \\ v \end{bmatrix} = A \, e \tag{5.22}$$

We can rewrite Equation 5.17 in:

$$\int_L r \, A \, \hat{e} \, dx \; = \int_L p \, \hat{e} \, dx \tag{5.23}$$

$$p = \begin{bmatrix} n \\ w \end{bmatrix} \tag{5.24}$$

And substituting the constitutive properties in 13.13 in 13.18 we have the general solution of the weak form:

$$\int_L D \, \varepsilon \, A \, \hat{e} \, dx \; = \int_L p \, \hat{e} \, dx \tag{5.25}$$

Now it is possible to describe a finite element formulation, which permits to describe the displacement, using polynomial functions; by means of a parabolic function for describing the axial displacements and a cubic polynomial for the deflections:

$$\begin{cases} u = a_0 + a_1 x + a_2 x^2 \\ v = b_0 + b_1 x + b_2 x^2 + b_3 x^3 \end{cases} \tag{5.26}$$

For evaluating the coefficient a_i and b_i it is possible to substitute the displacements with the displacements on the left, middle and right node:

$$u\,(x = 0) = a_0 = u_L \tag{5.27}$$

$$u\left(x = \frac{L}{2}\right) = a_0 + a_1 \frac{L}{2} + a_2 \left(\frac{L}{2}\right)^2 = u_M \tag{5.28}$$

$$u\,(x = L) = a_0 + a_1 L + a_2 (L)^2 = u_R \tag{5.29}$$

And reassembling according to the displacements:

$$a_0 = u_L \tag{5.30}$$

$$a_1 = -\frac{3u_L - 4u_M + u_R}{L} \tag{5.31}$$

$$a_2 = \frac{2(u_L - 2u_M + u_R)}{L^2} \tag{5.32}$$

Collecting the term in the Equation 5.26

$$u = u_L - \frac{3u_L - 4u_M + u_R}{L}\, x \, + \frac{2(u_L - 2u_M + u_R)}{L^2} x^2 \tag{5.33}$$

collecting all with the nodal displacements:

$$u = \left(1 \, - \, \frac{3\,x}{L} + \frac{2\,x^2}{L^2}\right) u_L + \left(1 \, - \, \frac{3\,x}{L} + \frac{2\,x^2}{L^2}\right) u_M + \left(1 \, - \, \frac{3\,x}{L} + \frac{2\,x^2}{L^2}\right) u_R \tag{5.34}$$

So in a compact way:

$$u = N_{u1} u_L + N_{u2} u_M + N_{u3} u_R \tag{5.35}$$

where:

$$N_{u1} = 1 \, - \, \frac{3\,x}{L} + \frac{2\,x^2}{L^2} \tag{5.36}$$

$$N_{u2} = \frac{4\,x}{L} \, - \, \frac{4\,x^2}{L^2} \tag{5.37}$$

$$N_{u3} = \frac{-x}{L} + \frac{2\,x^2}{L^2} \tag{5.38}$$

N_{ui} in **Figure 5.2** represent the shape functions of the element and describe the possible shape related to the nodal displacement, which is equal to one in the node with the displacement and zeroes in the other.

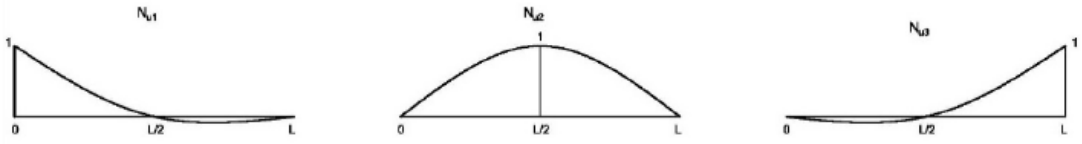

Figure 5.2 Shape functions for the approximation of u

In the same way, it is possible to define the displacement v:

$$v = \left(1 - \frac{3\,x^2}{L^2} + \frac{2\,x^3}{L^3}\right) v_L + \left(x - \frac{2\,x^2}{L} + \frac{x^3}{L^2}\right) \theta_L + \cdots$$
$$\ldots + \left(\frac{3\,x^2}{L^2} - \frac{2x^3}{L^3}\right) v_R + \left(-\frac{x^2}{L} + \frac{x^3}{L^2}\right) \vartheta_R \tag{5.39}$$

$$v = N_{v1} v_L + N_{v2} \theta_L + N_{v3} v_R + N_{v4} \vartheta_R \tag{5.40}$$

where:

$$N_{v1} = 1 - \frac{3\,x^2}{L^2} + \frac{2\,x^3}{L^3} \tag{5.41}$$

$$N_{v2} = x - \frac{2\,x^2}{L} + \frac{x^3}{L^2} \tag{5.42}$$

$$N_{v3} = \frac{3\,x^2}{L^2} - \frac{2x^3}{L^3} \tag{5.43}$$

$$N_{v4} = -\frac{x^2}{L} + \frac{x^3}{L^2} \tag{5.44}$$

where N_{vi} in **Figure 5.3** represent the shape functions of v:

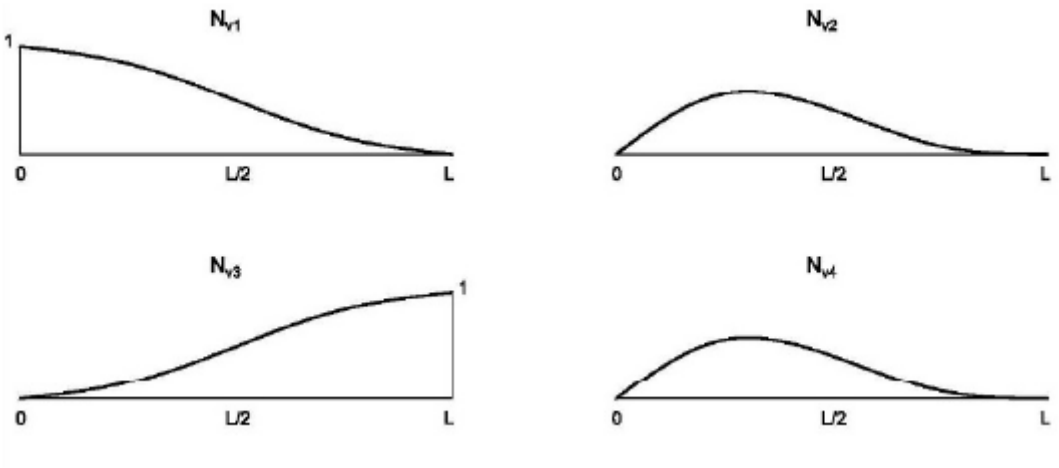

Figure 5.3 Shape functions for the approximation of v

Using a matrix formulation and remembering to use a 7-dof beam model as shown in **Figure 5.4**:

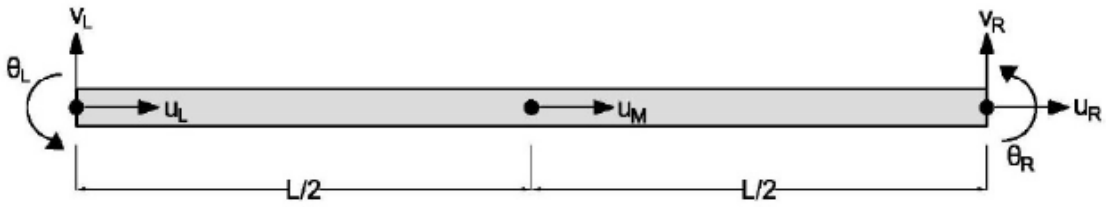

Figure 5.4 7-dof Bernoulli beam model

$$\begin{bmatrix} u \\ v \end{bmatrix} = \begin{bmatrix} N_{u1} & 0 & 0 & N_{u2} & N_{u3} & 0 & 0 \\ 0 & N_{v1} & N_{v2} & 0 & 0 & N_{v3} & N_{v4} \end{bmatrix} \begin{bmatrix} u_L \\ v_L \\ \vartheta_L \\ u_M \\ u_R \\ v_R \\ \theta_R \end{bmatrix} = N_e d_e \tag{5.45}$$

The strain can be expressed with this notation:

$$\varepsilon = A\, N_e d_e = B\, d_e \tag{5.46}$$

And substituting all in 13.20 we can define the stiffness relation of the finite element:

$$q_e = k_e d_e \tag{5.47}$$

5.3 Results of FEM and comparison with the code

The analysis developed is a FEA with 7 dof. The procedure involved in the calculation are defined by the following step:

a) assign a global system of coordinate

b) number the node

c) assign freedom at the node

d) calculate the stiffness matrix and the vector of force for each element in local coordinate

e) expand matrix and vector at the dimension of the structure

f) assemble all the elements in the global coordinate

g) solve respect to unknown displacements and reactions

For having a good comparison, it was used the same beam of the previous chapter with the same length and the same section and the only simplification concerns the position of the shear connectors.

The finite element model formulated is a simplification respect to the calculation defined by the code. The aim of this part is to understand the goodness of this element and demonstrate if the result of the code should be compared with the model adopted.

Inside the model was loaded:

a) the uniformly sitributed loads derived from stage 3, stage 5 to 6, short term, long term and shrinkage

b) the section properties of the beam

c) the material property

The model is implemented to give in output:

a) constraining reactions

b) unknown displacements

Table 5.1 shows all the displacements obtained by the FEM for all the length of the beam. In this case are defined all the component derived by the construction phases of the composite beam which subsequently need to be combined to obtain the total and incremental displacements.

Table 5.1 Displacements for all the construction phases defined by the FEM

Span	δ_{C13}	δ_{C56}		δ_{long}		δ_{short}		δ_{sh}	
[m]	[m]	[m]		[m]		[m]		[m]	
	FEM	FEM_s	FEM_c	FEM_s	FEM_c	FEM_s	FEM_c	FEM_s	FEM_c
0	0	0	0	0	0	0	0	0	0
1	-0.00517	-0.00109	-0.00047	-0.00197	-0.00085	-0.00218	-0.00094	0.00996	0.00429
2	-0.01019	-0.00215	-0.00093	-0.00387	-0.00167	-0.00431	-0.00185	0.01964	0.00845
3	-0.01494	-0.00315	-0.00136	-0.00568	-0.00244	-0.00631	-0.00271	0.02878	0.01238
4	-0.01929	-0.00407	-0.00175	-0.00733	-0.00315	-0.00815	-0.00350	0.03716	0.01599
5	-0.02314	-0.00489	-0.00210	-0.00879	-0.00378	-0.00977	-0.00420	0.04458	0.01918
6	-0.02641	-0.00558	-0.00240	-0.01004	-0.00432	-0.01115	-0.00480	0.05087	0.02189
7	-0.02902	-0.00613	-0.00264	-0.01103	-0.00475	-0.01226	-0.00527	0.05591	0.02405
8	-0.03093	-0.00653	-0.00281	-0.01175	-0.00506	-0.01306	-0.00562	0.05958	0.02563
9	-0.03209	-0.00678	-0.00292	-0.01220	-0.00525	-0.01355	-0.00583	0.06181	0.02660
10	-0.03248	-0.00686	-0.00295	-0.01234	-0.00531	-0.01371	-0.00590	0.06256	0.02692
11	-0.03209	-0.00678	-0.00292	-0.01220	-0.00525	-0.01355	-0.00583	0.06181	0.02660
12	-0.03093	-0.00653	-0.00281	-0.01175	-0.00506	-0.01306	-0.00562	0.05958	0.02563
13	-0.02902	-0.00613	-0.00264	-0.01103	-0.00475	-0.01226	-0.00527	0.05591	0.02405
14	-0.02641	-0.00558	-0.00240	-0.01004	-0.00432	-0.01115	-0.00480	0.05087	0.02189
15	-0.02314	-0.00489	-0.00210	-0.00879	-0.00378	-0.00977	-0.00420	0.04458	0.01918
16	-0.01929	-0.00407	-0.00175	-0.00733	-0.00315	-0.00815	-0.00350	0.03716	0.01599
17	-0.01494	-0.00315	-0.00136	-0.00568	-0.00244	-0.00631	-0.00271	0.02878	0.01238
18	-0.01019	-0.00215	-0.00093	-0.00387	-0.00167	-0.00431	-0.00185	0.01964	0.00845
19	-0.00517	-0.00109	-0.00047	-0.00197	-0.00085	-0.00218	-0.00094	0.00996	0.00429
20	0	0	0	0	0	0	0	0	0

To validate the model a comparison between: the value obtained and the deflection components found during the design computed by the code it was done.

Consulting **Table 5.2** it is possible to notice that only for the displacements related to the construction stage 3 and 5 to 6 the displacements are equal, so we obtain a good approximation in this case. However, there is a little gap among the other displacements due to the reason defined before.

Table 5.2 Different between displacements defined by the code and the FEM

Span	δ_{C13}		δ_{C56}		δ_{long}		δ_{short}		δ_{sh}	
[m]	[m]		[m]		[m]		[m]		[m]	
	FEM	code	FEM	code	FEM	code	FEM	code	FEM	code
0	0	0	0	0	0	0	0	0	0	0
1	-0.0052	-0.0052	-0.0006	-0.0006	-0.0012	-0.0008	-0.0013	-0.0009	-0.0059	-0.0095
2	-0.0102	-0.0102	-0.0013	-0.0013	-0.0023	-0.0015	-0.0025	-0.0018	-0.0115	-0.0177
3	-0.0149	-0.0149	-0.0018	-0.0018	-0.0033	-0.0021	-0.0036	-0.0025	-0.0167	-0.0248
4	-0.0193	-0.0193	-0.0023	-0.0023	-0.0042	-0.0027	-0.0046	-0.0032	-0.0213	-0.0308
5	-0.0231	-0.0231	-0.0028	-0.0027	-0.0050	-0.0031	-0.0055	-0.0038	-0.0252	-0.0357
6	-0.0264	-0.0264	-0.0031	-0.0031	-0.0056	-0.0035	-0.0061	-0.0043	-0.0284	-0.0396
7	-0.0290	-0.0290	-0.0034	-0.0033	-0.0061	-0.0037	-0.0066	-0.0046	-0.0308	-0.0424
8	-0.0309	-0.0309	-0.0035	-0.0035	-0.0064	-0.0038	-0.0070	-0.0049	-0.0324	-0.0442
9	-0.0321	-0.0321	-0.0036	-0.0036	-0.0065	-0.0038	-0.0071	-0.0050	-0.0331	-0.0451
10	-0.0325	-0.0325	-0.0036	-0.0035	-0.0065	-0.0037	-0.0071	-0.0050	-0.0331	-0.0450
11	-0.0321	-0.0321	-0.0036	-0.0036	-0.0065	-0.0038	-0.0071	-0.0050	-0.0331	-0.0451
12	-0.0309	-0.0309	-0.0035	-0.0035	-0.0064	-0.0038	-0.0070	-0.0049	-0.0324	-0.0442
13	-0.0290	-0.0290	-0.0034	-0.0033	-0.0061	-0.0037	-0.0066	-0.0046	-0.0308	-0.0424
14	-0.0264	-0.0264	-0.0031	-0.0031	-0.0056	-0.0035	-0.0061	-0.0043	-0.0284	-0.0396
15	-0.0231	-0.0231	-0.0028	-0.0027	-0.0050	-0.0031	-0.0055	-0.0038	-0.0252	-0.0357
16	-0.0193	-0.0193	-0.0023	-0.0023	-0.0042	-0.0027	-0.0046	-0.0032	-0.0213	-0.0308
17	-0.0149	-0.0149	-0.0018	-0.0018	-0.0033	-0.0021	-0.0036	-0.0025	-0.0167	-0.0248
18	-0.0102	-0.0102	-0.0013	-0.0013	-0.0023	-0.0015	-0.0025	-0.0018	-0.0115	-0.0177
19	-0.0052	-0.0052	-0.0006	-0.0006	-0.0012	-0.0008	-0.0013	-0.0009	-0.0059	-0.0095
20	0	0	0	0	0	0	0	0	0	0

In **Table 5.3** there is a combination of the displacements obtained before to derive the total and incremental displacements like done in Chapter 4. In this way we obtain a comparison between the most important parameter of the beam which govern the project in service condition. As well in this case, the difference between the result obtained by the code and by the model are comparable.

Table 5.3 Comparison between total and incremental displacements

Span [m]	δ_{incr} [m]		δ_{tot} [m]	
	FEM	code	FEM	code
0	0	0	0	0
1	-0.006	-0.007	-0.014	-0.017
2	-0.012	-0.014	-0.028	-0.032
3	-0.017	-0.020	-0.040	-0.046
4	-0.022	-0.024	-0.052	-0.058
5	-0.026	-0.028	-0.062	-0.069
6	-0.029	-0.032	-0.070	-0.077
7	-0.031	-0.034	-0.076	-0.083
8	-0.033	-0.035	-0.080	-0.087
9	-0.034	-0.036	-0.082	-0.090
10	-0.033	-0.036	-0.083	-0.090
11	-0.034	-0.036	-0.082	-0.090
12	-0.033	-0.035	-0.080	-0.087
13	-0.031	-0.034	-0.076	-0.083
14	-0.029	-0.032	-0.070	-0.077
15	-0.026	-0.028	-0.062	-0.069
16	-0.022	-0.024	-0.052	-0.058
17	-0.017	-0.020	-0.040	-0.046
18	-0.012	-0.014	-0.028	-0.032
19	-0.006	-0.007	-0.014	-0.017
20	0	0	0	0

In **Figure 5.5** are graphed the displacements in **Table 5.3** to check the difference. Despite the approximation of the model the values of total and incremental deflection are quite the same, in fact the max percentage variation for both case is about 10%.

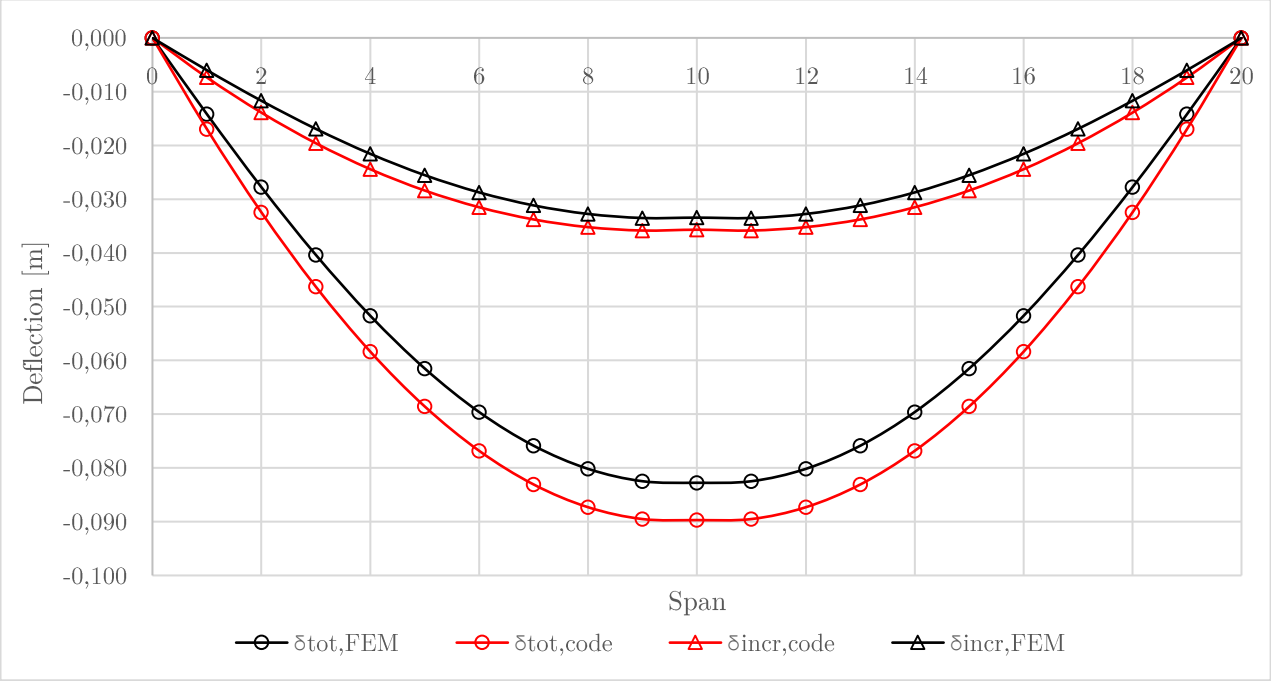

Figure 5.5 Deflections comparison between FEM and code results

To understand which parameters are more different, it is possible to analyze the ratio between the displacements obtained by the code and the FEM (**Table 5.4**).

Table 5.4 Ratio between displacements defined by code and FEM

Span [m]	$\delta_{C13,code}/\delta_{C13,FEM}$ [-]	$\delta_{C56,code}/\delta_{C56,FEM}$ [-]	$\delta_{long,code}/\delta_{long,FEM}$ [-]	$\delta_{short,code}/\delta_{short,FEM}$ [-]	$\delta_{sh,code}/\delta_{sh,code}$ [-]
0	1	1	1	1	1
1	1	0.998	0.672	0.700	1.599
2	1	0.996	0.662	0.700	1.539
3	1	0.993	0.652	0.700	1.490
4	1	0.991	0.641	0.700	1.451
5	1	0.989	0.630	0.700	1.420
6	1	0.986	0.619	0.700	1.396
7	1	0.984	0.608	0.700	1.378
8	1	0.981	0.596	0.700	1.367
9	1	0.978	0.584	0.700	1.361
10	1	0.976	0.572	0.700	1.361
11	1	0.978	0.584	0.700	1.361
12	1	0.981	0.596	0.700	1.367
13	1	0.984	0.608	0.700	1.378
14	1	0.986	0.619	0.700	1.396
15	1	0.989	0.630	0.700	1.420
16	1	0.991	0.641	0.700	1.451
17	1	0.993	0.652	0.700	1.490
18	1	0.996	0.662	0.700	1.539
19	1	0.998	0.672	0.700	1.599
20	1	1	1	1	1

And the ratio of the total and incremental deflection are presented in **Table 5.5**. It is possible to notice that the incremental deflection presents a good approximation, however, the some sentence is not correct for the total displacements.

Table 5.5 Ratio of total and incremental displacements defined by code and FEM

Span [m]	$\delta_{incr,code}/\delta_{incr,FEM}$ [-]	$\delta_{tot,code}/\delta_{tot,FEM}$ [-]
0	1	1
1	0.816	0.519
2	0.842	0.501
3	0.864	0.485
4	0.883	0.473
5	0.899	0.462
6	0.912	0.453
7	0.923	0.445
8	0.930	0.439
9	0.935	0.435
10	0.937	0.431
11	0.935	0.435
12	0.930	0.439
13	0.923	0.445
14	0.912	0.453
15	0.899	0.462
16	0.883	0.473
17	0.864	0.485
18	0.842	0.501
19	0.816	0.519
20	1	1

In **Figure 5.6** present a summary of all the concept defined previously. The ratio of the displacements permit to define the parameters which during the two analysis present a bigger gap respect to the other. At the end the effect of shrinkage, short and long term play a main role in the definition of the total deflection which cannot be approximated in a very precise way.

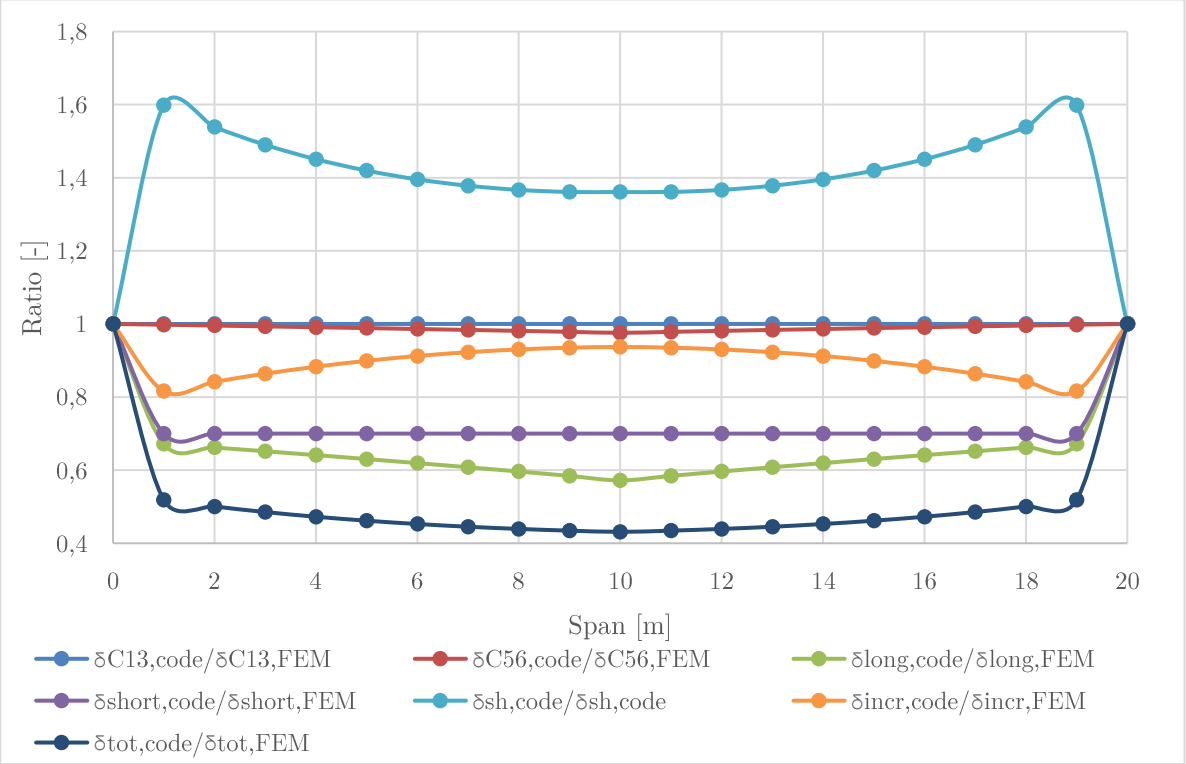

Figure 5.6 Comparison between displacement ratio of FEM and code

Chapter 6 Conclusions

6.1 Introduction

The results related to this thesis are summarized in this chapter followed by the recommendations for future work.

6.2 Concluding remarks

This thesis represents an evaluation of the design of composite beam and the behaviour in service condition. Particular attention is given to the long-term effect due to shrinkage in service limit state.

In Chapter 3, an evaluation of all the phases related to the design of a composite beam are demonstrated. The main parts are the design of strength and the design of serviceability which govern all the project. However, the design of serviceability is the most critical part; in fact, the deflection can create problems during the service life of this element. So, it is useful to analyse the history of displacements from the first construction

faces to the service condition and understand which parameters are the most dangerous. In the new Australian code, it is possible to notice that the effect of shrinkage played an important role and it is evaluated by the deformation produced by the equivalent actions and induced by the shrinkage strain.

In Chapter 4, a parametric analysis is carried out. The parameters involved in this case are: different level of spans, the ratio between moment, shear and displacement. It has proven that the main parameters which govern the serviceability design are the total and incremental displacement while the other will not influence a lot the problem. Moreover, in the new version of the code it not possible to use little steel sections like in the previous version because they suffer a lot of deflection and will not respect the limit. A comparison between all the deflection component of the two version of the code is done. It shows the bigger influence of shrinkage in AS/NSZ 2327:2017 due the new formulation of the code. In this chapter also, a stress analysis is performed to observe the behaviour of the stress along the beam.

In Chapter 5, a Finite Element Model is developed used to define the displacement during the service state of the composite beam. This element is validated using the results obtained before using the code. In fact, the values of displacements are quite the same and the gap between the two trends is related to some simplification adopted in the model.

Ultimately, by this work it is possible to understand that the effect of shrinkage in long-term changes a lot the displacement of a composite beam and the formulation of the new code is able to predict with good accuracy the value of shrinkage deflection respect to the old code in which this parameter did not influence the behaviour of the system.

6.3 Recommendations for future works

Considering this thesis possible future works should be defined as follow:

1) more refined Finite Element Model.

2) considering a nonlinear analysis using the Newton-Raphson Method which permit to define the development of curvature and stresses using an iterative procedure.

3) comparison between the model and real experiments for validate the model and understand if the model developed is suitable for predict the long-term effects in a composite beam.

Appendix I

In this appendix is provided the calculation of a composite beam for a single case in which are shown all the passage for the design of a composite beam.

The first step is to choose the type of steel section and concrete slab and the related property.

a) span of the primary beam L_1

b) span of the secondary beam L_2

c) define tributary area:

$$A_t = L_1 \; L_2$$

After it is possible to define all the loads and the combo acting on the beam:

d) define the loads acting on the beam:

$$G_{superimposed\,2} = L_2 \; \gamma_{superimposed}$$

in which $\gamma_{superimposed} = 1.5$

$$G_{slab\,2} = L_2 \; \rho_c \;\; t_c$$

in which ρ_c is the density of concrete and t_c is the thickness of the slab

$$G_{slab,ponding\,2} = G_{slab\,2}\ \phi_{ponding}$$

$$G_{reo} = 0.08\ \left(1 - \frac{\rho_c}{7850}\right) L_2$$

$$G_{adjust\ for\ deck} = 0.29$$

$$G_{steel\ sheeting} = \gamma_{steel\ sheeting}\ \ L_2$$

$$G_{superimposed\ slab\,2} = G_{superimposed\,2} + G_{slab\,2} + G_{slab,ponding\,2} + G_{reo} - G_{adjust\ for\ deck}$$

$$Q_2 = Q\ L_3$$

e) define all the geometry properties of the steel beam

f) define the lever of residual stress: LW (Lightly welded)

g) define the combinations of loads

$$G_{2\,tot} = \ SW_{steel} + G_{steel\ sheeting} + G_{superimposed\ slab\,2}$$

i) **for stage 3**:

$$G_{stage\,3} = \ SW_{steel} + G_{steel\ sheeting} + G_{slab\,2} + G_{slab,ponding\,2} + G_{reo} - G_{adjust\ for\ deck}$$

$$Q_{stage\,3} = f(A_t)$$

for strength:

$$COMB_{strength\ stage\,3,1} = \ 1.35\ G_{stage\,3}$$

$$COMB_{strength\ stage\,3,2} = \ 1.2\ G_{stage\,3} + 1.5\ Q_{stage\,3}$$

$$COMB_{strength\ stage\,3,3} = \ 1.2\ G_{stage\,3} + 1.5\ \psi_l\ Q_{stage\,3}$$

in which $\psi_l = 0.4$

$$COMB_{strength\ stage\ 3} = max(COMB_{strength\ stage\ 3,1};\ COMB_{strength\ stage\ 3,2};\ COMB_{strength\ stage\ 3,3})$$

for serviceability:

$$COMB_{service\ stage\ 3,1} = G_{stage\ 3}$$

$$COMB_{service\ stage\ 3,2} = \psi_s\ Q_{stage\ 3}$$

in which $\psi_s = 0.7$

$$COMB_{service\ stage\ 3,3} = \psi_l\ Q_{stage\ 3}$$

in which $\psi_l = 0.4$

$$COMB_{service\ stage\ 3} = max(COMB_{service\ stage\ 3,1};\ COMB_{service\ stage\ 3,2};\ COMB_{service\ stage\ 3,3})$$

ii) combo strength for design

$$COMB_{strength,1} = 1.35\ G_{2\ tot}$$

$$COMB_{strength,2} = 1.2\ G_{2\ tot} + 1.5\ Q_2$$

$$COMB_{strength,3} = 1.2\ G_{2\ tot} + 1.5\ \psi_l\ Q_2$$

in which $\psi_l = 0.4$

$$COMB_{strength} = max(COMB_{strength,1};\ COMB_{strength,2};\ COMB_{strength,3})$$

iii) combo serviceability for design

$$COMB_{service,1} = G_{2\ tot}$$

$$COMB_{service,2} = \psi_s\ Q_2$$

in which $\psi_s = 0.7$

$$COMB_{service,3} = \psi_l \, Q_2$$

in which $\psi_l = 0.4$

$$COMB_{service} = max(COMB_{service,1};\ COMB_{service,2};\ COMB_{service,3})$$

To understand where the load is loaded it is possible to analyze:

h) define effective section of the composite beam:

   i) in midspan or near an internal support:

$$b_{eff} = b_0 + \sum b_{ei}$$

   ii) end of support:

$$b_{eff} = b_0 + \sum \beta_i b_{ei}$$

i) define effective portion of steel beam:

   it is assumed $\beta = 0.5$

$$\lambda_{e,flange} = \frac{b}{t}\sqrt{\frac{f_y}{250}}$$

$$\lambda_{e,web} = \frac{d}{t}\sqrt{\frac{f_y}{250}}$$

   in which t is the thickness of the element

   and compare with λ_{ey} and λ_{ep} derived from the table in function of the part of the plate element and the residual stress

Now start the design of strength in which we need to do some verification:

j) $\phi V_u \geq V^*$

e) $M_R \geq M^*$

k) $\left(\frac{M}{M_{Rd}}\right)^3 + \left(\frac{V}{V_{comp}}\right)^6 = 1$

We start defining the design of composite action:

l) $n_i = \frac{F_{cp,i}}{P_{Rk}}$ which represent the minimum number of connectors

After we define on the beam the potentially critical cross section and the design the design for full shear connection:

m) $F_{cc} = min(N_{y,d}, N_{c,d})$

Then we define the design of vertical shear capacity:

n) $V_{comp} = V_{pl,Rd} + V_{slab}$

In function of γ and β it is possible to calculate:

o) M_{Rd}

Now it is possible to define the design of the shear connectors:

p) $n'_{ci} = \frac{F_{cc}}{P_{Rk}}$

where $P_{Rk} = k_l \ P_{Rk}$ in a composite slab

Now we define the design of longitudinal shear reinforcement:

q) $\nu_L^* = \frac{A_t \ y_c \ V^*}{I_t}$

r) Then we compare the design shear stress with the longitudinal shear strength

$$\nu_{Lp}^* \leq \phi \ \tau_u$$

After we use the minimum transverse reinforcement:

s) $\rho_{min} = \frac{0.08\sqrt{f'_c}}{f_{sy}}$

Now it is possible to start the design of serviceability:

t) Deflection for stage 1 to 3 and 5 to 6 is defined as in Science of Constructions:

$$\delta_{C\,i,j} = \frac{5\ q\ l^4}{384\ E_k\ I_k}$$

For stage 1 to 3 we consider only the steel part for the elastic modulus and the moment of inertia.

For stage 5 to 6 we consider the immediate deflection of steel beam and the immediate deflection of the composite member with complete interaction in which change the value of the moment of inertia. In this case, we define:

i) $\delta_{C\,5,6s}$

ii) $\delta_{C\,5,6c}$

And after we define the total deflection for this stage:

iii) $\delta_{\mathrm{C}\,5,6} = \left(1 + 0.3\ \left(1 - 0.85\ \frac{\mathrm{N}_i}{\mathrm{n}_f}\right)\left(\frac{\delta_{\mathrm{C}\,5,6\mathrm{s}}}{\delta_{\mathrm{C}\,5,6\mathrm{c}}}\right) - 1\right)\delta_{\mathrm{C}\,5,6\mathrm{c}}$

u) For the creep deflection we need to follow the same step but the value of the elastic modulus is:

$$E_{ef,cc} = \frac{E_c}{1 + \phi_{cc}}$$

And:

i) $\delta_{short} = \left(1 + 0.3\ \left(1 - \frac{\mathrm{N}_i}{\mathrm{n}_f}\right)\left(\frac{\delta_{\mathrm{short,s}}}{\delta_{\mathrm{short,c}}}\right) - 1\right)\delta_{\mathrm{short,c}}$

v) For the shrinkage deflection, we need to follow the same step but the value of the elastic modulus is:

$$E_{ef,cc} = \frac{E_c}{1 + 0.55\ \phi_{cc}}$$

And define the equivalent load which permit to define:

$$\text{i)} \quad \delta_{shrinkage} = \left(1 + 0.3\ \left(1 - 0.85\ \frac{\mathrm{N}_i}{\mathrm{n}_f}\right)\left(\frac{\delta_{shrinkage,\mathrm{s}}}{\delta_{shrinkage,\mathrm{c}}}\right) - 1\right) \delta_{shrinkage,\mathrm{c}}$$

Then we define the cracked and uncracked section which permit to define the I_{cr} and I_{uncr}

Appendix II

In this appendix are provided the flowcharts related to the project of the composite beam used for developing the MATLAB script. The main flowchart shows the general procedures to follow and the other flowcharts show the procedure to follow for complete all the steps.

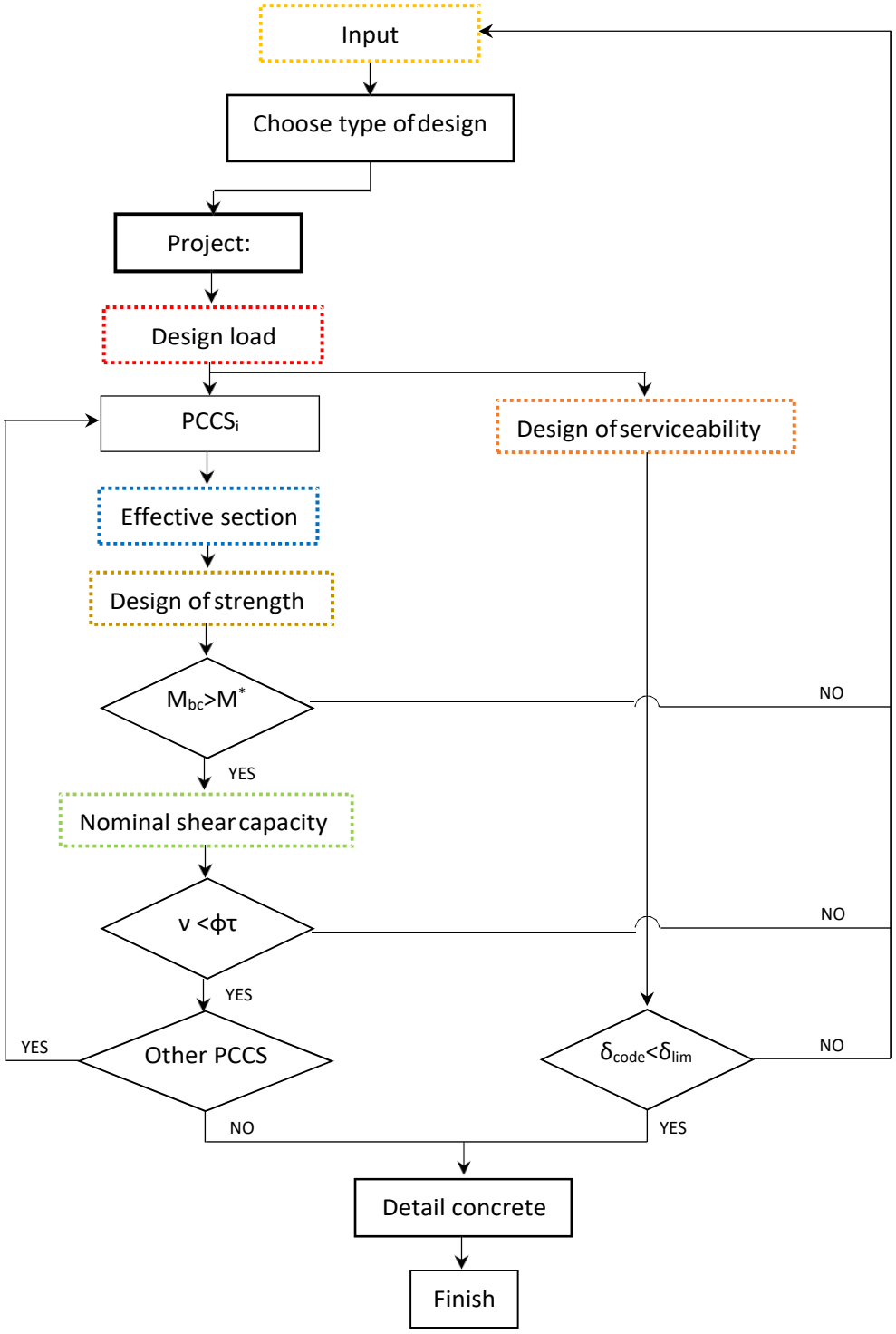
Input
Choose type of design
Project:
Design load
PCCS$_i$
Design of serviceability
Effective section
Design of strength
$M_{bc}>M^*$
NO
YES
Nominal shear capacity
$\nu < \phi\tau$
NO
YES
YES
Other PCCS
$\delta_{code}<\delta_{lim}$
NO
NO
YES
Detail concrete
Finish

Input data

Material property

- f'_c= compressive cylinder strength of concrete [kN/m^2]
- f_{cm}= f'_c + 8000
- f_{cmi}= 0.9 f_{cm}= 90% of the main value of the cylinder strength
- ρ_c= density of concrete [kN/m^3]
- ρ_s= density of steel [kN/m^3]
- E_c= elastic modulus of concrete (function of fcmi) [kN/m^2]
- E_s= elastic modulus of steel [kN/m^2]
- f_{uc}=410000 tensile strength of shear connector [kN/m^2]
- choose residual stresses (SR, HR, LW/CF, HW)

Section property

- t_c= thickness of slab depth
- β= degree of shear connection
- L_1= span of beam [m]
- L_2= span of secondary beam [m]
- L_3= span of secondary beam [m]
- Consider internal beam
- edge/internal beam
- b_{edge}= dimention of width overhang [m]
- solid (C)/composite slab (D)
- connector type: welded head stud (A), strength structural bolt (B)
- d_{bs}=0.019 (A) – 0.020 (B) [m] nominal shank diameter of a headed-stud
- hsc=0.092 (A) – 0.1 (B) [m] overall height of a shear connector
- s_{ribs}= transverse space of the ribs [m]
- $b_{sr,ribs}$= width of steel rib in a composite slab at its mid height [m]
- $b_{cr,ribs}$= s_{ribs} - $b_{sr,ribs}$ =width of concrete rib in a composite slab at its mid height of the steel ribs [m]
- $h_{r,ribs}$= 0.054 (D)- 0 (C) height of steel ribs in profiled steel sheeting [m]
- θ_{ribs}= acute angle between sheeting ribs and steel beam [°]
- A_t= L_2 L_3 tributary area [m^2]

Steel beam properties:

- SW_{steel}= selfweigth of steel section [kg/m]
- b_{fl}= width of flange
- d_s= depth of section
- t_{fl}= thickness of flange
- d_1= depth between flange
- t_w= thickness of web
- f_{yf}= yeld stress flange
- f_{yw}= yeld stress web
- A_s= gross area cross section
- I_x= moment of inertia about x axis
- I_y= moment of inertia about y axis
- Z
- J=torsional constant
- I_w= warping constant

Construction load

Slab:

- Q= live load [kN/m^2]
- Ψ_l= 0.4 = long term coefficient for load combination
- Ψ_s= 0.7 = short term coefficient for load combination
- $g_{ss,w}$=Steel sheeting weight [kg/m^2]
- ϕ_{prec}= 0 precamber coefficient
- $\phi_{ponding}$= 0.7 ponding slab coefficient
- $\phi_{dead\ load}$= 1.5 slab superimposed dead load
- $G_{2,\ slab}$= L_3 ρ_c t_c [kN/m]
- $G_{superimposed}$= L_3 $DL_{superimposed}$
- $G_{2,\ slab\ ponding}$= $G_{2,\ slab}$ $\phi_{ponding}$
- G_{reo}= 0.08 (1- ρ_c /7850) L_3
- $G_{adjustfor\ deck}$= 0.29
- $G_{2,\ superimposed\ slab}$= $G_{superimposed}$+ $G_{2,\ slab}$+ $G_{2,\ slab\ ponding}$+ G_{reo}- $G_{adjustfor\ deck}$
- Q_2= Q L_3
- $G_{steel\ sheeting}$= $\gamma_{steel\ sheeting}$ L_3

Composite beam (slab + steel beam)

- G_{2tot}= SW_{steel} +$G_{steel\ sheeting}$+ $G_{2,\ superimposed\ slab}$

Stage 3:

- $Q_{temporary\ stage3}$=α L_3 (α function of A_t)
- G_{stage3}= SW_{steel}+$G_{steel\ sheeting}$+ $G_{2,\ slab}$+ $G_{2,\ slab\ ponding}$+ G_{reo}+ $G_{adjustfor\ deck}$
- Q_{stage3}= $Q_{temporary\ stage3}$

Deflection

- $\delta_{dead\ load}$= 1/200 =deflection limit stage 3
- δ_{total}= 1/250 =total limit deflection
- δ_{Incr}= 1/500 =incremental limit deflection

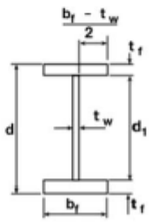

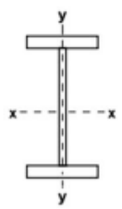

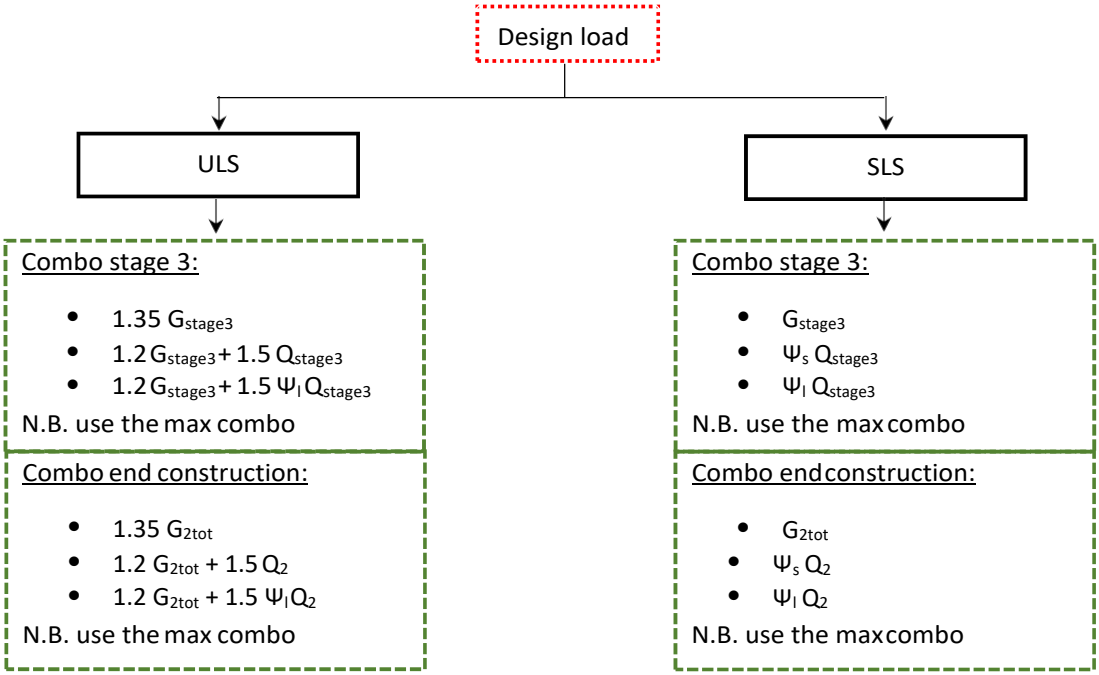
Design load
ULS
SLS
Combo stage 3:
1.35 G_{stage3}
1.2 G_{stage3} + 1.5 Q_{stage3}
1.2 G_{stage3} + 1.5 Ψ_l Q_{stage3}
N.B. use the max combo
Combo end construction:
1.35 G_{2tot}
1.2 G_{2tot} + 1.5 Q_2
1.2 G_{2tot} + 1.5 Ψ_l Q_2
N.B. use the max combo
Combo stage 3:
G_{stage3}
Ψ_s Q_{stage3}
Ψ_l Q_{stage3}
N.B. use the max combo
Combo end construction:
G_{2tot}
Ψ_s Q_2
Ψ_l Q_2
N.B. use the max combo

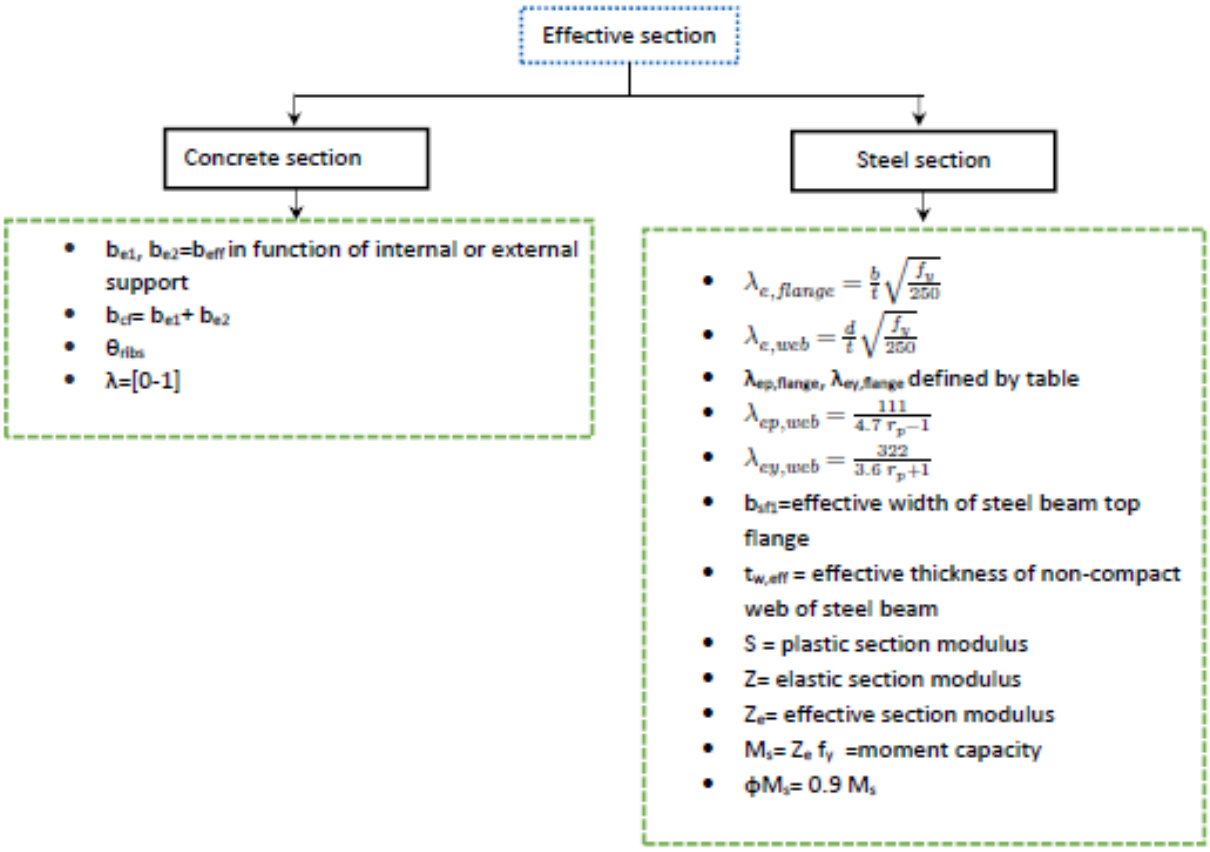
Effective section
Concrete section
Steel section
• b_{e1}, b_{e2}=b_{eff} in function of internal or external support
• b_{cf}= b_{e1}+ b_{e2}
• θ_{fibs}
• λ=[0-1]
• $\lambda_{e,flange} = \frac{b}{t}\sqrt{\frac{f_y}{250}}$
• $\lambda_{e,web} = \frac{d}{t}\sqrt{\frac{f_y}{250}}$
• $\lambda_{ep,flange}$, $\lambda_{ey,flange}$ defined by table
• $\lambda_{ep,web} = \frac{111}{4.7\, r_p - 1}$
• $\lambda_{ey,web} = \frac{322}{3.6\, r_p + 1}$
• b_{sf1}=effective width of steel beam top flange
• $t_{w,eff}$ = effective thickness of non-compact web of steel beam
• S = plastic section modulus
• Z= elastic section modulus
• Z_e= effective section modulus
• M_s= Z_e f_y =moment capacity
• ϕM_s= 0.9 M_s

Design of strength

PCCS

PCCS=2

Design action at support:

- $M^*_{stage3}=0$
- $M_{stage3}=0$
- $V^*_{stage3}= C_{combostrength\ stage\ 3} L/2$
- $V_{stage3}= C_{combostrength} L/2$
- $\beta^*=0$

Design action at mid-span:

- $M^*_{stage3}=C_{combostrength\ stage\ 3} L^2/8$
- $M_{stage3}= C_{combostrength} L^2/8$
- $V^*_{stage3}= 0$
- $V_{stage3}=0$
- $\beta^* = \beta$

N.B. use the max moment and shear

Effective section

Design member moment capacity

- A_{rt1}= area top flange
- A_{rt2}= area bottom flange
- A_w= area web in function of redial stresses
- $V_w=0.6*f_y*A_w$ Shear capacity
- $\phi V=0.9*\alpha^* V_w$
- $\gamma=V^*_{stage3}/ \phi V$

γ<0.5

- $F_{st}= (A_{rt1}+ A_{rt2}) f_{yf} + A_w f_{yw}$
- $d_{sc}= D_c+t_{rt1}+d_1/2=d_{sr}$
- $F_{c1}= 0.85 f_c b_{cf} (D_c-h_r)$
- $F_{c2}= 0.85 f_c b_{cf} h_r \lambda$
- $F_{scf}= f_{yf} b_{sf1} t_{r1}$

γ=1

- $F_{st}= (A_{rt1}+ A_{rt2}) f_{yf} + A_w f_{yw}$
- $d_{sc}= D_c+t_{rt1}+d_1/2=d_{sr}$
- $F_{c1}= 0.85 f_c b_{cf} (D_c-h_r)$
- $F_{c2}= 0.85 f_c b_{cf} h_r \lambda$
- $F_{scf}= f_{yf} b_{sf1} t_{r1}$

0.5<γ<1

- Define $M_{capacity}$ for γ=1 and γ<0.5

F_{cc}, F_{ccp}, $M_{capacity}$

γ>1

$M_{cap}= 0$

β=1

If PNA in solid slab $F_{st}\leq F_{c1}$

PNA between ribs and composite slab $F_{c1}< F_{st}\leq(F_{c1} + F_{c2})$

PNA in top steel flange $(F_{c1} + F_{c2}) < F_{st}\leq(F_{c1} + F_{c2} + 2 F_{sc})$

PNA in web $(F_{c1} + F_{c2}) < F_{st}\leq(F_{c1} + F_{c2} + 2 F_{sc})$

F_{cc}

d_c

d_h

M_{bc}

0<β<1

- Define:

  F_{scf}
- If PNA in solid slab $F_{st}\leq F_{c1}$

  PNA between ribs and composite slab $F_{c1}< F_{st}\leq(F_{c1} + F_{c2})$

  PNA in top steel flange $(F_{c1} + F_{c2}) < F_{st}\leq(F_{c1} + F_{c2} + 2 F_{sc})$

  PNA in web $F_{st}>(F_{c1} + F_{c2} + 2 F_{sc})$

  F_{cc}
- Define:

  $F_{cp}=\beta F_{cc}$ in function of connector

  $F_{sc}= F_{st}- F_{cp}$
- If $F_{cp}< F_{c1}$ or if $F_{cp}< F_{c1}$

  d_c
- Define:

  F_{scw}
- If $F_{sc}<2 F_{scf}$ or $2 F_{scf} < F_{sc} <(2 F_{scf} + 2 F_{scw})$ or $F_{cp}>(2 F_{scf} + 2 F_{scw})$

  d_h
- If $F_{cp}<2 F_{c1}$ & $F_{sc} < 2 F_{scf}$ or $F_{cp}<F_{c1}$ & $2 F_{scf} < F_{sc} < (2 F_{scf}+2 F_{scw})$ or $F_{cp}<F_{c1}$ & $F_{sc} > (2 F_{scf}+2 F_{scw})$ or $F_{cp}>F_{c1}$ & $F_{sc} < 2 F_{scf}$ or $F_{cp}>F_{c1}$ & $2 F_{scf}\leq F_{sc} > (2 F_{scf}+2 F_{scw})$ or $F_{cp}>F_{c1}$ & $F_{sc} < 2 F_{scf}+2 F_{scw}$

  M_b

- Define:

  F_{scf}, F_{scf}, F_{cc} (like β=1 and γ<0.5)
- If PNA in solid slab $F_{scf}\leq F_{c1}$

  PNA between ribs and composite slab $F_{c1}< F_{scf}\leq(F_{c1} + F_{c2})$

  PNA in top steel flange $(F_{c1} + F_{c2}) < F_{scf}\leq(F_{c1} + F_{c2} + 2 F_{scf})$

  F_{ccf}, d_c, d_h
- Define:

  $\Psi= F_{ccf}/ F_{cc}$
- When $\Psi<\beta<1$ if $F_{scf}\leq F_{c1}$ or $F_{c1}< F_{scf}\leq(F_{c1} + F_{c2})$ or $(F_{c1} + F_{c2}) < F_{scf}\leq(F_{c1} + F_{c2} + 2 F_{scf})$

  M_{bfc}
- When $0<\beta< \Psi$
  - if $F_{cpf}< F_{c1}$ or if $F_{cpf}< F_{c1}$

    F_{cpf}, F_{sc}, d_c
    - If $F_{sc}<2 F_{scf}$ or $F_{sc}>2 F_{scf}$

      d_h
    - If $F_{cpf}<2 F_{c1}$ & $F_{scf} < 2 F_{scf}$ or $F_{cpf}<F_{c1}$ & $F_{sc}>2 F_{scf}$ or $F_{cpf}>F_{c1}$ & $F_{sc} < 2 F_{scf}$ or $F_{cpf}>F_{c1}$ & $F_{sc}> 2 F_{scf}$

      M_{bf}
- Define:

  $M_{capacity}=\max(M_{bf}, M_{bfc})$

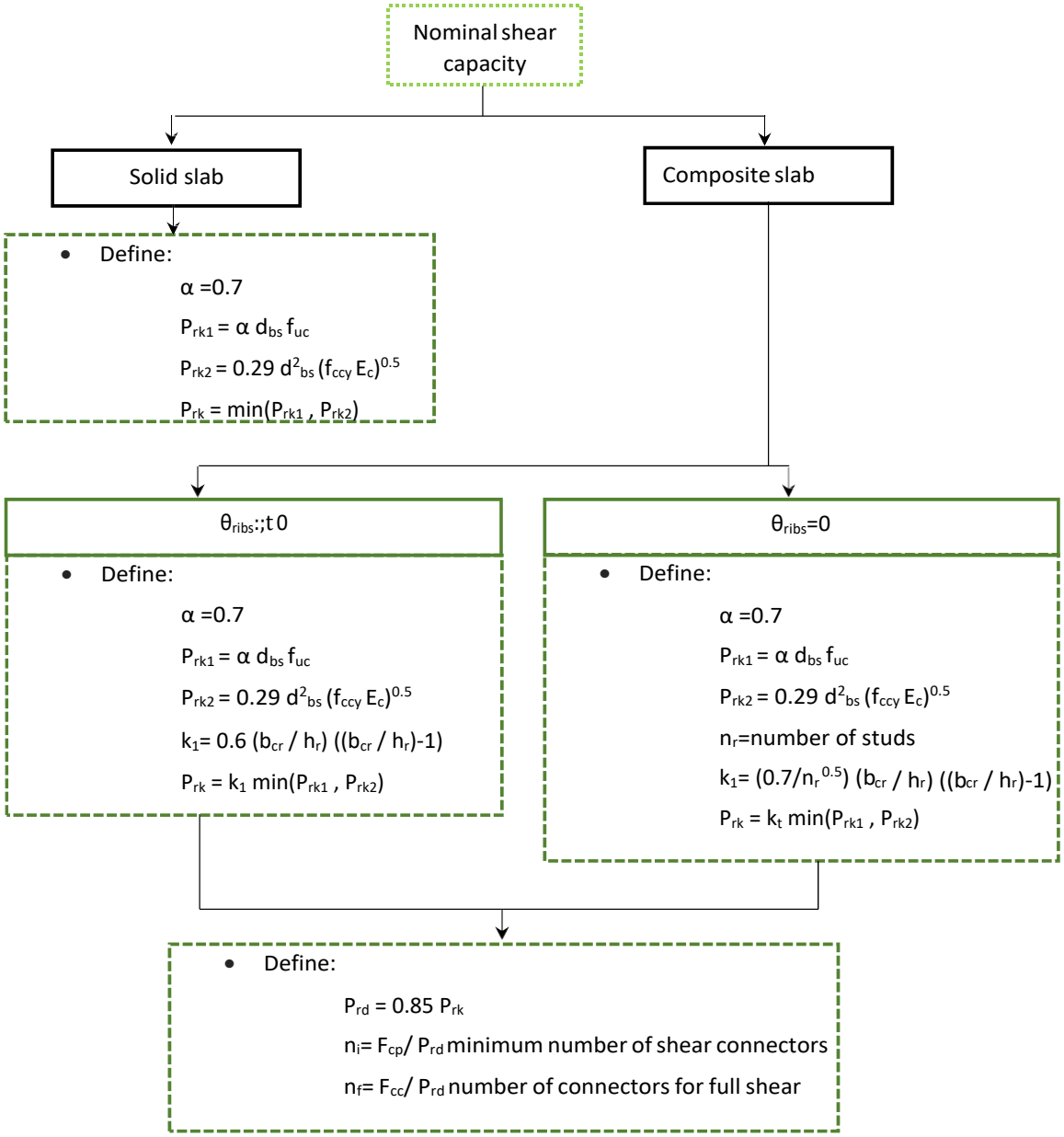
Nominal shear capacity
Solid slab
Composite slab
• Define:
α =0.7
$P_{rk1} = \alpha d_{bs} f_{uc}$
$P_{rk2} = 0.29 d^2_{bs} (f_{ccy} E_c)^{0.5}$
$P_{rk} = \min(P_{rk1}, P_{rk2})$
θ_{ribs}:;t 0
• Define:
α =0.7
$P_{rk1} = \alpha d_{bs} f_{uc}$
$P_{rk2} = 0.29 d^2_{bs} (f_{ccy} E_c)^{0.5}$
$k_1 = 0.6 (b_{cr} / h_r) ((b_{cr} / h_r)-1)$
$P_{rk} = k_1 \min(P_{rk1}, P_{rk2})$
θ_{ribs}=0
• Define:
α =0.7
$P_{rk1} = \alpha d_{bs} f_{uc}$
$P_{rk2} = 0.29 d^2_{bs} (f_{ccy} E_c)^{0.5}$
n_r=number of studs
$k_1 = (0.7/n_r^{0.5}) (b_{cr} / h_r) ((b_{cr} / h_r)-1)$
$P_{rk} = k_t \min(P_{rk1}, P_{rk2})$
• Define:
$P_{rd} = 0.85 P_{rk}$
$n_i = F_{cp} / P_{rd}$ minimum number of shear connectors
$n_f = F_{cc} / P_{rd}$ number of connectors for full shear

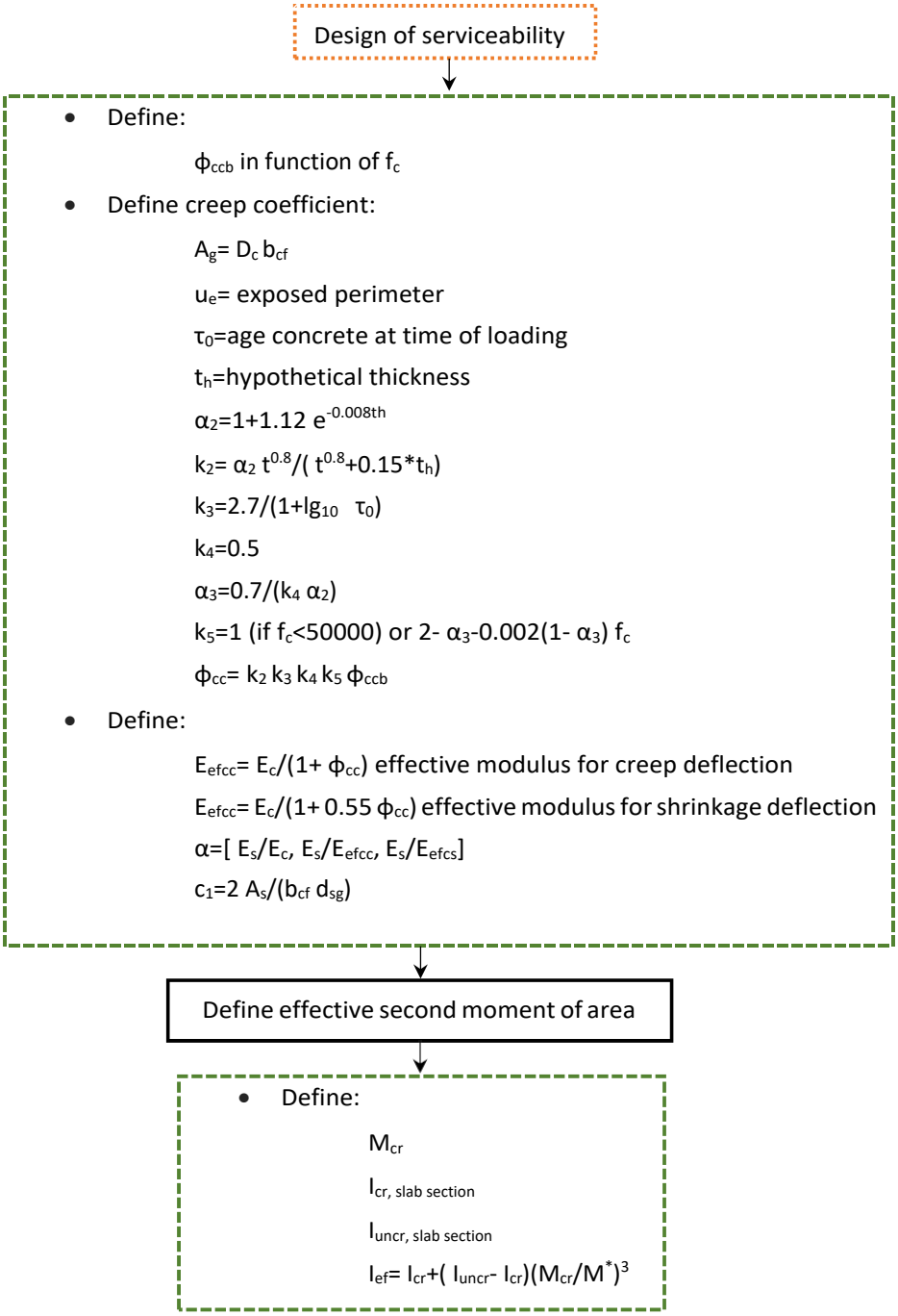
Design of serviceability
• Define:
ϕ_{ccb} in function of f_c
• Define creep coefficient:
$A_g = D_c\, b_{cf}$
u_e= exposed perimeter
τ_0=age concrete at time of loading
t_h=hypothetical thickness
$\alpha_2 = 1+1.12\, e^{-0.008th}$
$k_2 = \alpha_2\, t^{0.8}/(t^{0.8}+0.15*t_h)$
$k_3 = 2.7/(1+\lg_{10}\ \tau_0)$
$k_4 = 0.5$
$\alpha_3 = 0.7/(k_4\, \alpha_2)$
k_5=1 (if f_c<50000) or 2- α_3-0.002(1- α_3) f_c
$\phi_{cc} = k_2\, k_3\, k_4\, k_5\, \phi_{ccb}$
• Define:
$E_{efcc} = E_c/(1+\phi_{cc})$ effective modulus for creep deflection
$E_{efcc} = E_c/(1+0.55\,\phi_{cc})$ effective modulus for shrinkage deflection
α=[E_s/E_c, E_s/E_{efcc}, E_s/E_{efcs}]
$c_1 = 2\, A_s/(b_{cf}\, d_{sg})$
Define effective second moment of area
• Define:
M_{cr}
$I_{cr,\ slab\ section}$
$I_{uncr,\ slab\ section}$
$I_{ef} = I_{cr}+(I_{uncr}- I_{cr})(M_{cr}/M^*)^3$

Deflection component

- Define:

$\delta_{stage3}=G_{stage\_3}/(24\ E_s I_s)(L^3x-2Lx^3+x^4)$

$\delta_{s5to6}=G_{superimposed\_2}/(24\ E_s I_s)(L^3x-2Lx^3+x^4)$ (deflection steel)

$\delta_{c5to6}=G_{superimposed\_2}/(24\ E_s I_t)(L^3x-2Lx^3+x^4)$ (deflection concrete)

$\delta_{sshort}=\psi_s Q_2/(24\ E_s I_s)(L^3x-2Lx^3+x^4)$ (deflection steel in service stage)

$\delta_{cshort}=\psi_s Q_2/(24\ E_s I_t)(L^3x-2Lx^3+x^4)$ (deflection concrete in service stage)

$\delta_{slong}=(G_{superimposed\_2}+\psi_l Q_2)/(24\ E_s I_s)(L^3x-2Lx^3+x^4)$ (deflection steel in service stage)

$\delta_{clong}=(\ G_{superimposed\_2}+\psi_l Q_2)\ /(24\ E_s I_t)(\ 1/I_{t2}-1/I_{t1})(L^3x-2Lx^3+x^4)$ (creep deflection concrete in service stage)

$\delta_{precamber}=\rho_{recamber\_coeff}\ G_{stage\_3}/(24E_s I_s)(L^3\ x-2\ L\ x^3+x^4)$;

- Define long-term shrinkage deflection in service condition:

$\varepsilon_{cse1}=(0.06\ f_{cy}\ 10^{-3})-1)*50*10^{-6}$ = final autogenous shrinkage strain

$t_{drying}=3$

$t=t_{final}-t_{drying}$

$\varepsilon_{cse}=\varepsilon_{cse1}(1-e^{-0.1\,t})$ =autogenous shrinkage strain

$\varepsilon_{csdb1}=1000\ 10^{-6}$ final drying basic shrinkage strain

$\alpha_1=0.8+1.2\ e^{-0.005th}$

$k_1=\alpha_1\ t^{0.8}/(\ t^{0.8}+0.15*t_h)$

$k_4=0.5$

$\varepsilon_{csd}=k_1\ k_4\ e_{csdb}$ drying shrinkage strain

$\varepsilon_{cs}=\varepsilon_{cse}+\varepsilon_{csd}$ design shrinkage strain

Y_G=centroid of the composite cross-section

Solid slab

- Define:

$h_c=t_c-h_r$

$H_{sh}=h_c\ b_{cf}\ E_{efcs}\ \varepsilon_{cs}$

l_{cs}= lever arm

$M_{sh}=H_{sh}\ l_{cs}$

$\delta_{ssh}=M_{sh}/(2\ E_s\ I_{s\_}now)\ (L\ x-x^2)$

$\delta_{csh}=M_{sh}/(2\ E_s\ I_t)(L\ x-x^2)$;

Composite slab

- Define:

$\varepsilon_{csbtm}=0.2\ \varepsilon_{cs}$ shrinkage strain in the bottom of the slab

$\varepsilon_{cstop}=1.2\ \varepsilon_{cs}$ shrinkage strain in the top of the slab

$h_c=t_c-h_r$

$k_{cs}=(\varepsilon_{cstop}-\varepsilon_{csbtm})/t_c$ curvature of the shrinkage profile

$\varepsilon_{cseff}=\varepsilon_{cstop}-k_{cs}*h_c/2$ effective shrinkage strain

$H_{sh}=h_c\ b_{cf}\ E_{efcs}\ \varepsilon_{cseff}$

l_{cs}= lever arm

$M_{sh}=H_{sh}\ l_{cs}$

$\delta_{ssh}=M_{sh}/(2\ E_s\ I_{s\_}now)\ (L\ x-x^2)$

$\delta_{csh}=M_{sh}/(2\ E_s\ I_t)(L\ x-x^2)$;

- Define:

$\delta_{5to6}=1+0.3(1-\beta_{short}\ N_i/n_f)(\ \delta_{s5to6}/\ \delta_{c5to6}-1)\ \delta_{c5to6}$

$\delta_{short}=1+0.3(1-\beta_{short}\ N_i/n_f)(\ \delta_{sshort}/\ \delta_{cshort}\ -1)\ \delta_{cshort}$

$\delta_{long}=1+0.3(1-\beta_{short}\ N_i/n_f)(\ \delta_{slong}\ /\ \delta_{clong}\ -1)\ \delta_{clong}$

$\delta_{shrinkage}=1+0.3(1-\beta_{sh}\ N_i/n_f)(\ \delta_{ssh}\ /\ \delta_{csh}\ -1)\ \delta_{csh}$

$\delta_{tot}=\delta_{stage3}+\delta_{5to6}+\delta_{short}+\delta_{long}+\delta_{shrinkage}-\delta_{precamber}$

$\delta_{incr}=\delta_{short}+\delta_{long}+0.6\ \delta_{shrinkage}$

References

[1] G. L. R. Z. Gianluca Ranzi, "State of the art on the time-dependent bahaviour of composite steel-concrete structures," *Journal of Constructional Steel Research*, 2013.

[2] Z. P. BAZANT, "Prediction of Concrete Creep Effects," *Journal of the American Concrete Institute,* vol. Vol. 69, pp. 212-217, 1972.

[3] Gilbert, " Time effects in concrete structures," *Elsevier Science Publishers,* 1988.

[4] Gilbert, "Time-dependent analysis of composite steel–concrete sections," *Engineering MECHANICS*, 1990.

[5] U. B., " Uy B. Long-term service-load behaviour of simply supported profiled composite slabs," pp. 123:193-208, 1997.

[6] H. Koukkari, "Steel sheet in a post-tensioned composite slab" *Proceedings of Eurosteel*, p. 99, 1999.

[7] S. Shayan , S. Al-Deen , G. Ranzi and Z. Vrcelj , "Long-term behaviour of composite concrete slabs: an experimental study," . *Proceedings of the 4th International Conference,* 2010.

[8] S. Al-Deen , G. Ranzi and Z. Vrcelj, " Full-scale long-term and ultimate experiments of simply-supported composite beams with steel deck," *J Constr Steel,* pp. 67:1658-76, 2011.

[9] R. Gilbert , M. Bradford, A. Gholamhoseini and Z. Chang , "The effects of shrinkage on the long-term deformation of composite concrete slabs," 2011.

[10] Al Deen, Ranzi and Uy, "Non-uniform shrinkage in simply-supported composite steel-concrete slabs," 2015.

[11] Al-Deen and G. Ranzi , "Effects of Non-uniform Shrinkage on the Long-term Behaviour of Composite Steel-Concrete Slabs," 2015.

[12] Uy, "Long-term service-load behaviour of simply supported profiled composite slab," *Researchgate*, 1997.

[13] H. Koukkari, "Steel sheet in a post-tensioned composite slab," *Proceedings of Eurosteel,* 1999.

[14] K. Lambe and S. Siddh, " Analysis and design of composite slab by varing different parameters," *Materials Science and Engineering,* 2018.

[15] R. Gilbert, "Time-Dependent Analysis of Composite Steel-Concrete Sections," *Journal of Structural Engineering,* 1989.

[16] A. Gholamhoseini, R. Gilbert and M. Bradford, "Long-term deformations in continuous composite concrete slabs," *Australian Journal of Structural Engineering,* 2016.

[17] A. Gholamhoseini, R. Gilbert and M. Bradford, "Long-term deformations in continuous composite concrete slabs," *Australian Journal of Structural Engineering,* vol. 17, pp. 197-212, 2016.

[18] S. Al-Deen, "Hydro-mechanical analysis of non-uniform shrinkage development and its effects on steel-concrete composite slabs," *Steel and Composite Structures,* vol. 26, pp. 303-314, 2018.

[19] S. Al-Deen, "Hydro-mechanical analysis of non-uniform shrinkage development," *Steel and Composite Structures,* vol. 26, pp. 303-314, 2018.

[20] M. CJ, K. GL and S. G., "Deflections of a composite floor system," *Canadian Journal of Civil Engineering*, 1983.

[21] F. Roll , " Effects of differential shrinkage and creep on a composite steel–concrete structure," *ACI Spec Publ ,* pp. 27(8):263-8, 1971.

[22] A. Ghali and R. Favre, "Concrete structures: stresses and deformations," *Chapman and Hall,* 1986.

[23] R. Gilbert , "Time effects in concrete structures," *Elsevier Science Publishers,* 1988.

[24] T. Chicoine, B. Massicotte and R. Tremblay , "Long-term behavior and strength of partially encased composite columns made with built-up steel shapes," *J Struct Eng ASCE ,* pp. 129(2):141-50, 2003.

[25] W. Zuk , "Thermal and shrinkage stresses in composite beams," *ACI J ,* vol. 40, p. 327, 1961.

[26] M. Bradford and R. Gilbert, "Non-linear behaviour of composite beams at service loads," *Struct Eng ,* pp. 67(14):263-8, 1989.

[27] R. Lawther and R. Gilbert, "Deflection analysis of composite structures using the rate-of-creep method," *Struct Eng,* pp. 70(12):220-3, 1992.

[28] R. Lawther and R. Gilbert , "A rate-of-creep analysis of composite steel–concrete cross-sections," *Struct Eng ,* pp. 65(11):208-13., 1990.

[29] R. Gilbert and M. Bradford, "Time-dependent behaviour of continuous composite beams at service loads," *J Struct Eng ASCE ,* pp. 121(2):319-27, 1995.

[30] M. Bradford , H. Vu Manh and R. Gilbert, " Numerical analysis of continuous composite beams under service loading," *Adv Struct Eng ,* p. 5(1):1–12, 2002.

[31] M. Arockiasamy and M. Sivakumar, "Time-dependent behavior of continuous composite integral abutment bridges," *Pract Period Struct Des Constr ,* pp. 10(3):161-70, 2005.

[32] M. Tehami and K. Ramdane , "Creep behaviour modelling of a composite steel–concrete section," *J Constr Steel Res ,* pp. 65:1029-33, 2009.

[33] . J. Grant, A. John , Fisher and W. John , "SHEAR CONNECTOR BEHAVIOR IN COMPOSITE BEAMS WITH METAL DECKING," *Preprints - ASCE Convention & Exposition,* 1982.

[34] A. Tarantino and L. Dezi, "Creep effects in composite beams with flexible shear connectors," *Journal of structural engineering,* vol. 118, pp. 2063-2081, 1992.

[35] A. Tarantino and L. Dezi, "Creep effects in composite beams with flexible shear connectors," *J Struct Eng ASCE ,* pp. 118(8):2063-81, 1992.

[36] M. Bradford and R. Gilbert, "Composite beams with partial interaction under sustained loads," *J Struct Eng ASCE ,* pp. 118(7):1871-83, 1992.

[37] M. Bradford and R. Gilbert , "Time-dependent stresses and deformations in propped composite beams," *Proc Inst Civ Eng Struct Build ,* pp. 94:315-22, 1992.

[38] L. Dezi and A. Tarantino, "Creep in composite continuous beams — I: theoretical treatment," *J Struct Eng ASCE* , pp. 119(7):2095-111, 1993.

[39] L. Dezi and A. Tarantino , "Creep in composite continuous beams — II: parametric study," *J Struct Eng ASCE* , pp. 119(7):2112-33, 1993.

[40] L. Dezi , C. Ianni and A. Tarantino, "Simplified creep analysis of composite beams with flexible connectors," *J Struct Eng ASCE* , pp. 119(5):1484-97, 1993.

[41] C. Amadio and M. Fragiacomo, "A finite element model for the study of creep and shrinkage effects in composite beams with deformable shear connections," *Constr Met,* pp. 4:213-28, 1993.

[42] M. Bradford, "Shrinkage behaviour of steel–concrete composite beams," *ACI Struct J* , pp. 94(6):625-32, 1997.

[43] Reza Salari, Spacone, Benson Shing and Frangpol, "NONLINEAR ANALYSIS OF COMPOSITE BEAMS WITH DEFORMABLE SHEAR CONNECTORS," *JOURNAL OF STRUCTURAL ENGINEERING,* 1998.

[44] M. Bradford and R. Gilbert, "Time-dependent behaviour of simply supported steel–concrete composite beams," *Proc Inst Civ Eng Struct Build* , pp. 94:315-22, 1991.

[45] M. Bradford and R. Gilbert, "Experiments on composite beams at service loads," *Civ Eng Trans, Inst Eng* , pp. CE33(4):284-91, 1991.

[46] I. Alsamsam , "Shrinkage measurements in composite beam slabs. Proceedings of Non-destructive Testing of Concrete Elements and Structures," pp. p. 215-25, 1992.

[47] I. Alsamsam , "Serviceability criteria for composite floor systems," *PhD Thesis. The University of Minnesota ,* 1991.

[48] H. Wright , J. Vitek and S. Rakib , "Long-term creep and shrinkage in composite beams with partial connection," *Proc Inst Civ Eng Struct Build,* pp. 94:187-95, 1992.

[49] H. Kwak and Y. Seo, "Time-dependent behaviour of composite beams with flexible connectors," *Comput Methods Appl Mech Eng,* pp. 191:3751-72, 2002.

[50] M. Fragiacomo, C. Amadio and L. Macorini, " FrInfluence of viscous phenomena on steel–concrete composite beams with normal and high performance slab," *Steel Compos Struct ,* 2002;2(2):85-98.

[51] M. Fragiacomo, C. Amadio and L. Macorini , "Finite-element model for collapse and long-term analysis of steel–concrete composite beams," *J Struct Eng ASCE ,* pp. 130(3):489-97, 2004.

[52] F. Virtuoso and R. Vieira , "Time dependent behaviour of continuous composite beams with flexible connection," *J Constr Steel Res,* pp. 60(3–5):451-63, 2004.

[53] B. Jurkiewiez, S. Buzon and J. Sieffert , "Incremental viscoelastic analysis of composite beams with partial interaction," *Comput Struct ,* pp. 83:1780-91, 2005.

[54] G. Ranzi , "Short- and long-term analyses of composite beams with partial shear interaction stiffened by a longitudinal plate," *Steel Compos Struct ,* pp. 6(3)237-55, 2006.

[55] F. Gara , G. Ranzi and G. Leoni , "Time analysis of composite beams with partial interaction using available modelling techniques: a comparative study," *J Constr Steel Res ,* pp. 62(9):917-30, 2006.

[56] S. Chaudhary , U. Pendharkar and A. Nagpal, "Control of creep and shrinkage effects in steel concrete composite bridges with precast decks," *J Bridge Struct Eng ASCE,* pp. 14(5):336-45, 2009.

[57] S. Chaudhary , U. Pendharkar and A. Nagpal, "Hybrid procedure for cracking and time-dependent effects in composite frames at service loads," *J Struct Eng ASCE,* pp. 133(2):166-70, 2007.

[58] M. Sakr and S. Sakla, "Long-term deflection of cracked composite beams with nonlinear partial shear interaction: I — finite element modelling," *J Constr Steel Res,* pp. 64:1446-55, 2008.

[59] O. Mirza and B. Uy , "Finite element model for long-term behaviour of composite steel–concrete push tests," *Steel Compos Struct ,* pp. 10:439-61, 2010.

[60] R. Erkmen and M. Bradford , "Nonlinear quasi-viscoelastic behavior of composite beams curved in-plan," *J Eng Mech ,* pp. 137(4):238-47, 2011.

[61] C. Faella , E. Martinelli and E. Nigro, "Steel and concrete composite beams with flexible shear connection: "exact" analytical expression of the stiffness matrix and applications," *Comput Struct ,* pp. 80:1001-9, 2002.

[62] G. Ranzi , "Partial interaction analysis of composite beams using the direct stiffness method," *PhD thesis. The University of New South Wales,* 2003.

[63] G. Ranzi and M. Bradford , "Analysis of composite beams with partial interaction using the direct stiffness approach for time effects," *Int J Numer Methods Eng,* pp. 78(5):564-86, 2009.

[64] Q. Nguyen , M. Hjiaj and B. Uy , "Time-dependent analysis of composite beams with continuous shear connection based on a space-exact stiffness matrix," *Eng Struct,* pp. 32:2902-11, 2010.

[65] Q. Nguyen , M. Hjiaj and J. Aribert , "A space-exact beam element for time-dependent analysis of composite members with discrete shear connection," *J Constr Steel Res,* pp. 66:1330-8., 2010.

[66] G. Ranzi, M. A. Bradford and B. Uy, "Analytical Solutions for the Viscoelastic Response of Composite Beams Including Partial Interaction," *Advances in Structural Engineering ,* vol. Vol. 9 No. 1 , 2006.

[67] T. Xiang, C. Yang and G. Zhao, "Stochastic Creep and Shrinkage Effect of Steel-Concrete Composite Beam," *Advances in Structural Engineering ,* vol. Vol. 18 No. 8 , 2015.

[68] P. Criel, R. Caspeele, S. Matthys and L. Taerwe, "Creep experiments and analysis of T-shaped beams subjected to loading and unloading at young age," *Conference Paper ,* November 2014.

[69] K. Furtak, "Evaluation of the influence of shrinkage strain on the fatigue strength of the connection in steel–concrete composite beams," *Elsevier,* 2015.

[70] J. Ducret and J. Lebet , "Effects of concrete hydration on composite bridges," *IABSE reports,* vol. 999, 1997.

[71] G. Bertagnoli, D. Gino and E. Martinelli, "A simplified method for predicting early-age stresses in slabs of steel-concrete composite beams in partial interaction," *Engineering Structures ,* vol. 140 , p. 286–297, 2017.

[72] K. Furtak, "Evaluation of the influence of shrinkage strain on the fatigue strength of the connection in steel-concrete composite beams," *Archives of Civil and Mechanical Engineering,* vol. 15, pp. 767-774, 2015.

[73] H. Ban, B. Uy, S. Pathirana, I. Henderson, O. Mirza and X. Zhu, "Time-dependent behaviour of composite beams with blind bolts under sustained loads," *Journal of Constructional Steel Research,* vol. 112, pp. 197-207, 2015.

[74] T. Tong, Q. Yu and Q. Su, "Coupled Effects of Concrete Shrinkage, Creep, and Cracking on the Performance of Postconnected Prestressed Steel-Concrete Composite Girders," *Journal of Bridge Engineering,* vol. 23, 2018.

[75] Z. Yuan, P. Ng, D. Bačinskas and J. Du, "Analysis of non-uniform shrinkage effect in box girder sections for long-span continuous rigid frame bridge," *Baltic Journal of Road and Bridge Engineering,* vol. 13, pp. 146-155, 2018.

[76] G. Cao, L. Yang, W. Zhang, X. Peng and Y. Dai, "Long-term mechanical properties of steel-concrete connectors subjected to corrosion and load coupling," *Journal of Materials in Civil Engineering,* vol. 30, 2018.

[77] Paul Kuhn, "Approximate stress analysis of multi-stringer beams with shear deformation of the flanges," *T.R. ,* p. No. 636 , 1938.

[78] Schule, "Mitteilungen der eidgenossischen materialprufungsanstalt," *Zurich,* 1909.

[79] Bortsch, "Der bauingenieur," p. p. 662, 1921.

[80] T. Karman, "Beitrage zur technischen Mechanik und technischen PhysiK," *Berlin,* 1923.

[81] W. Metzer, "Die mittragende breite," *Luftfahrtforschung,* vol. 4, pp. pp. 1-20 (in German), , 1929 .

[82] L. Dezi, F. Gara, G. Leoni and A. Tarantino, "Time-dependent analysis of shear lag effect in composite beams," *Journal of Engineering Mechanics, ASCE, ,* Vols. vol. 127, No. 1, pp. pp. 71-79, Jan. 2001.

[83] M. Chiewanichakorn, I. Ahn, A. Aref and S. Chen, "The development of revised effective slab width criteria for steel-concrete composite bridges," *Structures Congress, George. E. Blandford-Editor,,* pp. pp. 22-26, May 2004.

[84] A. Aref, M. Chiewanichakorn, S. Chen and S. Ahn, "Effective slab width definition for negative moment regions of composite bridges," *Journal of Bridge Engineering,* Vols. ASCE, vol.12, No.3, pp. pp. 339-349, May 2007.

[85] L. Fa-Xiong and N. Jian-Guo , "Elastic analytical solutions of shear lag effect of steel-concrete composite beam," *Gongcheng Lixue/Engineering Mechanic,* Vols. v 28, n 9, pp. p 1-8, September 2011.

[86] H. Yu-Liang , X. Yi-Qiang, L. Shao-Jun and L. Li-Si, "Analysis on shear-lag effect of composite of composite girders based on a different parabolic warping dispalcement function," *Journal of Zhejang University,* vol. 48 n 11, pp. 1993-1940, 2014.

[87] M. Lin and C. De-Wei , "Long-term behavior of composite beam incorporating shear lag effect," *Gongcheng Lixue/Engineering Mechanics,* Vols. v 29, n 9, pp. p 252-258, September 2012.

[88] L. Dezi, F. Gara, G. Leoni and A. Tarantino, "Time-dependent analysis of shear-lag effect in composite beams," *Journal of Engineering Mechanics, ,* Vols. v 127, n 1, pp. p 71-79, January 2001.

[89] S. Fei-Fei and L. Guo-Qiang , "Closed-form solution for steel-concrete composite beams with slip, shear lag and shear deformation," *Gongcheng Lixue/Engineering Mechanics,* Vols. v 22, n 2, pp. p 96-103, , April 2005.

[90] R. Su and L. Zhu, "Analytical solutions for composite beams with slip, shear-lag and time-dependent effects," *Engineering Structures,* vol. v 152, pp. p 559-578, 1 December 2017.

[91] H. Mohannad , Al-Sherrawi Ghaidak and Ahmed Fadhil Ef, "Effect of Stiffeners on Shear Lag in Steel Box Girders," *Department of Civil Engineering/ College of Engineering/University of Baghdad.*

[92] G. Ranzi and A. Zona, "A steel-concrete composite beam model with partial interaction including the shear deformability of the steel component," *Proceedings of the 3rd International Conference on Steel and Composite Structures,* pp. 231-236, 2007.

[93] F. Gara, S. Carbonari, G. Leoni and L. Dezi, "A higher order steel-concrete composite beam model," *Engineering Structures,* vol. v 80, pp. p 260-273, December 2014.

[94] G. Ranzi, A. Zona and Z. Vrcelj, "Effects of the shear deformability of the steel member in the short- and long-term partial interaction analysis of steel-concrete composite beams," *Futures in Mechanics of Structures and Materials ,* pp. 683-688, 2008.

[95] H. Saadatmanesh, P. Albrecht and B. Ayyub, "Static strength of prestressed composite steel girders," *Civil Engineering Report, Univ. of Maryland, College Park, Md,* 1986.

[96] Hamid Saadatmanesh, Pedro Bilal and Ayyub Albrech, "EXPERIMENTAL STUDY OF PRESTRESSED COMPOSITE BEAMS," 1989.

[97] L. Dezi , G. Leoni and A. Tarantino , "Time-dependent analysis of prestressed composite beams," *J Struct Eng ASCE ,* pp. 121(4):621-33, 1995.

[98] A. Dall'Asta , L. Dezi and G. Leoni , "Long-term analysis of externally prestressed composite posite beams," *Proceedings of the 2nd International Conference on Advances in Steel Structures ,* pp. 631-938, 1999.

[99] B. Uy, "Long Term Behaviour of Composite Steel-Concrete Beams Prestressed with High Strength Steel Tendons," *Advances in Steel Structures ,* 2007.

[100] W. Xue , M. Ding , C. He and J. Li , "Long-term behavior of prestressed composite beams at service loads for one year," *J Struct Eng ASCE ,* pp. 134(6):930-7, 2008.

[101] F. Giussani and F. Mola , " Giussani F, Mola F. Displacement method for the long-term analysis of steel–concrete beams with flexible connection," *J Struct Eng ASCE* , pp. 265-74, 2010.

[102] M. Gilbert and A. Bradford , "Time-Dependent Behavior of Continuous Composite Beams at Service LoadsArticle," *Journal of Structural Engineering* , 1995.

[103] R. I. Gilbert and G. Ranzi, Time-Dependent Behaviour of, 2011.

[104] Hyo-Gyoung Kwak and Young-Jae Seo, "Time-dependent behavior of composite beams," *Elsevier,* 2002.

[105] C. Faella, E. Martinelli and E. Nigro, "Steel and concrete composite beams with flexible shear connection: ''exact'' analytical expression of the stiffness matrix and applications," *Computers and Structures,* 2000.

[106] G. Ranzi, M. A. Bradford and B. Uy, "A direct stiffness analysis of a composite beamwith partial interaction," *INTERNATIONAL JOURNAL FOR NUMERICAL METHODS IN ENGINEERING,* vol. 61, pp. 657-672, 2004.

[107] B. Jurkiewiez and S. Braymand, "Experimental study of a pre-cracked steel–concrete composite beam," *Journal of Constructional Steel Research 63 (2007) 135–144,* 2006.

[108] S. Chaudhary, U. Pendharkar and A. K. Nagpal, "Hybrid Procedure for Cracking and Time-Dependent Effects in Composite Frames at Service Load," *JOURNAL OF STRUCTURAL ENGINEERING,* vol. 133(2), pp. 166-175, 2007.

[109] W. Yu and M. Blair, "GEBT: A general-purpose nonlinear analysis tool for composite beams," *Composite Structures,* pp. 2677-2689, 2012.

[110] C. Zanuy, "Analytical equations for interfacial stresses of composite beams due to shrinkage," *International Journal of Steel Structures,* vol. 15, pp. 999-1010, 2015.

[111] M. Dias, J. Tamayo, I. Morsch and A. Awruch, "Time dependent finite element analysis of steel-concrete composite beams considering partial interaction," *Computers and Concrete,* vol. 15, pp. 687-707, 2015.

[112] A. Gholamhoseini, I. Gilbert and M. Bradford, "Calculation of time-dependent deflection of composite concrete slabs: Simplified design approach," *Practice Periodical on Structural Design and Construction,* vol. 20, 2015.

[113] W. Siekierski, "Analysis of concrete shrinkage along truss bridge with steel-steelconcrete," *Steel and Composite Structures,* vol. 20, pp. 1237-1257, 2016.

[114] A. Gholamhoseini, A. Khanlou, G. MacRae, A. Scott, S. Hicks and R. Leon, "An experimental study on strength and serviceability of reinforced and steel fibre reinforced concrete (SFRC) continuous composite slabs," *Engineering Structures,* vol. 114, pp. 171-180, 2016.

[115] T. Guo, Z. Chen, T. Liu and D. Han, "Time-dependent reliability of strengthened PSC box-girder bridge using phased and incremental static analyses," *Engineering Structures,* vol. 117, pp. 358-371, 2016.

[116] Q. Nguyen and M. Hjiaj, "Nonlinear Time-Dependent Behavior of Composite Steel-Concrete Beams," *Journal of Structural Engineering (United States),* vol. 142, 2016.

[117] P. Bernardi, R. Cerioni, E. Michelini and A. Sirico, "Numerical simulation of early-age shrinkage effects on RC member deflections and cracking development," *Frattura ed Integrita Strutturale,* vol. 10, pp. 15-21, 2016.

[118] M. A. Uddin, A. H. Sheikh, D. Brown, T. Bennett and B. Uy, "A higher order model for inelastic response of composite beams with interfacial slip using a dissipation based arc-length method," *Engineering Structures 139 (2017) 120–134,* p. 120–134, 2017.

[119] Q. Nguyen, M. Hjiaj and A. Asce, "Nonlinear Time-Dependent Behavior of Composite Steel-Concrete Beams," *American Society of Civil Engineers,* 2016.

[120] G. Bertagnoli and G. Mancini, "EFFECT OF ENDOGENOUS DEFORMATIONS IN COMPOSITE BRIDGE BEAMS," *Conference paper,* 2016.

[121] L. Zhu and R. Su, "Analytical solutions for composite beams with slip, shear-lag and time-dependent effects," *Engineering Structures ,* vol. 152 , p. 559–578, 2017.

[122] S. Altoubat, K. Rieder and M. Junaid, "Short- and long-term restrained shrinkage cracking of fiber reinforced concrete composite metal decks: an experimental study," *Materials and Structures* , p. 50:140, 2017 .

[123] L. Zhu and R. Su, "Analytical solutions for composite beams with slip, shear-lag and time-dependent effects," *Engineering Structures,* vol. 152, pp. 559-578, 2017.

[124] "Influence of shrinkage and temperature on a composite pretensioned reinforced concrete structure," *Procedia Engineering* , vol. 193 , p. 96 – 103, 2017.

[125] G. Cao, L. Yang, W. Zhang, X. Peng and Y. Dai, "Long-Term Mechanical Properties of Steel–Concrete Connectors Subjected to Corrosion and Load Coupling," *J. Mater. Civ. Eng.,* 2018.

[126] B. Klemczak, M. Batog, Z. Giergiczny and A. Z˙mij, "Complex Effect of Concrete Composition on the Thermo-Mechanical Behaviour of Mass Concrete," *Materials,* Vols. 11, 2207, 2018.

[127] Mohamed Tehami and Kheir-Eddine Ramdane, "Creep behaviour modelling of a composite steel-concrete section," *Journal of Constructional Steel Research,* 2009.

[128]

[129] L. Dezi, G. .. Leoni and A. M. Tarantino, "Creep and shrinkage analysis of composite beams," vol. 1(2), pp. 170-177, 1998.

[130] Hyo-Gyoung Kwak, Young-Jae Seo and Chan-Mook Jung, "Effects of the slab casting sequences and the drying shrinkage of concrete slabs on the short-term and long-term behavior of composite steel box girder bridges. Part 2," *Elsevier,* 2000.

[131] A. Marı´, E. Mirambell and I. Estrada, "Effects of construction process and slab prestressing on the serviceability behaviour of composite bridges," *Journal of Constructional Steel Research, Elsevier,* 2001.

[132] A. M. Tarantino and L. Dezi, "CREEP EFFECTS IN COMPOSITE BEAMS WITH FLEXIBLE SHEAR CONNECTORS," *J.Struct. Eng.,* vol. 118(8), pp. 2063-2081, 1992.

[133] O. Mirza and B. Uy, "Finite element model for the long-term behaviour of composite steel-concrete push tests," *Steel and Composite Structures,* vol. 10, pp. 45-67, 2010.

[134] Q.-H. Nguyena, M. Hjiaj and B. Uy, "Time-dependent analysis of composite beams with continuous shear connection based on a space-exact stiffness matrix," *Engineering Structures,* vol. 32, pp. 2902-2911, 2010.

[135] G. Ranzi and A. Zona, "Finite elementmodelsfornonlinearanalysisofsteel–concretecomposite beams with partial interaction in combined bending and shear," in *Finite ElementsinAnalysisandDesign47*, 2011, pp. 98-118.

[136] R. E. Erkmen and M. A. Bradford, "Time-dependent creep and shrinkage analysis of composite beams curved in-plan," *Computers and Structures 89 (2011) 67–77,* vol. 89 , p. 67–77, 2010.

[137] C. Amadio, M. Fragiacomo and L. Macorini , "Evaluation of the deflection of steel-concrete composite beams at serviceability limit state," *Journal of Constructional Steel Research,* vol. 73, pp. 95-104, 2012.